A HYDROGEOLOGICAL AND GEOCHEMICAL STUDY OF THE ORIGIN AND NATURE OF THE PRAIRIE FLATS URANIUM DEPOSIT, SUMMERLAND, BC

by

Kathy Rossel

BASc, Queen's Univeristy, 1996

A THESIS SUBMITTED IN PARTIAL FULFILLMENT OF
THE REQUIREMENTS FOR THE DEGREE OF
MASTER OF APPLIED SCIENCE

in

THE FACULTY OF GRADUATE STUDIES
(Department of Geological Engineering)

We accept this thesis as conforming
to the required standard:

THE UNIVERSITY OF BRITISH COLUMBIA

April, 1999

In presenting this thesis in partial fulfilment of the requirements for an advanced degree at the University of British Columbia, I agree that the Library shall make it freely available for reference and study. I further agree that permission for extensive copying of this thesis for scholarly purposes may be granted by the head of my department or by his or her representatives. It is understood that copying or publication of this thesis for financial gain shall not be allowed without my written permission.

Department of **Earth and Ocean Sciences**

The University of British Columbia
Vancouver, Canada

Date **April 29 '99**

ABSTRACT

An investigation of the hydrogeology and groundwater geochemistry was carried out at the Prairie Flats surficial uranium deposit in Summerland, B.C. The deposit contains an estimated 230 tonnes of uranium, most of which is concentrated in the upper half-metre of soil. It is believed to have formed out of the discharge of uraniferous groundwaters into organic-rich sediments over a period of 10,000 years. Objectives of this study were 1) to trace the origins of the groundwaters transporting uranium into the site, 2) to measure current rates of groundwater discharge and uranium deposition, 3) to identify the mechanism(s) of uranium retention, such as adsorption, reductive precipitation or evaporative precipitation, and 4) to comment on the likelihood of uranium remobilization. A literature review was first carried out to characterize the area's local and regional groundwater systems. Next, a network of 13 piezometers was installed across the site, with completion depths ranging from 1 to 3 metres. Using these, hydraulic conductivities of the hydrostratigraphic units were measured, and relative head values were monitored at four different times of year. Groundwater and surface waters were tested for pH, Eh, conductivity, and concentrations of U, Ca, Mg, Na, K, NO_3, HCO_3, SO_4, and Cl. Measurements of groundwater discharge into Prairie Creek, which crosses the site, were also carried out.

Results show that the flats are a discharge zone for locally recharged groundwaters, that is groundwaters that infiltrate within a few kilometers of the site and travel at depths of less than 100m within glacial deposits and shallow bedrock. These groundwaters are neutral in pH, relatively oxidizing, and enriched in calcium and bicarbonate. Discharge rates are on the order of 9450 m^3/year, most of which flows vertically upward from below the deposit. As uranium concentrations in the incoming groundwaters are up to 100μg/L, current uranium deposition rates are estimated to be around 1 kg/year. This is at least ten times lower than that calculated using the estimated size and age of the deposit, which suggests that uranium deposition rates were higher in the past than they are today. A major fraction of the uranium is held by adsorption to organics, however desorption by the formation of soluble complexes with bicarbonate is also evident. Two field observations show that soil aeration or exposure to septic discharge may also remobilize uranium. Uranium which is not held by adsorption is precipitated as a reduced uranium mineral, probably $UO_{2(c)}$. Relatively more reducing conditions near ground surface than at depth may help to explain the high concentrations of uranium within the top half-metre of soil.

TABLE OF CONTENTS

LIST OF TABLES

LIST OF FIGURES

LIST OF PLATES

ACKNOWLEDGEMENTS

I would like to state first and foremost that this project was made possible by the combined efforts of many different people. Among them are

- my field assistants: **Khaled Shahin, Craig Nichol, Rina Mackillop, Tracy Bellehumeur,** and **Melody Taylor**

- friends and acquaintances in Summerland: **Coral, Dave, and Dawn Knight, Yvonne and Vince Stelzer, Allen Wiens, Mark Siemens, Dr Tom Northcoat, Bernie Zebarth, George Redlich, Peter Rodd, Ron Mraz, Barry Cowan, Darrol Colgar, Malcolm Lane, Jacob Schulte, Peter Peto,** and **Tito Canape**

- technicians: **Roy Rodway, Doug Polson, Bryon Cranston,** and **Marc Baker, Bert Mueller, Susan Harper, Paula Parkinson, Maureen Soon, Richard Friedman** and **Herb Lans**

- UBC faculty and grad students: **Dr Ken Hall, Dr Marc Bustin, Dr Lee Groat, Dr Jim Mortensen, Dr Kristin Orians, Dr Mike Church,** and **Dr Les Lavkulich, Dr K Fletcher, Cari Deyell, Kristina Laretei, Rich Harris, Dr Chris Daughney, Raphael Wüst**

- other scientists outside the UBC community: **Doug Leighton, David Morley, Dr Fred Michel, Dr Richard Culbert, Dr Robert Zielinski** and **Dr James Otton**

- my thesis committee members: **Myles Parsons, Dr Leslie Smith, Dr Oldrich Hungr,** and **Dr Greg Dipple**

I would like to especially thank my advisor, **Dr Roger Beckie**, for his encouragement, great ideas, and ever-reliable open-door policy, and **Sebastien Tixier** for his unfailing love and understanding.

1 INTRODUCTION

The Prairie Flats uranium deposit in the Okanagan region of British Columbia is one of the largest and most studied of its kind. It is a secondary, surficial enrichment wherein organic-rich sediments have stripped uranium from discharging groundwaters. While studies of uranium concentrations in the host soils, crop cover, and surrounding surface waters and well waters have been carried out, no detailed investigation of the hydrogeology and groundwater geochemistry has ever been attempted. Therefore, questions regarding the origins of these uraniferous groundwaters, the mechanisms of uranium entrapment, and the history of the deposit remain unanswered.

This thesis addresses these questions using published hydrogeological and geochemical data from the surrounding region, as well as data collected in a field study at the Prairie Flats. The thesis is divided into eight chapters. Chapter 1 introduces the deposit and summarizes what is known about it to date. Chapters 2 and 3 place the deposit within a more regional geological and hydrogeological context. Chapter 2 maps out the bedrock geology and glacial deposits and highlights the most likely source rocks of uranium. Both the local and regional groundwater flow regimes are traced and characterized in Chapter 3. This information helps to form hypotheses on where the uranium came from, whether it be local or regional bedrock sources.

Chapter 4 presents the results of the hydrogeological and geochemical field study carried out by the author from July 1997 to May 1998. This began with the installation of a network of 13 piezometers across the flats, which provided a better picture of the hydrostratigraphy. Using the piezometers, hydraulic conductivities were measured and hydraulic heads were monitored at different times of year. Groundwater and surface water samples were also collected for chemical analysis.

Interpretation of this data is divided into two chapters. Chapter 5 identifies the source of Prairie Flats groundwaters based on their geochemical signature and presents a simplified

hydrologic budget for the site. It quantifies groundwater discharge into the deposit and uses this figure to comment on its formational history. Chapter 6 reviews aspects of uranium geochemistry that are relevant to the understanding of uranium mobility in natural environments. Chapter 7 applies these principles to the geochemical data collected on site, looking at adsorption, reductive precipitation, and evaporitive precipitation as likely uranium retention mechanisms. New theories explaining the spatial distribution of uranium are presented, as well as hypotheses regarding its potential remobilization.

1.1 SITE DESCRIPTION

This section summarizes what was already known about the Prairie Flats uranium deposit before the start of this thesis. The first section describes the site's general location, climate, hydrology, stratigraphy and uranium distribution. The second section presents current theories about the nature of uranium fixation, including the conclusions drawn from isotope analyses and bench-scale leaching experiments done on soil cores taken from the flats.

Terrain

The Prairie Flats deposit is located in the centre of the Summerland basin in the Okanagan region of BC. It underlies a hay field at the base of Prairie Valley, just south of the Summerland town centre (see **Figure 1-1**). It is surrounded by a number of small mountains: Cartwright Mountain to the northwest, Mount Conkle to the south and Giant's Head to the east. This topographic setting prompted Culbert and Leighton (1988) to identify it as a "collector basin" type of uranium deposit, where "upwelling groundwaters, surface waters, and runoff meet in a marshy bowl." The flats were formerly a marshland up until the end of this century when drainage ditches were dug across it to drain the land for cultivation (personal communication
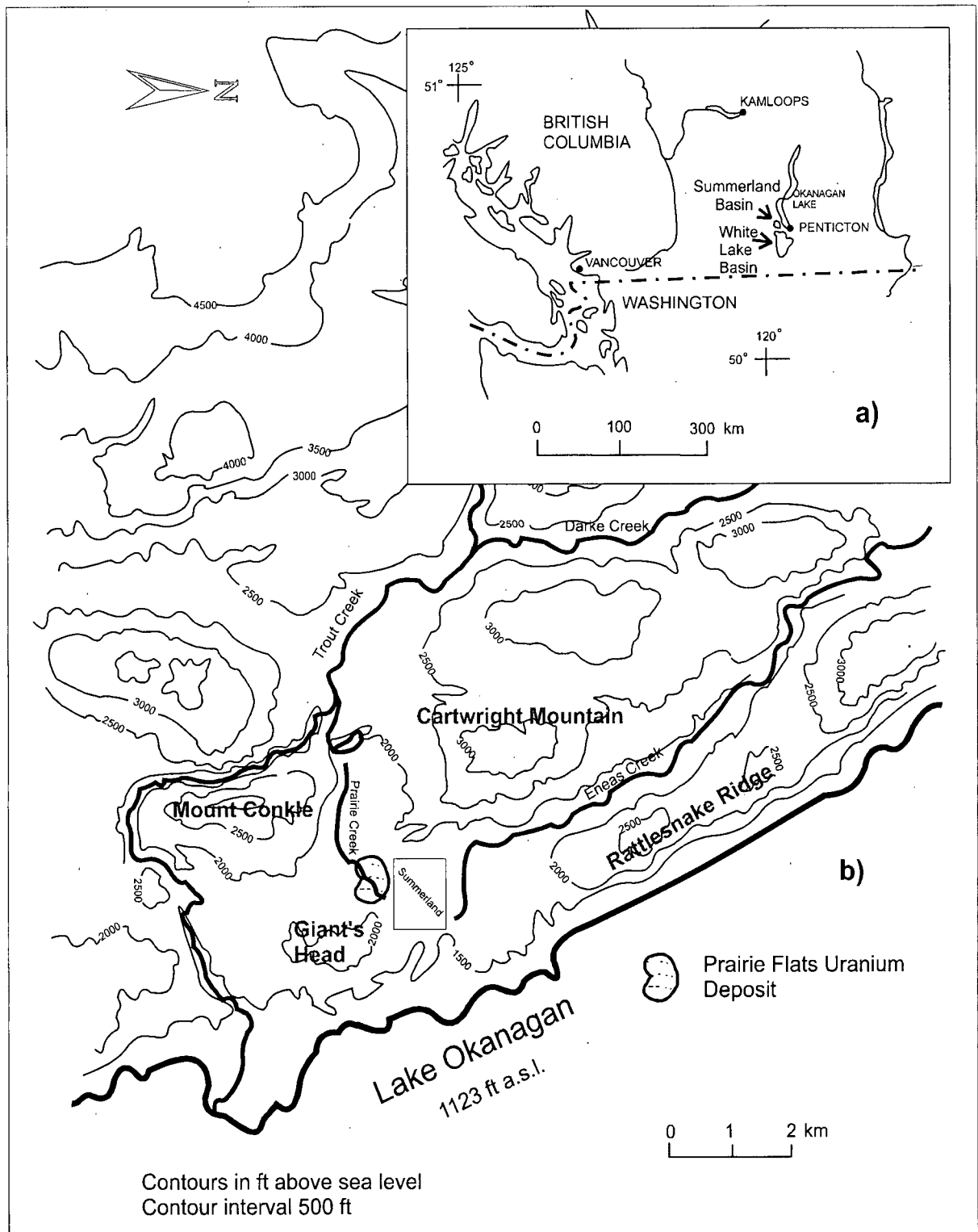
Figure 1-1 Location of the (a) Summerland and White Lake basins and (b) Prairie Flats uranium deposit

with the Summerland Museum, 1998). These drainage ditches direct Prairie Creek across the flats, as is illustrated in **Figure 1-2**.
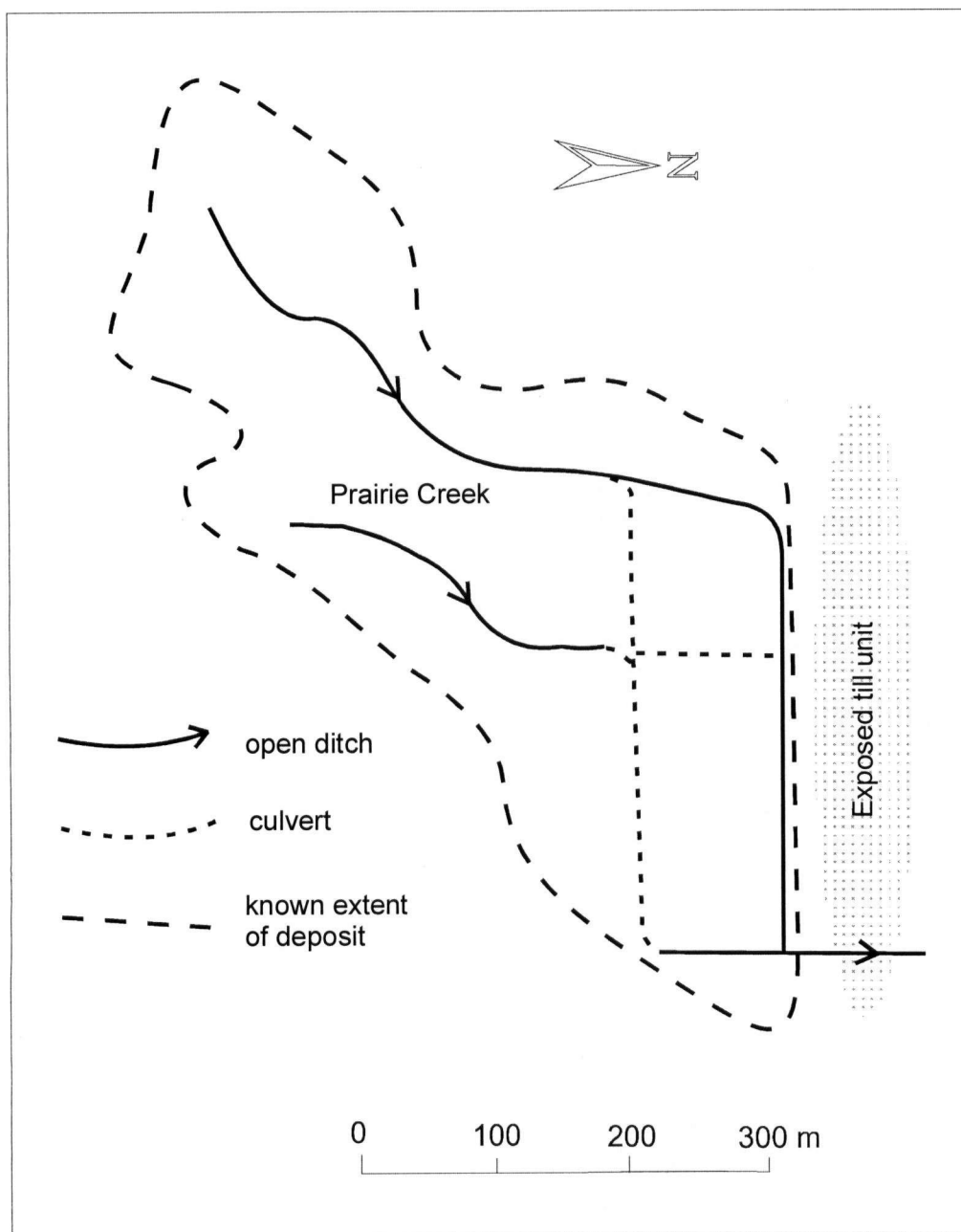
Figure 1-2 Site map showing the known extent of the Prairie Flats uranium deposit

Climate

The climate of the Summerland area is generally arid with hot summers and cold winters. Mean annual precipitation, including snow and rain, is around 300 mm (Piteau & Associates, 1984). Monthly precipitation values measured at the Summerland Agricultural Research Station in 1995 were highest in late spring and mid winter, and lowest in late winter and mid fall, as shown in **Figure 1-3**. Average temperatures are lowest in January (-2.7 °C) and highest in July (20.9 °C) (Piteau & Associates, 1984). The combination of low rainfall rates, warm summer temperatures, and high sun exposure results in a high potential evapotranspiration rate of approximately 652 mm per year (Piteau & Associates, 1984). Potential evapotranspiration rate is the amount of water that would be removed from the land surface by evaporation and transpiration processes if sufficient water were available in the soil to meet the demand.
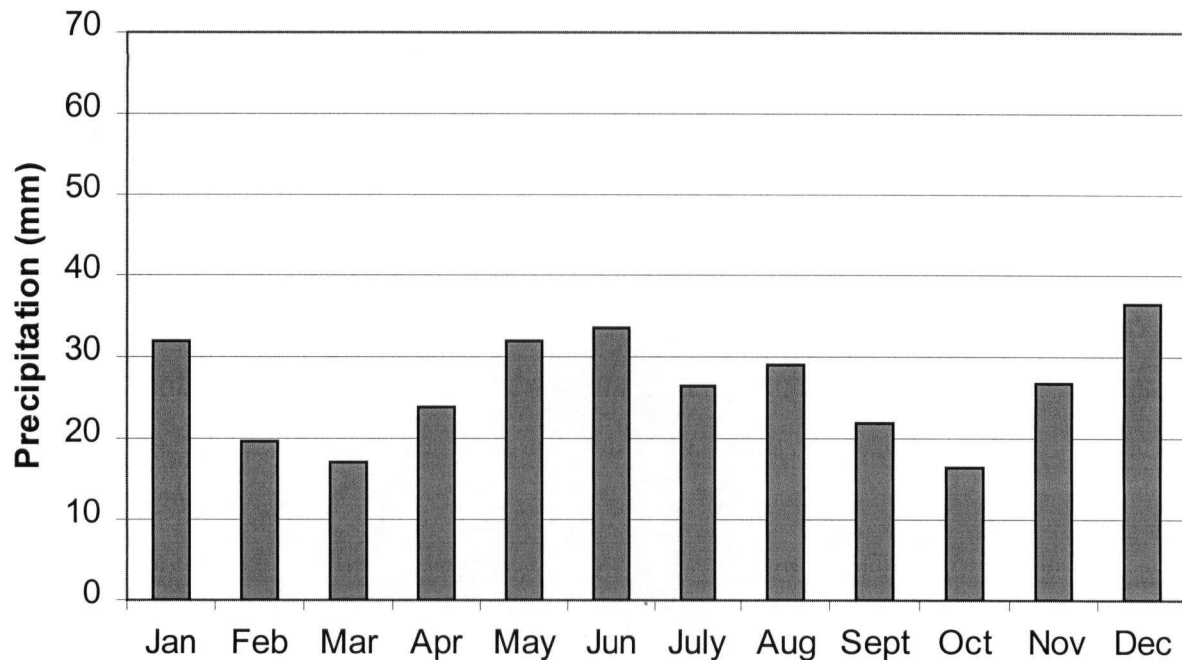
Figure 1-3 Histogram of precipitation data measured at the Summerland Agricultural Research Station, 1995.

Stratigraphy

The near-surface stratigraphy of the flats consists of four principal lithologic units: peat, glaciolacustrine silty clay, glaciofluvial till, followed by bedrock. The peat unit is a highly-organic mixture of fine silts and decomposing plant material that accumulated before the marshland was drained for cultivation. The silty clay occurs either as lenses within the peat or as a continuous unit below the peat. It was deposited by a lake that covered most of Prairie valley during the late stages of glacial retreat (Nasmith, 1962; Kvill, 1976), which is explained further in section 2.3. The collective thickness of the peat and silty clay units ranges from roughly 0.5 m to 3 m across the flats. It is thickest on the south end of the deposit and thins out to the north, exposing the underlying till unit (see **Figure 1-2**).

The till unit is probably an extension of the "kame terrace and meltwater channel" deposit (Nasmith, 1962) bordering the north side of the deposit (see section 2.3). Culbert (1980) proposes that this deposit may have been the original barrier which impounded the marsh whose peat now underlies the flats. The till consists of sand and gravel and occasional pebbles, fining downwards. It is called "till" because of its variety of grain sizes, and should not be thought of as hydraulically impermeable, as is often the nature of till. It is estimated to be less than 2 metres thick since drilling records for a well bordering the flats log bedrock at a depth of seven feet (Ministry of Environment, Lands and Parks B.C., 1998).

Hydraulic conductivity measurements of fractured bedrock in the Summerland basin and Trapping Creek Basin (near Kelowna) suggest that the bedrock underlying the till unit is relatively less permeable. In-situ packer testing in a test drillhole for the Summerset Inn on Giant's Head (Golder Associates, 1980) gave a 10^{-10} to 10^{-7} m/s range in hydraulic conductivity at depths of less than 10m. Lawson's (1968) estimates of hydraulic conductivity in the Trapping Creek basin were between 10^{-9} and 10^{-5} m/s at less than 30 metres' depth. Based on this information, Piteau & Associates assigned bulk hydraulic

conductivity values on the order of 10^{-8} m/s to bedrock in a regional groundwater flow model of the Summerland basin.

Uranium Distribution

Culbert (1980) also states that "it is very unusual to find so thin a topsoil over apparently well-drained till which has concentrated uranium to the extent shown here." In 1980, D.G. Leighton & Associates made approximately 35 auger holes across Prairie Flats and sampled these at every half-meter depth. Soil uranium concentrations were reported as pounds of uranium oxide (as U_3O_8) per square metre, and are contoured in plan view in **Figure 1-4a**. In total, approximately 250 000 kg of uranium as U_3O_8 are estimated to underlie the flats (Culbert, 1979). The formula U_3O_8 is used as a stoichiometric quantity, and does not describe the actual form of uranium. Church et al. (1990) also found the uranium to be most concentrated in the east-central part of the deposit.

In vertical profile (see **Figure 1-4b**), the highest concentrations of uranium were found within the top half-metre of soil, except near the southern edge of the site where it is concentrated at a few metres depth (Culbert, 1980). Similarly, a more recent soil survey measured highest uranium concentrations in the 8 to 16-inch depth interval, and a few at greater depth (Ministry of Health B.C., 1981).

1.2   DEPOSITIONAL CONTROLS

The Prairie Flats uranium deposit is a post-glacial, secondary deposit resulting from the mixing of uraniferous groundwaters with organic-rich sediments. Levinson et al. (1984) measured $^{234}U/^{230}Th$ ratios on soil cores taken from the flats and used these to estimate the age of the deposit. This method assumes that the ^{230}Th nuclide is created in-situ by the decay of ^{234}U, therefore the higher the $^{234}U/^{230}Th$ ratio, the younger the deposit. Ages were found to increase with depth (see **Figure 1-5a**), and were everywhere less than 10 000 years, calculated from the $^{234}U/^{230}Th$ ratio and half life of ^{234}U. Because the uranium was deposited recently enough so as not to attain equilibrium with it's shorter-lived

daughter products, it is not highly radioactive. Many other post-glacial uranium deposits exist in the Okanagan region of BC and the northwestern United States and are further described in Culbert et al. (1984) and Culbert and Leighton (1988).
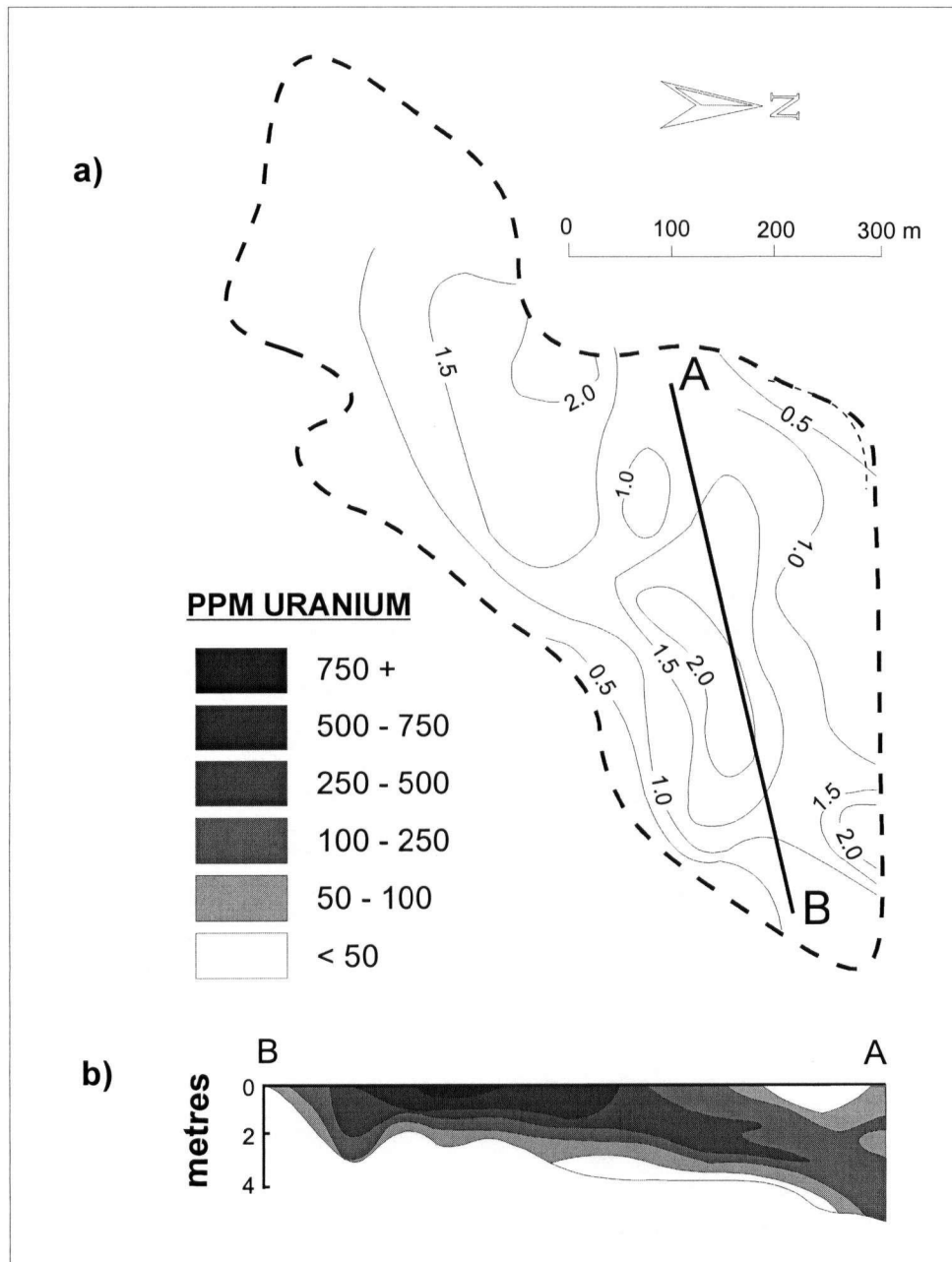
Figure 1-4 (a) Plan view of uranium distribution in uraniferous layer in lbs U_3O_8/m^2, modified from Culbert (1979), and (b) Uranium distribution in cross-section, modified from Culbert and Leighton (1988)

The patchy uranium distribution at the Prairie Flats suggests a complex combination of depositional controls, of which topography, evaporation, and adsorption onto organics are thought to dominate (Culbert et al, 1984). Levinson et al. (1984) found uranium concentrations to correlate very closely to the organic contents of the soils (as is measured by Loss on Ignition or LOI in **Figure 1-5b**) which was reaffirmed later by Church et al. (1991). Levinson et al. (1984) believe that "the uranium was initially concentrated in the surface layers and, with subsequent burial and compaction, has not been removed from the organic matter." Therefore, they proposed that adsorption is the major process of uranium concentration, minimizing but not eliminating the role of evaporation.

In addition to adsorption, reductive precipitation of uranium is also likely occurring at the flats, however the actual mineral form has yet to be identified. Between 40 and 60% of the uranium is in an unstable, remobilizable form, based on bench-scale leaching experiments of two soil samples (Culbert, 1980). This fraction is retained by adsorption onto organics, while the remaining fraction is held by "precipitation as a micron-sized four-valency mineral, probably uraninite ($UO_{2(c)}$)" (Culbert, 1980).

Because such a significant portion of the uranium is loosely-held, it could be remobilized under the right geochemical conditions. Culbert (1980) stated that re-release of the uranium could be initiated by as little as one unit increase in pH of the waters in contact with the peat. Culbert (1980c) also states that "if [the uranium] was combined with an early spread of nitrate fertilizer, then conditions could exist where this loosely-held uranium would be naturally eluted and would join the drainage runoff, and would report into the lake, or even into the local water supplies." Therefore although the uranium does not impose a radioactive health hazard, it may threaten water quality if land-use practices in and around Prairie valley are not carefully managed.
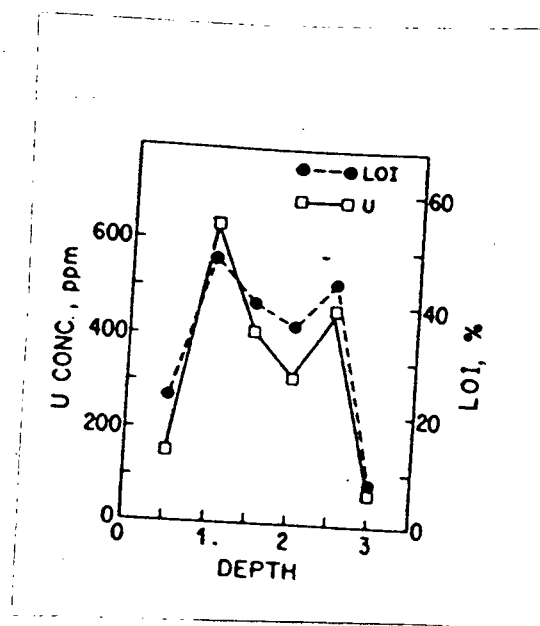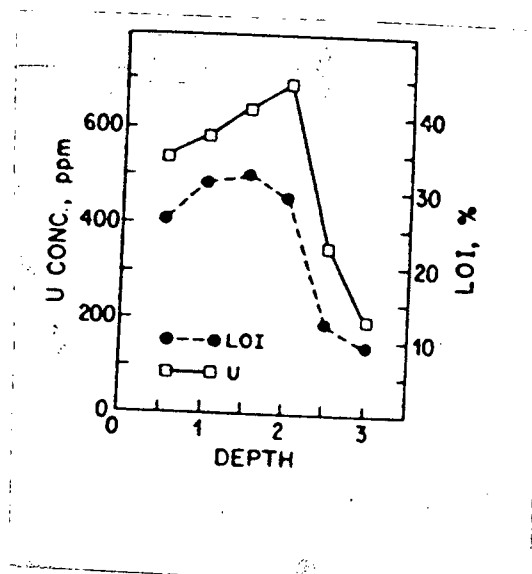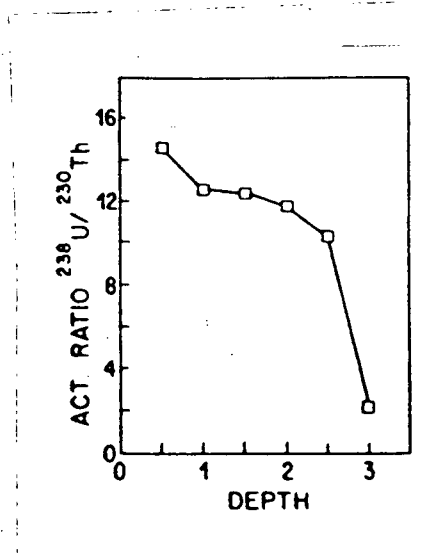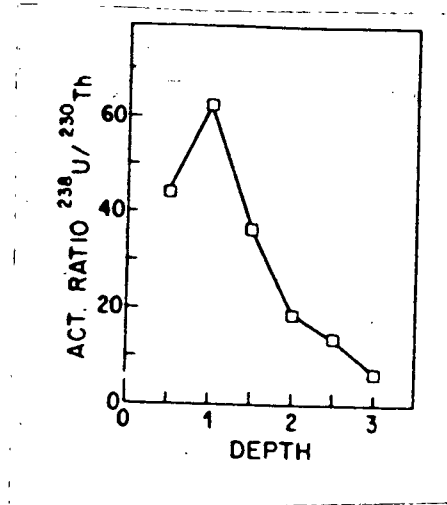
Figure 1-5 Variations with depth of (a) uranium content and organic content (measured by Loss on Ignition, or LOI) and (b) $^{238}U/^{230}Th$ activity ratio, for two peat core samples taken from Prairie Flats, from Levinson et al. (1984)

2 REGIONAL GEOLOGY

This chapter examines the bedrock and surficial geology of the Summerland basin and identifies possible source rocks of uranium. The geology and hydrogeology of the White Lake basin is also reviewed because of its similarity to the Summerland basin. Due to a lack of well data in the Summerland basin, well data collected in the White Lake basin will be used in upcoming chapters to make inferences about the Summerland basin groundwater regime.

2.1   BEDROCK GEOLOGY

The Prairie Flats deposit lies in the middle of the Summerland basin, which covers approximately 28 square kilometers between Okanagan Lake to the east and the Summerland reservoir to the west (see **Figure 2-1**). According to Church (1973), crustal extension along the Okanagan valley 50 million years ago caused rift and graben development which tilted and folded these rocks into an elliptical 5 by 10 kilometre synclinal trough. They have also undergone significant fabric loosening by folding and faulting. Down-faulted volcanic beds meet Giant's Head along the Summerland fault, which defines the southern boundary of the Summerland basin. Other major faults run approximately north-south along Eneas and Darke Creek Valleys **(Figure 1-1)**.

Both the Summerland and White Lake basins are made up of Tertiary volcanic and sedimentary rocks overlying pre-Tertiary basement granites. The Tertiary volcanic rocks belong to the "Penticton Tertiary Outlier," (Jessop and Church, 1991), which is believed to be a remnant of a continuous belt of volcanic rocks passing through central Washington and south-central BC (Lewis, 1984). Cross sections of both the Summerland basin and White Lake basin are given in **Figures 2-3** and **2-4**, and their approximate locations in **Figure 2-2**.

EOCENE

WHITE LAKE FORMATION

MOSTLY POLYMICTIC VOLCANIC CON-
GLOMERATE AND SANDSTONE WITH
MINOR CARCONACEOUS SEAMS

MARAMA FORMATION

DACITE LAVA AND BRECCIA

MARRON FORMATION

NIMPIT LAKE MEMBER: TAN TRACHYTE
AND TRACHYANDESITE LAVA AND
ASH FLOWS

KITLEY LAKE MEMBER: MOSTLY FELD-
SPATHIC TRACHYANDESITE LAVA

YELLOW LAKE MEMBER: RHOMB-POR-
PHYRY SIL

KETTLE RIVER FORMATION

MOSTLY GRANITE BOULDER CONGLOM-
ERATE AND BRECCIA

PENTICTON GROUP

PRE-TERTIARY

GRANITIC BASEMENT ROCKS

5502000N

UTM

303000E

RATTLESNAKE RIDGE

ENEAS CREEK

SUMMERLAND

HWY 97

OKANAGAN LAKE

FIG.

W ——————————— E

PRAIRIE FLATS

RESERVOIR

GIANTS HEAD

N

E

TROUT CR.

SUMMERLAND

FAULT

RAILWAY

49°33'
119°44'

	Miles	2
0		

	Km	3
0		

Figure 2-1 Geology of the Summerland basin, from Jessop and Church (1991)
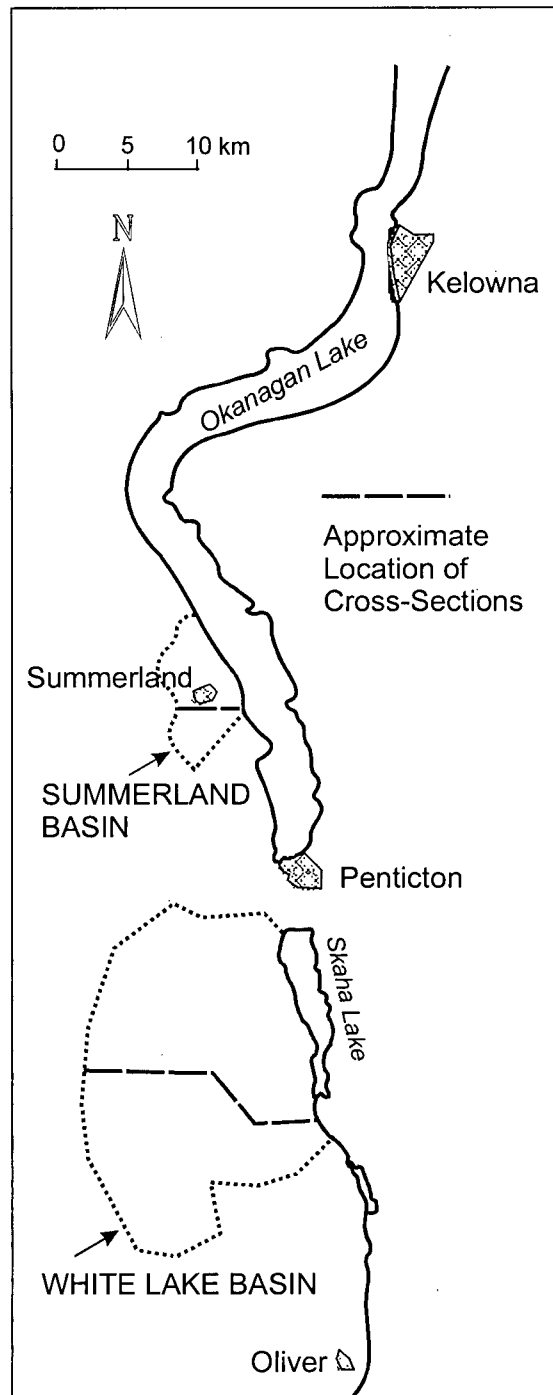
Figure 2-2 Location of the Summerland and White Lake basins, showing approximate locations of cross-sections

13
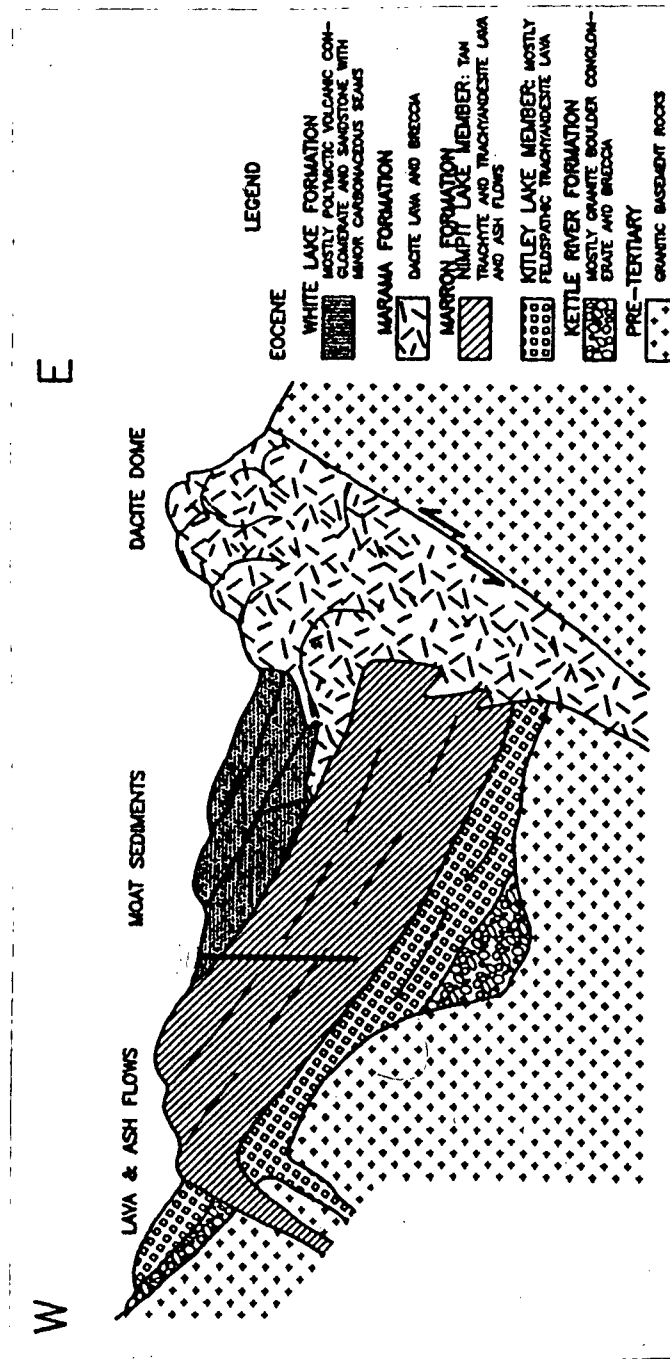
Figure 2-3 Diagrammatic cross-section of the Summerland basin, from Jessop and Church (1991)

14
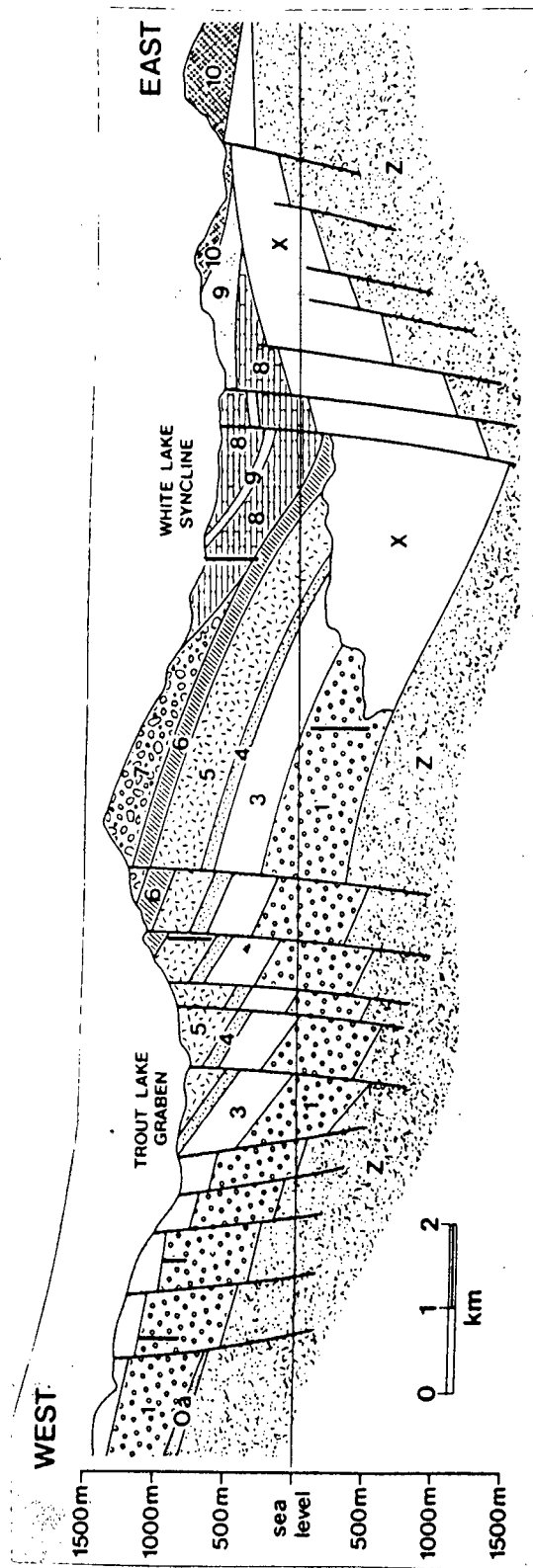
Figure 2-4 Cross-section of the White Lake basin, from Church (1973). Symbols: Z = pre-Tertiary basement rocks; O= Springbrook Formation; X = Undivided Marron Formation; 1= Yellow Lake Member, Marron Formation; 3 = Kitley Lake Member, Marron Formation; 5 = Nimpit Lake Member, Marron Formation; 6 = Park Rill Member, Marron Formation; 7 = Marama Formation; 8 = volcanic conglomerate, sandstones, and shales, White Lake Formation; 0 = mostly volcanic breccias, White Lake Formation; 10 = Skaha Formation.

15

The Penticton Tertiary Outlier consists of sedimentary rocks belonging to the White Lake Formation overlying an alternating series of lava flows and ash flows belonging to the Marama and Marron Formations. At the base of these is the Kettle River Formation, consisting of conglomerates and breccia. The total thickness of this assemblage is greater than 1000 metres (Jessop and Church, 1991). Underlying the Penticton Tertiary Outlier are the pre-Tertiary basement granites originating from two periods of intrusions. The oldest is Nelson intrusive series (Little, 1961), followed by the Okanagan Highlands Intrusive Complex (Boyle, 1982).

Detailed descriptions of the lithologies of the Tertiary and pre-Tertiary rocks are listed from oldest to youngest in **Table 2-1**. This is a compilation of the works of Church (1982), Little (1961), and Boyle (1982).

Table 2-1 Bedrock lithologies in the Summerland and White Lake basins

GEOLOGIC PERIOD	NAME	LITHOLOGIES
TERTIARY	PENTICTON TERTIARY OUTLIER (White Lake Basin)	
	White Lake Formation	polymictic volcanic conglomerate and sandstone with carbonaceous seams, shale
	Marama Formation	dome-forming dacite lava and breccias
	Marron Formation: Yellow Lake member Kitley Lake member Nimpit Lake member	rhomb-porphyry sill feldspathic trachyandesite lavas tan trachyte and trachyandesite lava and ash flows
	Kettle River Formation	granite boulder conglomerates and breccias
PRE-TERTIARY (MESOZOIC) Late Cretaceous-Paleocene	OKANAGAN HIGHLANDS INTRUSIVE COMPLEX	granitoids: quartz monzonite, porphyritic granite, pegmatite
Jurassic-Early Cretaceous	NELSON INTRUSIONS	granitoids: granodiorite, diorite, granite, monzonite

2.2   SOURCES OF URANIUM

It is generally believed that the uranium found in surficial uranium deposits dotting the Okanagan Valley is coming from diffuse sources, rather than a single weathering ore body, as stated by Culbert (1980b):

".. originally we viewed [the deposits] at least to a major extent as so-called geochemical anomalies, and we tried to follow them up until we found that there was just so many of them, that it wasn't necessarily any primary deposit from which they were coming."

Therefore, knowledge of the weatherability and uranium-content of bedrock in this region helps to highlight which rocks are the most likely sources.

Pre-Tertiary Granites

In their investigation of surficial uranium deposits in the Okanagan area, Culbert et al. (1984) state that "virtually all deposits always occur in areas underlain by intrusive rocks varying from intermediate to felsic in composition." The Okanagan Highlands Intrusive Complex has the highest labile (ie. leachable) uranium content of all the intrusive rocks in the Okanagan region (Boyle, 1982). These rocks have relatively high carbon contents (Boyle, 1982), which enhances uranium leaching by forming highly soluble uranyl-carbonate complexes.

Tertiary Volcanics and Sedimentary Rocks

Another potential source of uranium is the Tertiary Volcanics, particularly the Nimpit lake member of the Marron formation. This ash flow sequence has an average uranium content of 6 ppm, and consists of partially welded fragments of potassium-rich glass that can be easily devitrified (Church, 1979; Zielinski, 1981). Furthermore, the Nimpit Lake member is widely exposed and stratigraphically thick throughout the Summerland basin. All of the cuttings from a 715 metre deep borehole (EPB/GSC 495) just outside of

Summerland (see **Figure 3-1**) were identified as Nimpit Lake volcanics (Jessop and Church, 1991).

2.3   SURFICIAL GEOLOGY

The surficial geology of the Summerland basin consists mainly of glaciofluvial deposits, glaciolacustrine deposits, and exposed bedrock. Those deposits underlying or adjacent to the Prairie Flats deposit are shown in **Figure 2-5**.

Glacial activity which shaped the landscape of the Summerland basin has been described in detail by Nasmith (1962) and Kvill (1976). Nasmith has divided the deglaciation period into 4 distinct stages. During the first stage, a thick ice sheet covered all of Prairie Valley, the town of Summerland, and the main valley that currently hosts Lake Okanagan. During the next stage, the west margin of this ice sheet started to retreat, leaving a lobe of ice extending up Prairie Valley as far as the Summerland reservoir. This ice lobe retreated further east in stage three, and meltwaters obstructed by the local topography ponded to form a proglacial lake covering Summerland and the base of Prairie Valley. During the last stage of glacial retreat, the proglacial lake disappeared and ice sheet in the main valley melted to yield the present-day Lake Okanagan.

In the vicinity of the Prairie Flats there are two classes of glacial deposits: glaciofluvial sands and gravels and glaciolacustrine silts and clays. Each is described further in the following paragraphs.

At the top of Prairie Valley is a series of steep-sided sediment ridges between which the Summerland reservoir currently sits. These consist primarily of coarse sand with pebble-sized inclusions. Nasmith (1962) identifies the ridges as a moraine which was deposited directly by the ice lobe that occupied Prairie Valley. Evidence of sorting and stratification in this deposit led Kvill (1976) to call it a kame deposit, which implies that the depositional medium was meltwater, not ice. Therefore, this is a glaciofluvial deposit.

Legend:

- Pre-Tertiary Granites
- Tertiary Volcanics and Sedimentary Rocks
- Glaciolacustrine deposits
- Glaciofluvial deposits
  - 1 kame deposit
  - 2 kame terrace and meltwater channel
  - 3 fan or outwash terrace
- Prairie Flats Uranium Deposit
- Summerland Reservoir
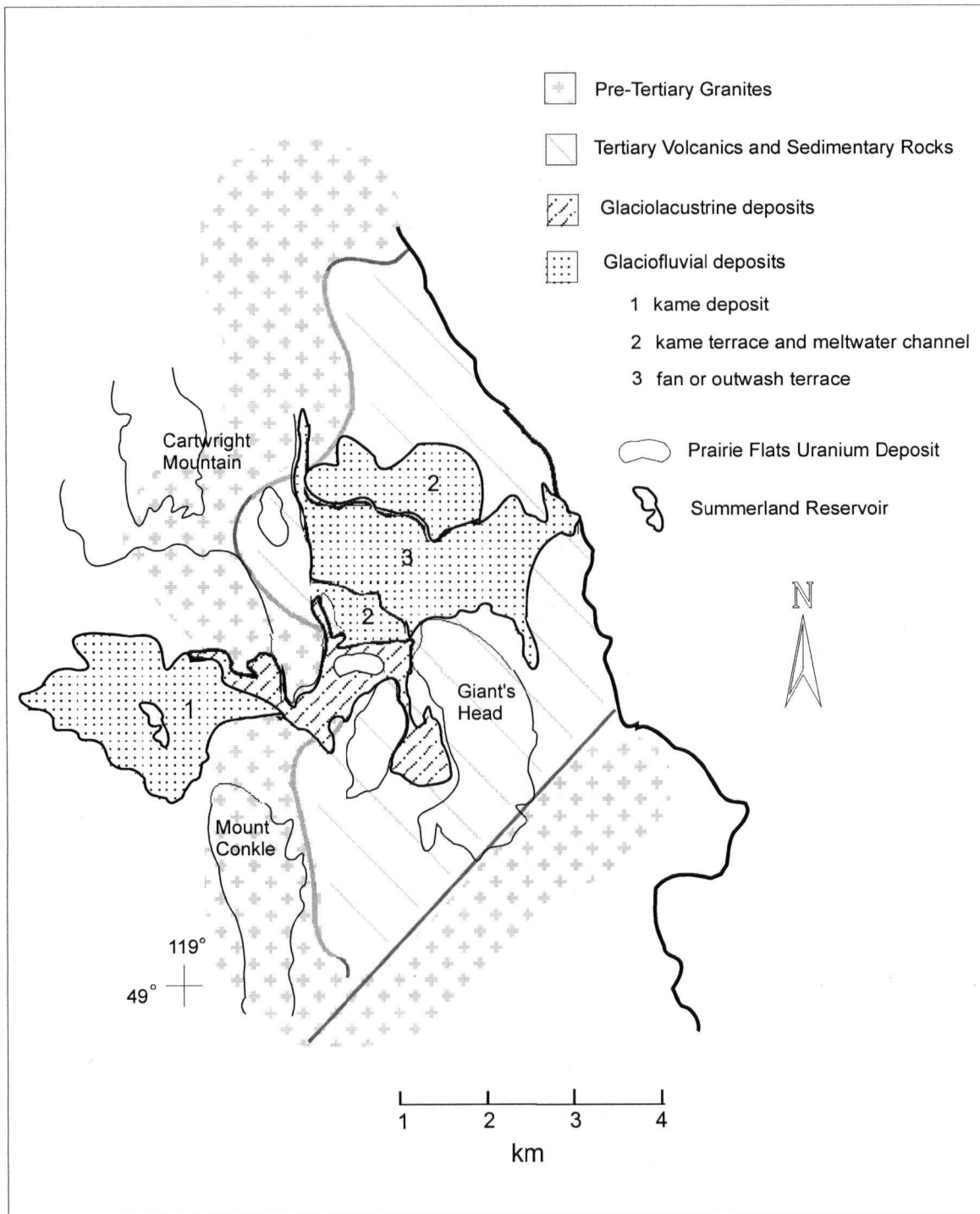
Figure 2-5 Surficial geology surrounding the Prairie Flats, modified from Nasmith (1962) and Kvill (1976)

19

The rest of Prairie valley including the Prairie Flats is blanketed by a thin layer of glaciolacustrine deposits. Nearby bedrock outcrops and a slightly irregular surface morphology in this area suggest that bedrock is not far below ground surface (Kvill, 1976). These deposits consist of silt and clay that was deposited by the proglacial lake that occupied this area during stage three of deglaciation.

Extending north of the Prairie Flats to the outlet of Eneas Creek (Garnet Valley) is a broad, flat apron of well-rounded, moderately sorted and stratified sands and gravels (Kvill, 1976). Kvill (1976) identifies it as a "fan," which is a glaciofluvial/alluvial deposit formed when meltwater streams draining upland areas emerge into a larger valley and drop their sediment load in response to the decrease in gradient and widening of the valley. This deposit formed during the last stage of deglaciation after the drainage of the proglacial lake covering Prairie Valley.

Nasmith (1962), however, refers to this "fan" as an "outwash terrace" and places a "kame terrace and meltwater channel" deposit on either side of it (see **Figure 2-5**). A kame terrace is material that was deposited along the floor of streams occupying the space between a stagnant ice lobe and a valley wall. Therefore, these "kame terrace and meltwater channel" deposits were created while blocks of ice were still present at base of Garnet Valley and Prairie Valley, and before the glaciolacustrine silt and clay deposits were complete. Of particular interest is the kame terrace and meltwater channel deposit adjacent to the north side of the Prairie Flats. This may be the same "till or outwash barrier" referred to by Culbert (1980) (see Chapter 1).

In more recent times, a considerable thickness of peat has accumulated on top of the silt and clay deposits covering the Prairie Flats. Most of this peat accumulated when the Prairie flats was a marshland, receiving water from natural groundwater drainage and runoff coming down Prairie Valley. In the later part of this century, it was drained for cultivation by means of drainage ditches which currently relay Prairie Creek across it (personal communication with Summerland Museum, 1998). To the author's knowledge, no dating of this peat has ever been done, however Levinson (1984) analyzed the

^{238}U/^{230}Th activity ratios of the uranium on two peat cores and calculated ages of the uranium ranging from approximately 8000 years (0.5 m depth) to 13000 years (2.5 m) for one core and 1900 (1.0 m) to 18000 years (3.0 m depth) for the other. Still, it is impossible to tell the age of the peat since the accumulation of peat and uranium may not have been coincident.

The above history explains the origins of the uppermost stratigraphic units of the Prairie Flats, which are referred to as "peat," "clay," and "till" throughout this thesis. The till unit is glaciofluvial material which was deposited by the lobe of ice that once extended up Prairie Valley. It is probably an extension of Nasmith's "kame terrace and meltwater channel deposit" on the north side of the flats, which precedes the glaciolacustrine silts and clays. Its western extent up Prairie Valley or possible connection to Kvill's "kame" deposit around the Summerland reservoir remain unclear. Further borehole drilling in and around the flats would help to clarify the origin of the till. The "clay" unit comes from the pro-glacial lake and the "peat" unit from more recent detrital accumulation.

SUMMARY

The Prairie Flats lie in the middle of the Summerland basin, which consists of faulted lava and ash flow sequences on top of granitic basement rocks. The volcanic rocks are a remnant of the Penticton Tertiary Outlier, which also underlies the White Lake basin. Both the Tertiary volcanic rocks and pre-Tertiary granites are potential sources of uranium to the Prairie Flats. During glacial retreat, coarse-grained glaciofluvial material was deposited at the top of Prairie Valley and just north of Prairie Flats, and silts and clays were deposited under a meltwater lake. The uraniferous peats sit on top of these silts and clays and the underlying till is connected to the glaciofluvial deposits.

3 REGIONAL AND LOCAL GROUNDWATER SYSTEMS

The Prairie Flats deposit was created by discharging uraniferous groundwaters, however the origins of these groundwaters, whether they be regional or local, remains unclear. This chapter defines regional and local groundwaters in terms of their flow paths and aqueous geochemistry. Evidence is taken from studies carried out in both the Summerland and White Lake basins, which is reasonable given their geological similarity.

3.1 REGIONAL GROUNDWATER FLOW

For this thesis, the term "regional" is used for groundwaters recharged several kilometers outside of the Summerland topographic basin and which descend to depths of over 100m in the bedrock. They either discharge within the basin or into Lake Okanagan (see **Figure 3-1a**). To discharge within the basin, they would have to migrate up through the thick sequence of Tertiary volcanics that overlie the basement granites (see **Figure 3-1b**).

Boyle (1982) believes that regional groundwaters percolating in the Okanagan Highlands Intrusive Complex (pre-Tertiary granites) are discharging along major fault zones. These basement granites are an ideal setting for a deep-seated, regional groundwater flow regime owing to numerous interconnected faults and fracture systems created by tectonic and intrusive activity (Boyle, 1982). Water samples taken from creeks and boreholes along these fault zones were highly uraniferous (10 to 50 µg/L), enriched in carbonate (150 to 400 mg/L), and slightly oxidizing (dissolved oxygen 4 to 6 mg/L), which Boyle (1982) assumes to be representative of these regional groundwaters. Such high dissolved oxygen concentrations have been reported in other granitic environments (Leenheer et al., 1974), and can be sustained in the basement rocks of the Summerland basin because of the scarce presence of reductants such as organic matter and sulfide (Boyle, 1982).
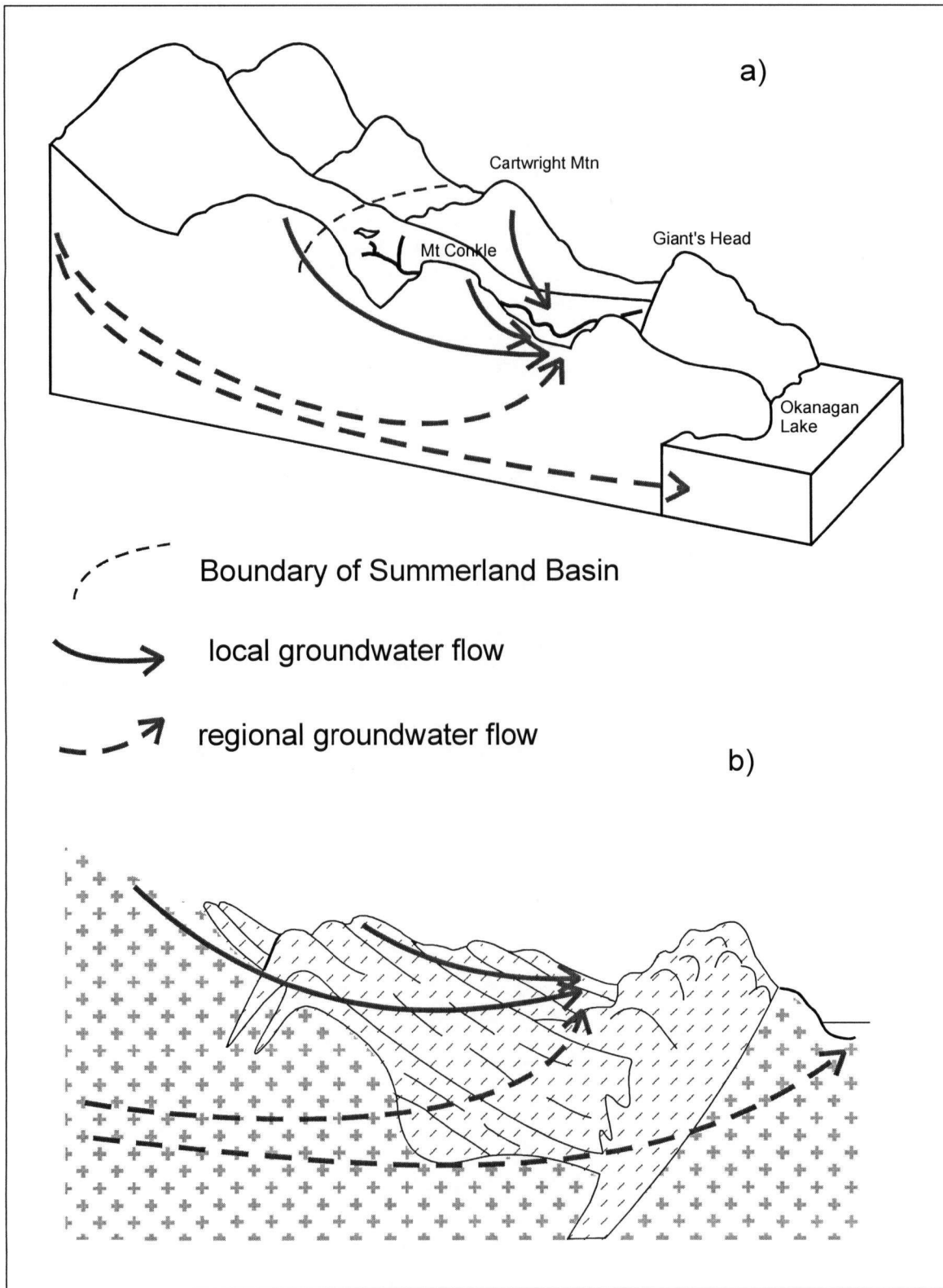
Figure 3-1 Regional and local groundwater flow paths in (a) aerial view and (b) geological cross-section, modified from Jessop and Church, 1991

23

Increasing uranium concentrations with distance along Eneas and Darke creeks, which overlie two of these fault zones, support Boyle's hypothesis. Water samples taken from Darke creek and nearby boreholes show increasing uranium concentrations and decreasing tritium counts in the downstream direction. This suggests that older (> 25 years) groundwaters flowing southward along the fault zone are discharging in the downstream sections of the creek. Sampling of Eneas Creek (Ministry of Health B.C. and Ministry of Energy, Mines and Petroleum Resources B.C., 1981) also found a consistent increase in uranium concentration in the downstream direction, doubling between the Garnet Lake spillway and a site 10km downstream (Ministry of Health B.C. and Ministry of Energy, Mines and Petroleum Resources B.C., 1980 and 1981). An increase in concentration of this magnitude cannot be caused by evaporation alone, but is likely due to the discharge of increasingly uranium-enriched groundwaters in the downstream direction.

On the contrary, Piteau and Associates (1984) believed that shallow (10 to 50m deep) groundwater flow systems are recharged in the local upland areas and discharge into Darke, Eneas and Trout creeks; while deeper flow systems are recharged several to tens of kilometers away and discharge into Lake Okanagan or along the lake shore. If deep groundwaters are discharging into these creeks, Piteau and Associates (1984) claim that dilution by shallow groundwaters prevents their chemical identification. They estimate that only 5% of the total groundwater recharge in the Summerland basin goes into the deep, regional flow system, which is comparable to Lawson's (1968) estimate of 2% in the Trapping Creek Basin just south of Kelowna.

Deep boreholes in the Tertiary volcanics of the Summerland basin provide limited evidence of regional groundwater flow. Two boreholes drilled in the White Lake formation (depth on the order of 100m) are artesian and are still flowing today (personal communication with driller, Ron Mraz, 1997). These are labeled Mraz well and Mraz well #2 on **Figure 3-2**. However, the White Lake formation would make a poor regional

24
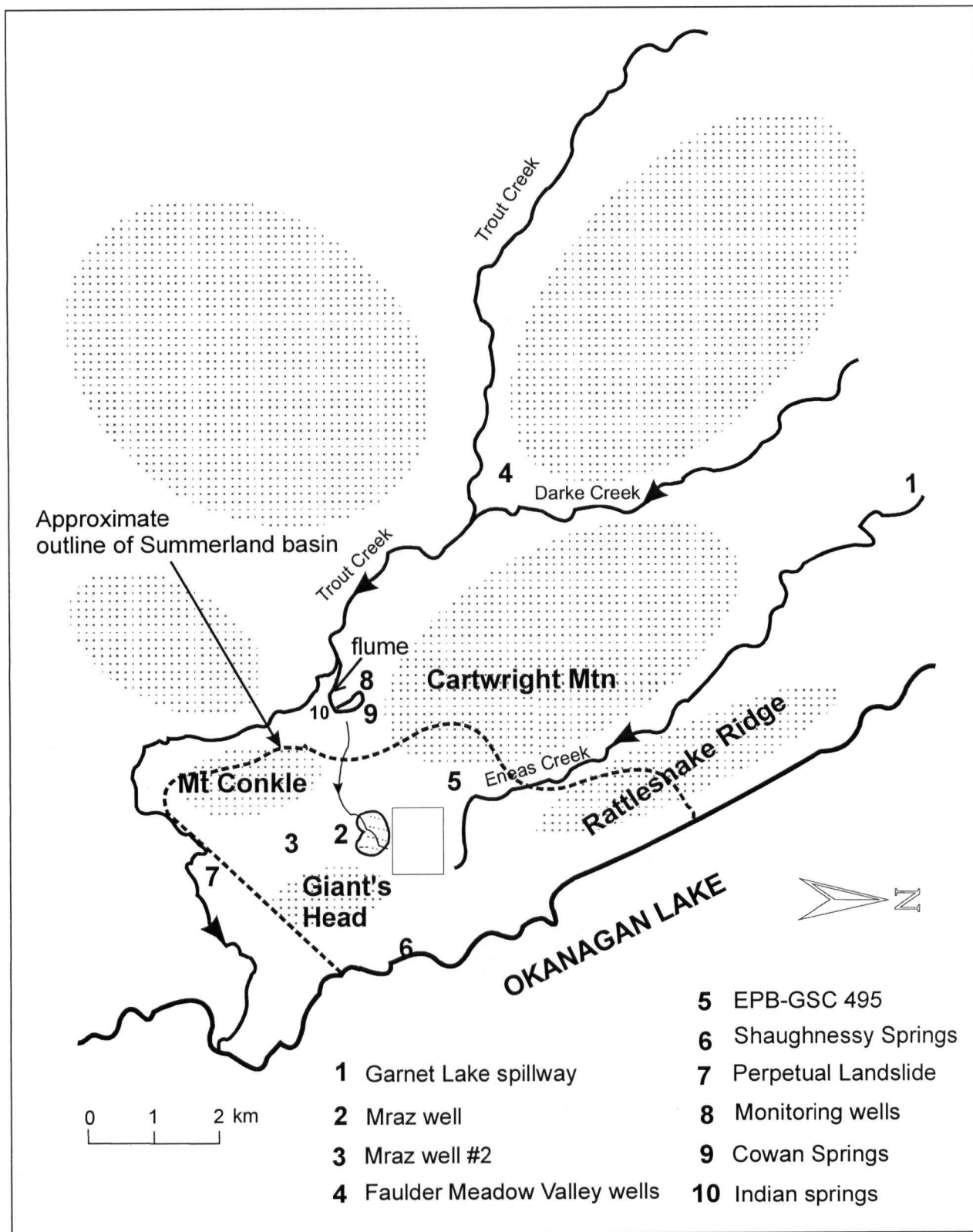
Figure 3-2 Hydrogeological features in the Summerland basin

Approximate
outline of Summerland basin

Trout Creek

Darke Creek

1

Trout Creek

flume

8

10 9

Cartwright Mtn

Mt Conkle

5 Eneas Creek

Rattlesnake Ridge

3 2

Giant's
Head

7

6

OKANAGAN LAKE

N

0   1   2 km

1 Garnet Lake spillway
2 Mraz well
3 Mraz well #2
4 Faulder Meadow Valley wells

5 EPB-GSC 495
6 Shaughnessy Springs
7 Perpetual Landslide
8 Monitoring wells
9 Cowan Springs
10 Indian springs

25

aquifer since it is discontinuous and local in extent (Grant and Michel, 1983). In 1990, a 715m deep well (EPB-GSC 495) was drilled just outside of Summerland in hopes of locating a geothermal groundwater reservoir in the brecciated fault zones of the Kettle River formation (Jessop and Church, 1991). Although brief flows of groundwater and evidence of hydrothermal alteration were found at depth, no hot water reservoir was located.

As part of a geothermal exploration program in the White Lake Basin, Lewis (1984) tested five deep boreholes (on the order of 400m deep) completed in the Tertiary volcanics. Among these are two artesian boreholes, the P-Well and 78-4, which are 390m and 450m deep, respectively. Measured temperature profiles indicate upward-flowing waters, probably recharged at White Lake and moving up-dip to the west (Lewis, 1984). No large reservoir of hot water was identified, and large differences in water flows and heat flows between boreholes was noted. Therefore these groundwaters appear to be isolated and structurally controlled, confined to fractures sets, faults, the tops of lava flows, and interbeds of conglomerates and sands (Church and Jessop, 1991, Lewis, 1984).

Geochemical sampling of groundwater in these and other deep boreholes (> 100m) in the White Lake Basin have been carried out by Grant and Michel (1983) and by Piteau & Associates (1984), and are plotted in **Figure 3-3**. Both parties found the groundwater to be older (greater than 30 yrs) and more chemically evolved, based on their isotope ratios, Na-Cl chemistries and high dissolved solids concentrations. Water from 78-4 had elevated temperatures (11-14 °C) and a measured Eh of -210 mV, which is typical of waters isolated from atmospheric influence (Piteau & Associates, 1984). Grant and Michel (1983) found that the P-Well, 78-4, and three other bedrock wells had very different chemistries, leading them to conclude that deep bedrock groundwaters reflect local rock-water interactions and flow very slowly or not at all. Because of geological similarity, the behaviour of deep-seated, regional groundwaters in the Summerland basin is inferred to be similar to that of the White Lake basin.
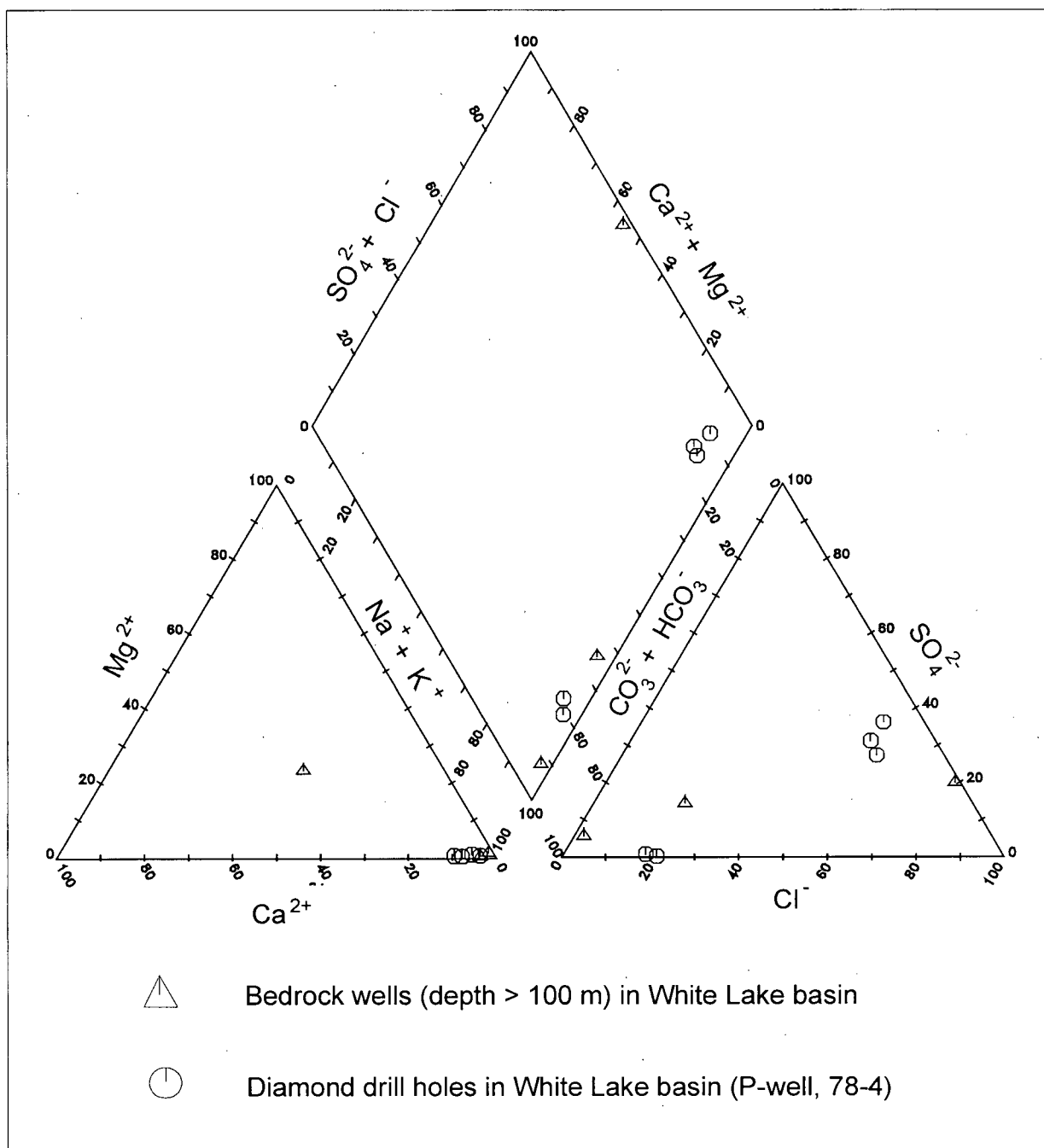
Figure 3-3 Piper plot of regional groundwaters sampled in the Summerland and White Lake basins. Data from Piteau & Associates (1984) and Grant and Michel (1983)

3.2 LOCAL GROUNDWATER FLOW

Local groundwaters are defined as those recharged within or slightly outside the Summerland basin and flowing at depths less than 100m through the bedrock and surficial sediments. The hydrogeological features referred to in this section are found in **Figure 3-2**.

Small mountains such as Mt Conkle, Giant's Head, Rattlesnake Ridge, and Cartwright mountain (see **Figure 3-2**) provide suitable recharge areas for shallow groundwater aquifers in the Summerland basin. These mountains are made up of exposed bedrock with well-developed fracture sets (Piteau & Associates, 1984). Lawson's (1968) measurements of hydraulic conductivities of shallow volcanic rocks (< 30m) in the Trapping Creek Basin just south of Kelowna were between 10^{-9} and 10^{-5} m/s. A similar range of 10^{-10} m/s to 10^{-7} m/s was measured by Golder Associates (1980) at depths of up to 84 m in a test hole for sewage effluent disposal on Giant's Head.

Most creek valleys in and around Summerland are filled with unconsolidated glacial sediments that comprise ideal aquifers. When drilling the EPB-GSC 495 well at the base of Eneas creek valley, 56 metres of gravel and glacial till were penetrated before encountering bedrock. The Faulder-Meadow Valley district, which runs northward from the junction of Trout and Darke Creeks (see **Figure 3-2**), sits on top of a gravel aquifer that fills the valley. A report by Pacific Hydrology Consultants Ltd (1983) states that "this buried valley acts as a drain with water flowing through the gravel southward and then eastward, probably under Summerland to Okanagan Lake." The kame deposit surrounding the Summerland reservoir (see **Figure 2-5**) may be a connecting aquifer which directs groundwater into Prairie Valley. In addition to natural groundwater flow, significant amounts of water are diverted from Trout Creek Valley to Prairie Valley via the flume connecting Trout Creek to the Summerland reservoir. In turn, this water is transferred to Prairie Valley through irrigation lines and reservoir seepage.

These aquifers contribute significant baseflow to local creeks within the basin. A year-long sampling program of Eneas Creek and a nearby water well gave consistent groundwater to surface water uranium concentration ratios of between 0.8 and 1.30, thereby indicating significant groundwater baseflow contribution to the creek (Ministry of Health B.C. and Ministry of Energy, Mines and Petroleum Resources B.C., 1980). Both also followed parallel cycles in uranium concentration over the year (Ministry of Health B.C. and Ministry of Energy, Mines and Petroleum Resources B.C., 1980). Darke creek and adjacent well waters, as well as Trout creek waters show the same pattern (Ministry of Health B.C. and Ministry of Energy, Mines and Petroleum Resources B.C., 1980).

The following sections present geochemical evidence that the groundwater in these aquifers is locally recharged and can be distinguished from regional groundwaters described in the previous section. Water quality analyses from the following features are found on the Piper plot of **Figure 3-4**.

Shaughnessy Springs

A large groundwater reservoir is believed to occupy the glacial overburden and shallow bedrock channels beneath the Summerland business district and to receive waters from Prairie and Eneas Creek valleys (Piteau & Associates, 1984, Ministry of Environment, Lands and Parks B.C., 1986). Kvill (1976) states that discharge from Eneas Creek infiltrates the coarse-textured fan material north of Summerland town centre and flows towards the lake as groundwater. Shaughnessy springs (see **Figure 3-2**), whose outlet lies at the base of the silt cliffs just off Highway 97, is believed to be a discharge point for this aquifer. The springs supply the Summerland Trout hatchery with a steady year-round flow rate of 67.5 L/s at a temperature of 11 °C (Piteau & Associates, 1984).
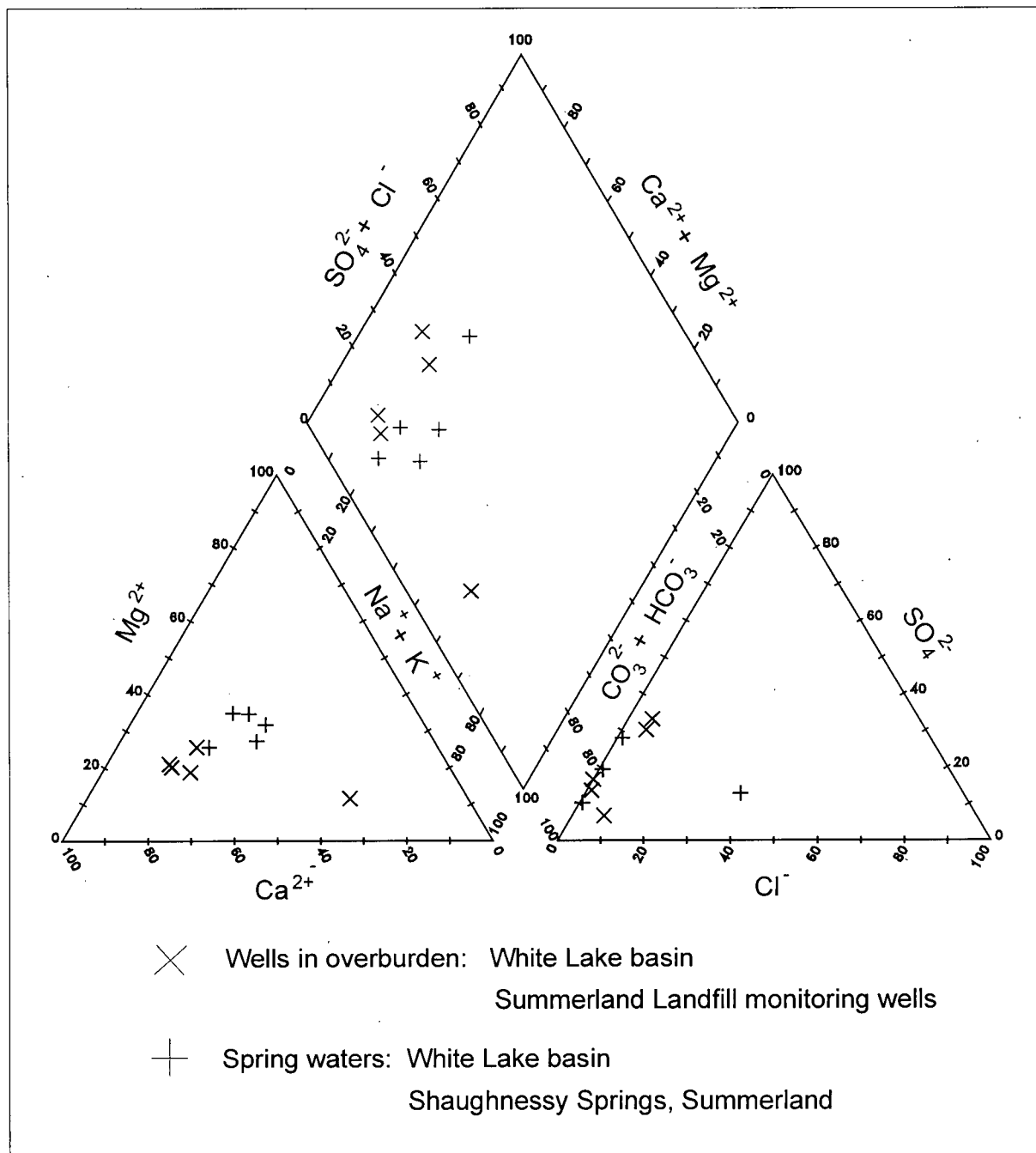
Figure 3-4 Piper plot of local groundwaters in the Summerland and White Lake basins. Data from Grant and Michel (1983) and Piteau & Associates (1984)

The chemistry of Shaughnessy springs waters points to local sources of recharge, including rainfall, irrigation water, and local creeks. Tritium levels measured in 1986 dated the water to be less than 30 years old, and hydrogen and oxygen isotope ratios were found to match those of local creeks and irrigation waters. (Ministry of Environment, Lands and Parks B.C., 1986). Other analyses showed these waters to be relatively oxidizing (Eh +180 mV), slightly alkaline (pH = 7.90), with moderate amounts of dissolved solids (roughly 300 mg/L), and a $Ca-HCO_3$ chemistry (Ministry of Environment, Lands and Parks B.C., 1997 and Piteau & Associates, 1984). This chemical signature is typical of locally recharged groundwaters circulating in shallow glacial sediments that have undergone carbonate-mineral dissolution under open or partially open CO_2 conditions (Freeze and Cherry, 1979, p. 284). Since the early 1990's, increases in concentrations of nitrate and coliform bacteria have been noted in the spring water, which probably comes from agricultural runoff and septic discharge in Eneas and Prairie valleys (Ministry of Environment, Lands and Parks, B.C., 1997).

Perpetual Landslide

Another example of a surficial aquifer receiving significant recharge from agricultural activity is the "Perpetual Landslide," located on the north side of Trout Creek Canyon. Here unconsolidated Quaternary deposits are in a state of constant creep, made worse in recent years by the increased pore water pressures from diffuse groundwater discharge (Piteau Associates, 1984). Roughly a dozen spring pools were identified on the side of the landslide by the author in May '97. This is likely irrigation water from the nearby golf course and fruit orchards. Church (1980) measured a uranium concentration of 43 μg/L in some of these springs.

Summerland reservoir

A network of shallow monitoring wells was installed in the kame deposit at the top of Prairie Valley just above the town reservoir (Golder Associates Ltd., 1994) to monitor the

migration of landfill leachate. Groundwaters were found to be migrating eastward, and groundwater samples taken from a background well were neutral to alkaline (pH 7.5 to 8), with low dissolved solids (230 mg/L), significant Ca (50 mg/L), and minor Mg and Na concentrations (9 mg/L each). Uranium concentrations of 1 μg/L have been detected in the reservoir itself (Church, 1980).

Indian Springs

A uranium concentration of 1 μg/L was measured at Indian Springs, located just west of the town reservoir (see **Figure 3-2**) (Church, 1980). This spring discharges at a rate of 2 L/s, and is slightly acidic (pH 5.8) with low dissolved solids (conductivity of 170 μS/cm). The dominant ions were HCO_3 and Ca, with minor but equal concentrations of Mg and Na. This is believed to represent even shallower groundwaters recharged within a few kilometers of the springs.

Cowan Springs

A number of springs surface just downgradient from the Summerland reservoir. One of these is Cowan Springs, located in the backyard of Barry Cowan. These were sampled by the author in March '98 and their analyses are plotted later in **Figure 5-1**. Compared to Indian springs waters, concentrations of Cl were slightly elevated (possibly due to mixing with leachate from the landfill upgradient of the reservoir), but the overall chemistry was the same.

White Lake Basin

Groundwaters sampled in surficial wells in the White Lake basin had chemistries typical of shallower, more locally recharged groundwaters than those sampled in bedrock (Grant and Michel, 1983). Tritium counts indicated recharge in the mid 1970's; and their ion composition was predominantly $Ca-HCO_3$ and $Ca-Mg-Na-HCO_3$ with low concentrations

of dissolved solids.

SUMMARY

For this thesis, regional groundwaters are defined as originating several kilometers west of the Summerland basin and flowing at depths of over 100m within the bedrock toward Lake Okanagan. They are generally older than 25 years and have high levels of dissolved solids. Borehole testing in the White Lake basin further characterized regional groundwaters as relatively reducing, enriched in Na and Cl, and confined to poorly-connected fracture sets and porous units deep underground. However, Boyle (1982) argues that regional groundwaters form a well-established flow regime rising along major fault zones in and around the Summerland basin, and are relatively oxygenated and enriched in HCO_3.

Creeks and springs in the Summerland basin are discharge points for local groundwaters. These are defined as being recharged within or slightly outside the basin and flowing at depths of less than 100m in the shallow bedrock and glacial deposits. Evidence supporting their recent recharge and short travel times include their $Ca-HCO_3$ chemistries, young age (< 25 years) relatively oxidizing Eh, and low dissolved solids concentrations. If regional groundwaters are discharging within the Summerland basin, they are probably diluted beyond chemical recognition. Therefore, evidence of regional uranium transport into the Summerland basin is scarce.

4 RESULTS OF FIELD INVESTIGATION

This chapter presents the results of a field program designed to further characterize the hydrogeology and groundwater geochemistry of the Prairie Flats. It begins with a general outline of the field program carried out from July '97 to May '98. This is followed by a more detailed characterization of the topography and hydrogeology of the flats, including measurements of hydraulic conductivities and hydraulic gradients in the peat, clay and till units. Streamflow measurements are also presented, as well as the geochemical sampling results. This data is used in Chapters 5 and 7 to construct hypotheses regarding the origins and nature of the uranium deposit.

4.1   OUTLINE OF FIELD PROGRAM

A network of 13 piezometers was installed across the Prairie Flats in July and August '97 (see **Figure 4-1**). Four deep piezometers (labelled –01) were completed in the till unit at depths of about 3 metres. Nine shallow piezometers (labelled –02) were completed in the peat and clay units at depths of about 1 metre, which is just below the water table. The deep and shallow piezometer pairs (101/102, 401/402, 601/602, 701/702) were each installed within 50 cm of each other to measure vertical hydraulic gradients and changes in chemistry with depth. Further details on piezometer installation are given in **Appendix A**, and piezometer logs are located in **Appendix B**.

Slug tests were carried out in the piezometers to measure horizontal hydraulic conductivities of the peat, clay and till units, and a borehole infiltration test was used to measure the vertical hydraulic conductivity of the peat unit. Hydraulic heads were measured across the site over four seasons (late July/early August '97, late September '97, early March '98, and mid May '98) to determine lateral and vertical components of the hydraulic gradient and the general direction of groundwater flow.

E

o
502

o
302

601/602
□ o

□ o 701/
o 702

401/402
□
o

202 o D

o
Shallow Piezometer

□
Deep Piezometer

802
o

□o 101/
102

C

902
o

B

A

open ditch

culvert

| 0 | 100 | 200 | 300 m |
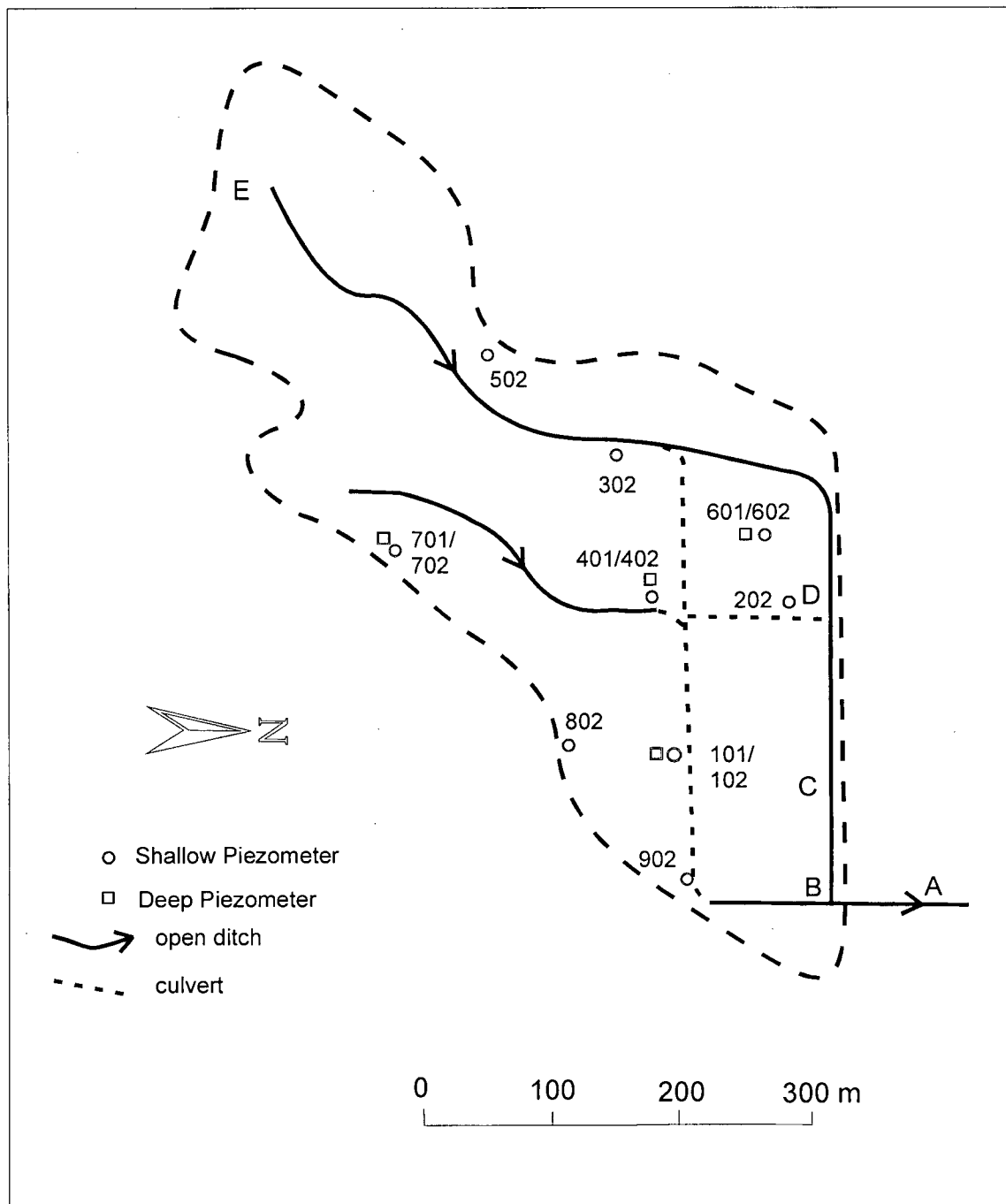
Figure 4-1 Piezometer and stream measurement locations on the Prairie Flats

35

Measurements of groundwater-surface water interaction were made at locations A, B, C, and D on Prairie Creek using mini piezometers and seepage meters. Field methods for these tests are described in detail in **Appendix A**, and the slug test data can be found in **Appendix C**.

Water samples were collected from the piezometers and from surrounding springs and creeks in September '97 and March '98. Parameters tested in September included pH, temperature, conductivity, and dissolved uranium. A more thorough analysis was carried out in March with the addition of ferrous iron, dissolved carbon (total, inorganic, and organic), major cations (Ca, Na, K, Mg, Fe_{TOT}), major anions (HCO_3, Cl, SO_4) and nitrate. Field and laboratory methods are explained further in **Appendices D** and **E**, and are summarized in **Table 4-1**.

4.2 TOPOGRAPHY

The topography of the Prairie Flats is shown in plan view in **Figure 4-2**, based on a level survey carried out in August, '97. The ground surface rises gently to the southwest with an average gradient of 0.5%. At the east end of the flats the gradient flattens to about 0.1% and the topographic contours curve around an elevation low. West of the deposit the terrain continues to climb up Prairie Valley to the Summerland reservoir, and about half a kilometer to the east it encounters the steep cliffs of Giant's Head.

4.3 HYDROSTRATIGRAPHY

The near-surface lithology of the Prairie Flats consists of four principal units: peat, clay, till, and bedrock. These can be grouped into three hydrostratigraphic units: a low permeability peat & clay unit, a higher permeability till unit, followed by low permeability, fractured bedrock. Further discussion of the field results will be presented from this hydrostratigraphic perspective.

Table 4-1 Field and laboratory methods used for geochemical analyses

Parameter	Method	Sample Treatment	Sample Storage
pH	Hanna HI 9025C pH probe	unfiltered	measured in the field
temp	Temperature probe	"	"
Conductivity	Hanna Dist WP 3 conductivity probe	"	"
Bicarbonate	Electrometric alkalinity titration	"	"
Fe2+	HACH test kit: 1,10 Phananthroline indicator method	"	"
Eh	Cole-Palmer ORP combination electrode	"	"
Ca, K, Fe	Atomic Absorption	filtered, acidified	acid-washed nalgene bottles, refrigerated
Na, Mg	Atomic Emission		
NO3 (Sept)	Hach Kit: Cadmium reduction method	filtered	nalgene bottles, refrigerated 6 hours
NO3, SO4, PO4, Cl	Ion Chromatography	filtered	nalgene bottles, frozen
TC, IC, OC	Combustion Infrared		
U	ICP-MS	filtered, acidified	acid-washed nalgene bottles, refrigerated

Total thicknesses of the peat & clay unit encountered during this field program ranged from 0.5 to 2.5 m, and are contoured in **Figure 4-3.** The base of the till unit is below the deepest piezometer, therefore the total thickness of the till unit was not measured.
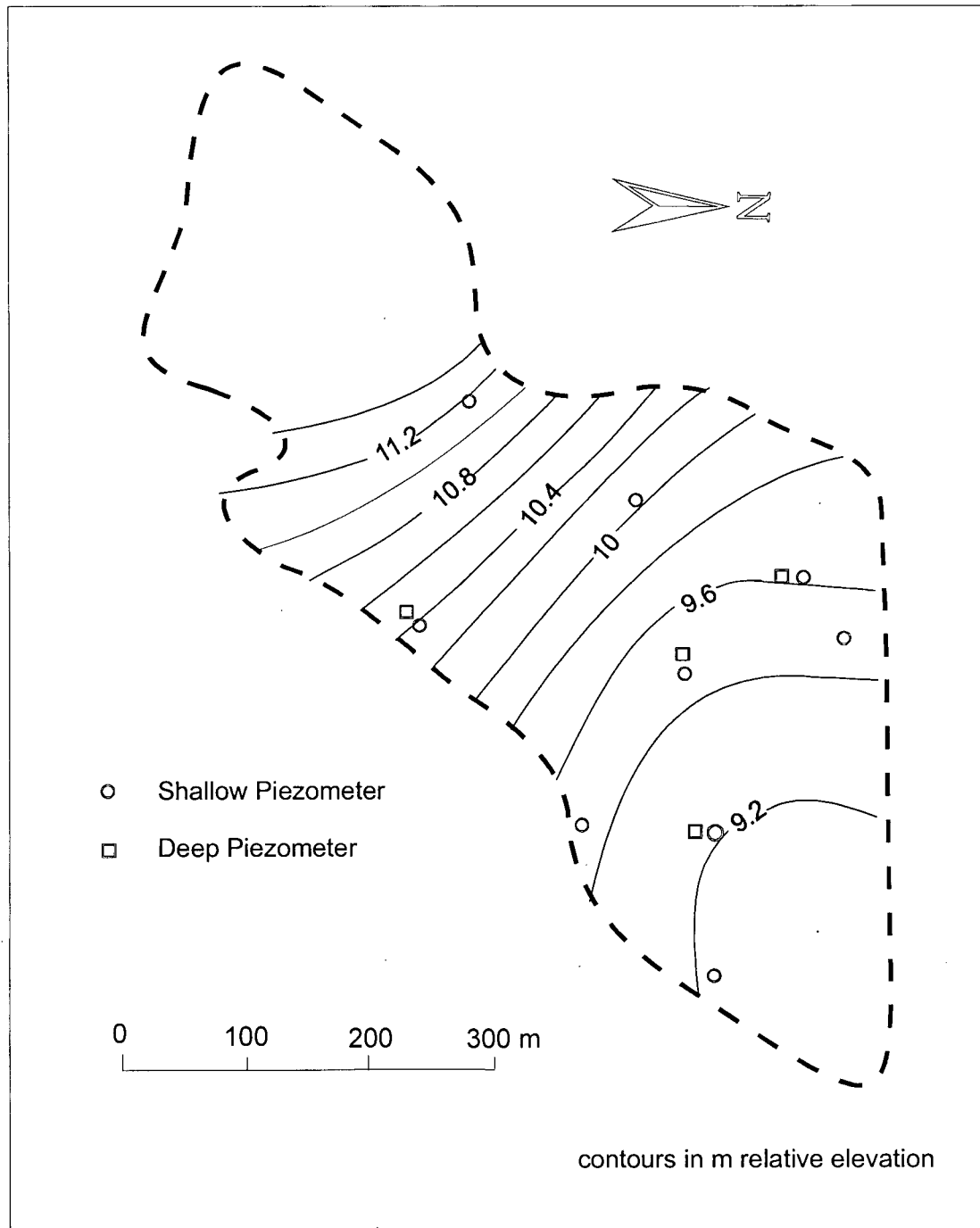
Figure 4-2 Topography of the Prairie Flats
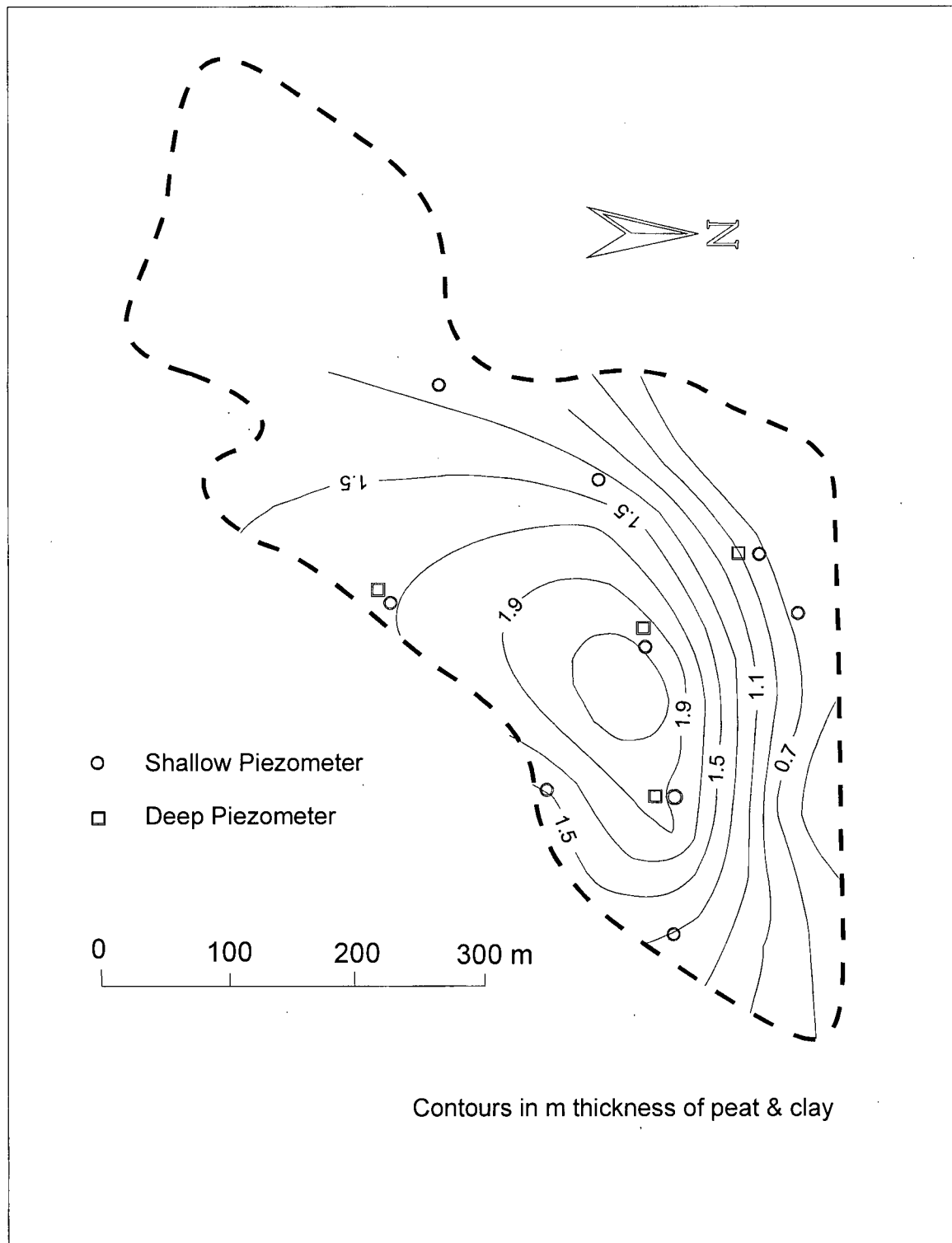
Figure 4-3 Isopach map showing thicknesses of peat & clay unit

39

4.4   HYDRAULIC CONDUCTIVITY

Horizontal Hydraulic Conductivity

Slug tests were performed to measure the horizontal hydraulic conductivity, K_H, of the peat & clay and till units. This data can be found in **Appendix C**. The data was analyzed by the Hvorslev (1951), Cooper-Bredehoeft-Papadopulos (1967), and Bouwer-Rice (1976) methods (using AQTESOLV™ for the latter two).   All three approaches were tried since the site doesn't perfectly fit any of their sets of geometrical conditions. These discrepancies are discussed below.

The Hvorslev method assumes a fully completed well in a homogeneous, isotropic, perfectly confined aquifer of infinite lateral extent and unlimited thickness. However, the peat & clay unit is unconfined and the piezometers are not fully completed (ie. screened across the entire thickness of peat & clay). Also, both the Bouwer-Rice (1976) and Hvorslev methods neglect specific storage. Demir and Narasimhan (1994) pointed out that specific storage effects cause head data on a semi-log plot to deviate from a straight line (ie. bend concave upward), which was observed at a few piezometers (202, 402, and 902). The Cooper- Bredehoeft-Papadopulos (1967) method assigns a specific storage value to the data, but the assumptions of Hvorslev are also inherent in this method.

Despite the limitations of these three methods, calculated hydraulic conductivity values were within the same order of magnitude for both the peat & clay unit (10^{-7} m/s) and the till unit (10^{-5} m/s), as shown in **Table 4-2**. Furthermore, the frequency distribution of all hydraulic conductivity values (see **Figure 4-4**) is bimodal, with peaks corresponding to the peat & clay unit (3×10^{-7} m/s) and till unit (6×10^{-6} m/s).

Table 4-2 Summary chart of horizontal hydraulic conductivities calculated using 3 methods

Piezometer	Lithology at screen intake	Hvorslev K (m/s)	Cooper & Bredehoeft K(m/s)	Bower & Rice K (m/s)
101	till	7.0E-07	3.7E-07	1.4E-06
101	till	1.1E-05	6.9E-06	3.3E-05
601	till	2.6E-05	2.1E-05	4.5E-05
601	till	2.1E-05	2.2E-05	6.9E-05
102	peat, clay	2.0E-07	1.7E-08	3.7E-07
202	till	2.5E-07	n/a	n/a
302	clay	4.7E-07	1.0E-06	8.6E-07
402	peat	6.6E-07	1.8E-06	1.5E-06
602	clay	6.7E-07	1.1E-06	1.3E-06
602	clay	1.2E-06	1.3E-06	2.2E-06
602	clay	1.0E-06	1.3E-06	1.9E-06
802	peat	6.0E-07	8.9E-07	1.1E-06
902	clay	1.5E-07	1.4E-07	5.0E-07
902	clay	3.5E-07	4.5E-07	5.9E-07
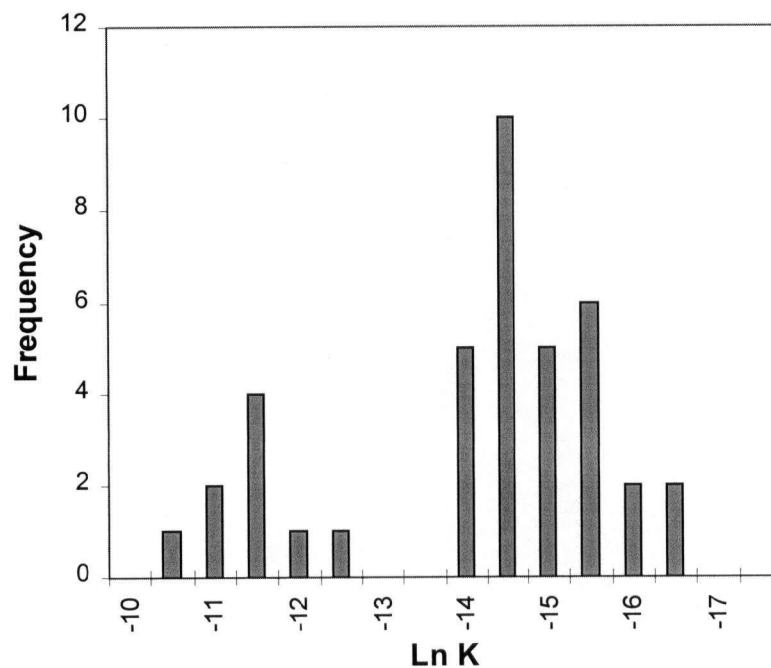
Figure 4-4 Frequency distribution of all calculated horizontal hydraulic conductivities

The alignment of head recovery data in the Cooper-Bredehoeft plots provides insight on the homogeneity of the peat & clay unit and the till unit. **Figure 4-5a** suggests that hydraulic conductivities of the peat & clay unit are relatively uniform across the site. Deviation from this trend at piezometers 102 and 202 may be due to the persistence of fines in the piezometer after development. The hydraulic conductivities measured in till unit (see **Figure 4-5b**) are not as uniform, which is reasonable given the unsorted nature of till.
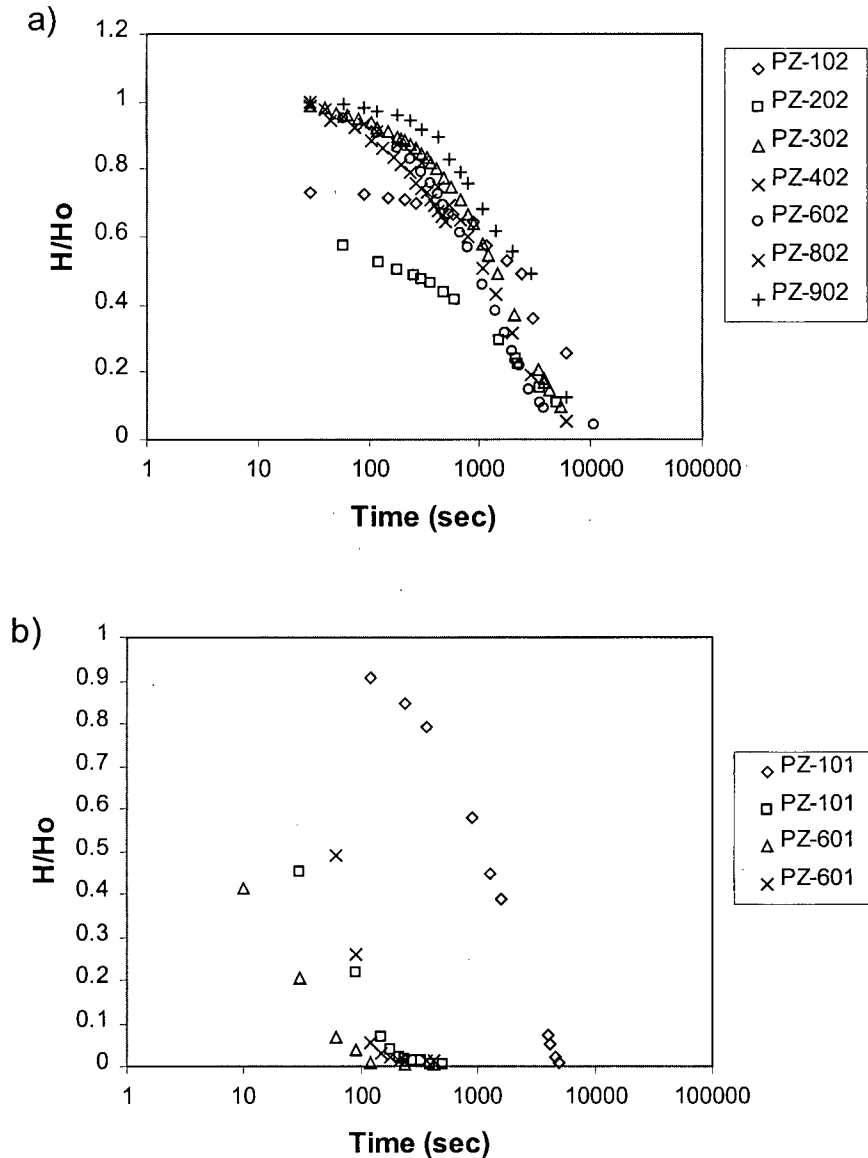
Figure 4-5 Cooper-Bredehoeft plots of slug test data in a) shallow piezometers (peat & clay) and b) deep piezometers (till). H_0 is the initial hydraulic head value, and H is the subsequent hydraulic head value after start of the test

Representative hydraulic conductivity values of 6×10^{-7} m/s for the peat & clay unit, and 2×10^{-5} m/s for the till unit were calculated from the curves of best fit to the Cooper-Bredehoeft-Papadopulos plots. These values are considered to be the best estimates of hydraulic conductivity because they account for specific storage effects. Hydraulic conductivities calculated using the Bouwer-Rice method were consistently higher than those calculated using the other two methods and thus are likely to be less representative.

Some piezometers were slug-tested repeatedly in order to detect any dependence of head recovery on the initial displacement, H_0, or to detect the possible evolution of a low permeability well-skin, as is recommended by Butler et al. (1996). On the contrary, hydraulic conductivity values tended to increase, which means that some piezometers may not have been optimally developed before slug testing.

Vertical Hydraulic Conductivity

A borehole infiltration test was carried out to estimate the vertical hydraulic conductivity, K_V of the peat & clay unit. The test method is described in **Appendix A** and the resultant head data is plotted in **Figure 4-6**.

The Hvorslev method was used to interpret the data since it is only when measuring the horizontal hydraulic conductivity (ie. radial-flow across the piezometer screen) that the neglect of specific storage incurs significant error (Demir and Narasimhan, 1996). A shape factor appropriate to the flow geometry was chosen (case C: "flush bottom in uniform soil" Hvorslev, 1951) and the mean hydraulic conductivity was calculated using:

$$K_m = \pi D / 11 \, T \qquad\qquad (4.1)$$

where $K_m = \sqrt{K_H} \times \sqrt{K_V}$ is the mean hydraulic conductivity (cm/sec)

K_H and K_V are the horizontal and vertical hydraulic conductivities (cm/sec)

D is the diameter of the casing (cm)

T is the basic time lag (sec)
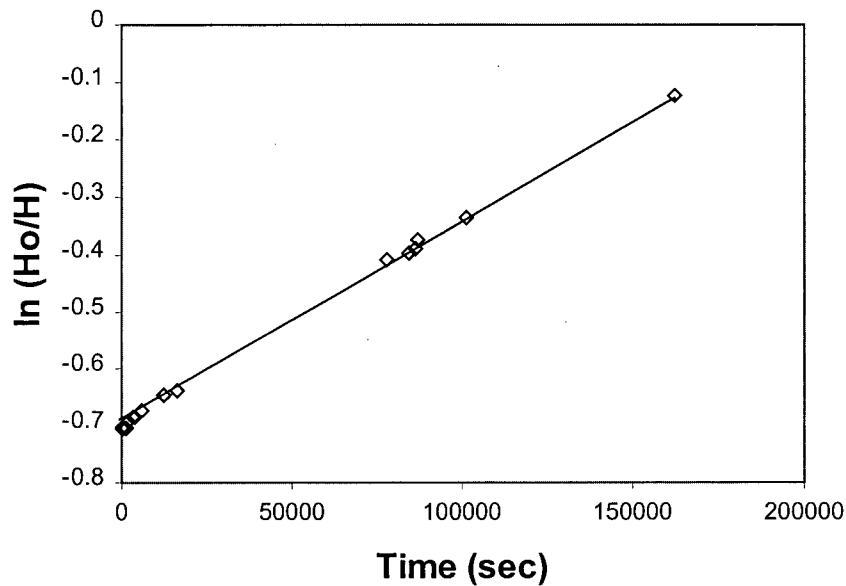
Figure 4-6 Plot of infiltration test data in peat & clay unit. H_0 is the initial hydraulic head value, and H is the subsequent hydraulic head value after start of the test

To calculate K_v, a representative K_H value of 6×10^{-5} cm/sec was used for the peat & clay unit. This gave a K_v of about 4.4×10^{-7} cm/sec or 4×10^{-9} m/s, about two orders of magnitude lower than the horizontal hydraulic conductivity. A lower K_v is reasonable given that this material is made up of peat intermixed with silt and clay that has been repeatedly compacted by the heavy farming machinery. However, 10^{-9} m/s is an order of magnitude lower than the 10^{-8} assigned to the underlying bedrock by Piteau & Associates (1984), and corresponds to the hydraulic conductivity of shale (10^{-11} to 10^{-7}, Freeze and Cheery, 1979, p. 29), which is more compact and impermeable than peat. Therefore, 10^{-8} m/s was chosen as a more reasonable value for the K_v of the peat & clay unit.

4.5   FLOW PATHS

Contour plots of measured head values enable the lateral component of the hydraulic gradient to be calculated and the general groundwater flow direction to be traced.

44

Lateral Flow in the Peat & Clay and Till Units

A representative contour plot of the hydraulic heads in the peat & clay unit is shown in plan view in **Figure 4-7**. This head pattern changed minimally throughout the year. By comparing **Figure 4-7** and **Figure 4-2**, it is evident that the head contours closely mimic the topographic contours. The lateral component of groundwater flow is generally west to east, and the gradient ranges from 0.009 on the west end of the flats to 0.001 on the east end.

Because of the different completion depths of the deep piezometers, hydraulic heads measured here offer only an approximate measure of the lateral component of groundwater flow through the till unit, which is illustrated in **Figure 4-8**. The lateral component of the hydraulic gradient in the till is about half that in the peat & clay because of the higher hydraulic conductivity of the till.

Measurements taken the morning after a rainfall event showed a surprising rearrangement of heads in the till unit (see **Figure 4-9**), which returned to normal the next day. No such perturbation was noted in the peat & clay unit. This quick response suggests that the till unit is connected to nearby sources of recharge, possibly storm runoff that collected on residential streets and infiltrated along the northern boundary of the flats where the peat & clay unit is thinner.
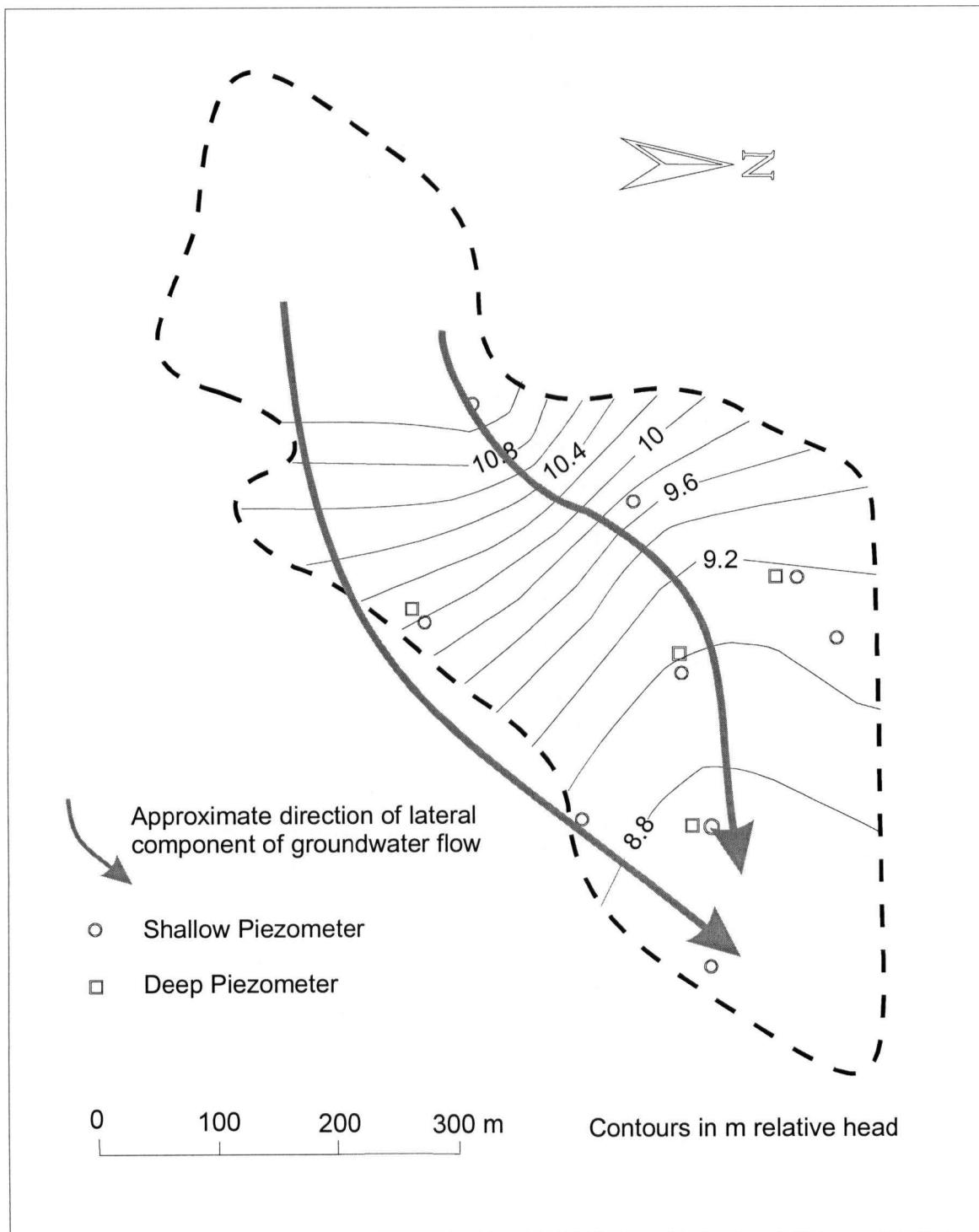
Figure 4-7 Contour plot of relative head values measured in shallow piezometers (peat & clay) on Aug 1, '97

46
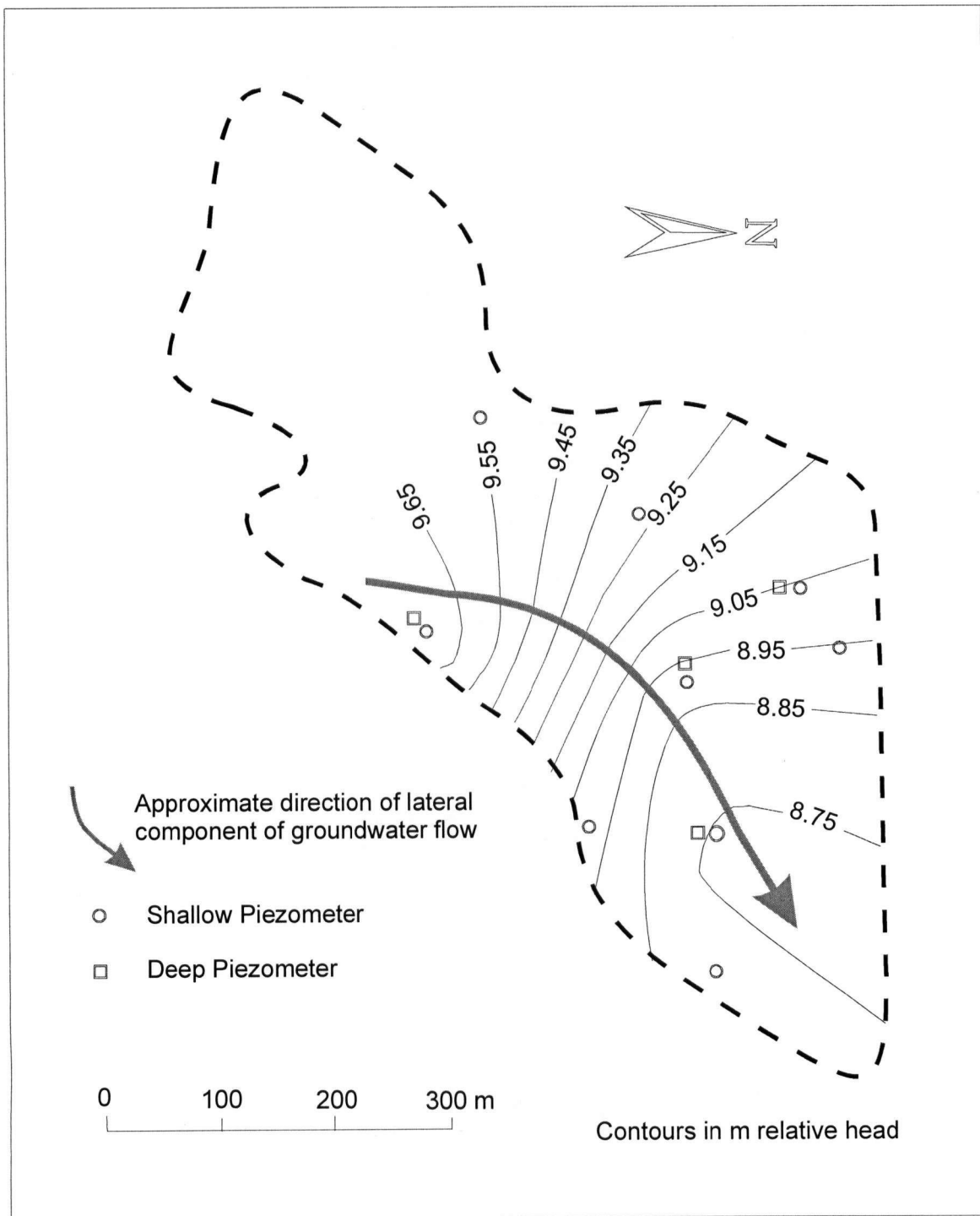
Figure 4-8 Contour plot of relative head values measured in the deep piezometers (till) on Aug 3, '97

47
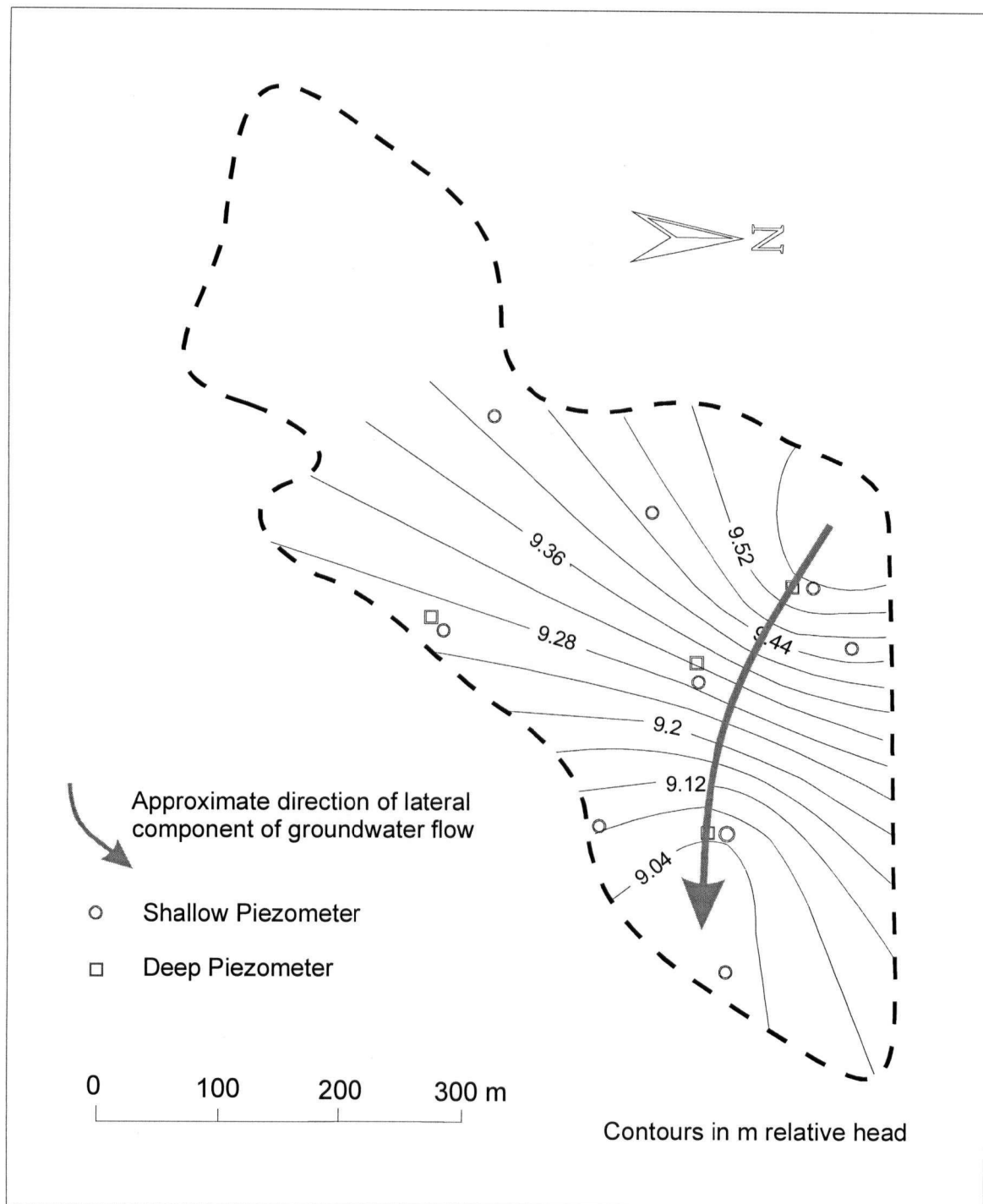
Figure 4-9 Contour plot of relative head values measured in the deep piezometers (till) on Sept 26, '97, the morning after a rainfall event

Vertical Flow in the Peat & Clay Unit

Table 4-3 summarizes the measurements of the vertical component of the hydraulic gradient taken at the four nested pairs of piezometers. These gradients were calculated from the head difference between a point just below the water table in the peat & clay unit (shallow piezometer) and a point at the top of the till unit (deep piezometer), over a difference in elevation of at least 110 cm, (except for 28 cm at 601/602). Given the difference in hydraulic conductivity between the peat & clay unit and the till unit, most of the head losses occur across the peat & clay, therefore these measurements represent the vertical component of the hydraulic gradient across the peat & clay unit. Gradients are described as upward where the head at depth exceeds that above, thus where groundwater would tend to flow upwards across the peat & clay unit (and vice versa).

Unlike the lateral component of the hydraulic gradient through the peat & clay unit, temporal variations were noted in the vertical component. The piezometer pairs located in the middle of the deposit, 401/402 and 601/602, show both downward and upward hydraulic gradients. The downward hydraulic gradients are probably an expression of recent climatic events, such as rainfall or snowmelt, rather than seasonal trends. However, upward gradients persist throughout most of the year, and average 0.04. More frequent head measurements are necessary to confirm seasonal and shorter-term trends.

Piezometers 101/102 and 701/702 show consistent upward gradients at all sampling times, averaging 0.04 and 0.10 respectively. 101/102 are located near an impermeable clay liner that was put in place under the Giant's Head School playfield to prevent ponding during wet periods. Groundwaters that formerly ponded in the middle of the field are now forced to surface along its edge, creating these upward gradients. Piezometers 701/702 are located near the base of a hill, where springs have been located by local residents (personal communication, 1997, 1998) and by Piteau & Associates (1985). Therefore these upward gradients are probably topographically-driven.

Table 4-3 Vertical hydraulic gradients measured throughout the year at Prairie Flats

Location	Jul-23	Jul-24	Aug-01	Aug-02	Aug-03 (am)	Aug-03 (pm)	Sep-24	Sep-26	Sep-28	Mar-03	Mar-05	Mar-06	May-11	May-12
101/102	0.04	0.02	0.03	0.04	0.04	0.05	0.02	0.03	0.02	0	0.01	0.02	0.04	0.04
401/402	n/a	n/a	0.02	0.02	0.03	0.02	-0.15	-0.14	-0.17	-0.06	n/a	n/a	-0.01	-0.01
601/602	n/a	n/a	0	0.03	0.03	0.02	-0.02	-0.04	-0.02	-0.07	-0.04	-0.05	-0.02	-0.03
701/702	n/a	n/a	0.06	0.06	0.06	0.06	0.05	n/a	0.08	0.11	0.16	0.15	0.08	0.08

4.6 STREAM MEASUREMENTS

Prairie Creek flows through a series of open drainage and underground culverts from entry point (E) to the Prairie Flats to exit point (A) (see **Figure 4-1**). Mini piezometers and seepage metres were installed in the creek bed at points B, C, and D to measure the vertical component of the hydraulic gradient and the seepage rate between the creek and the underlying groundwater. These field methods are further described in **Appendix A**, and their results are listed in **Table 4-4**.

Table 4-4 Hydraulic gradient and seepage results for Prairie Creek

Location	Date	Vertical Hydraulic Gradient	Seepage Rate $(m^3\ yr^{-1}m^{-2})$
B	July 19, 1997	0.13	25
C	July 22, 1997	-0.06	-10
D	July 20, 1997	-0.32	not measured

* positive gradients and seepage rates indicate upward discharge of groundwater into the stream

From the above data set, it is difficult to state in general terms whether groundwaters contribute to streamflow across the flats or vice versa. Vertical hydraulic gradients and seepage rates varied significantly in both magnitude and direction between locations B, C, and D, and possibly across the rest of the site. This may be attributed to natural variations in creek bed topography or hydraulic conductivity, or to changes in the natural hydrology due to culvert installation or nearby residential development. For example, the relatively large upward gradient and seepage rate measured at B may be explained by its proximity to the impermeable liner under Giant's Head School playing field.

4.7   GEOCHEMISTRY

Results of geochemical sampling in and around the Prairie Flats are found in **Table 4-5**. The waters are generally neutral, with pH values between 6.5 and 8.0. They are enriched in Ca and HCO_3, with minor Na. Uranium concentrations span a large range, from 10 to nearly 1000 ppb. NO_3 and Cl may be coming from fertilizer, septic discharge, or landfill leachate (from the Summerland landfill behind the town reservoir) migrating eastward down Prairie Valley. Further discussion of these results is given in the upcoming chapters.

SUMMARY

Borehole logs, slug tests, hydraulic head measurements, and a water sampling program provide further insight into the groundwater regime underlying the Prairie Flats. The hydrostratigraphy consists of a low-permeability peat & clay unit 0.5 to 2.5 metres thick, followed by a higher permeability till unit of unknown thickness. Average lateral hydraulic conductivity measurements in the till unit were around $2x10^{-5}$ m/s, and $6x10^{-7}$ m/s in the peat & clay unit. A vertical hydraulic conductivity of 10^{-8} m/s was assigned to the peat & clay. While the lateral component of hydraulic gradient in the peat & clay unit was small (0.005) and relatively unchanging throughout the year, the vertical component of the hydraulic gradient was an order of magnitude greater (0.04) and more variable. This is attributable to the varying effects of evapotranspiration, rainfall, and snowmelt at different times of year. A summary sketch of the hydrostratigraphy and summer groundwater flow conditions across Prairie Flats is given in **Figure 4-10**.

Table 4-5 Geochemical sampling results from September, 1997 and March, 1998

Location	Sampling Depth (m)	Exposed unit	Sampling Date	pH	Temp C	Cond uS/cm	Meas Eh mV	Fe^{2+} mg/L	Total Fe mg/L	HCO_3 mg/L
PZ-101	2.58	till	Mar 05 1998	7.84	8.6	350	153.6	0.0	0.0	239
			Sep 25 1997	7.49	14.6	250				
PZ-401	2.47	till	Mar 07 1998	7.72	7.8	670	233.9	0.0	0.1	604
			Sep 25 1997	6.66	15.8	1300				
PZ-601	1.24	till	Mar 05 1998	6.7	6.9	640	154.5	1.8	1.2	549
			Sep 24 1997	7.19	15.5	420				
PZ-701	2.29	till	Mar 06 1998	7.68	6.6	625	358.7	<0.1	0.0	464
			Sep 26 1997	6.8	16.5	530				
PZ-102	0.98	peat, clay	Mar 05 1998	6.83	5.2	880	191	3.2	7.0	525
			Sep 24 1997	7.02	18	420				
PZ-202	0.88	till	Mar 06 1998	7.18	5.9	3300	155.6	3.6	7.5	1354
PZ-302	1.70	clay	Mar 07 1998	7.19	6.5	500	263.9	0.7	0.2	610
PZ-402	1.12	peat	Mar 07 1998	6.82	6.5	1440	231.4	3.8	12.0	647
			Sep 25 1997	6.58	16.6	1550			6.7	
PZ-502	1.16	peat	Mar 06 1998	7.3	7.4	650	196.6	2.7	9.5	498
			Sep 26 1997	6.8	16	660				
PZ-602	0.97	clay	Mar 05 1998	6.84	6	750	198.8	2.1	3.1	573
			Sep 24 1997	7.05	16.8	490				
PZ-702	1.14	peat	Mar 06 1998	7.53	6.7	670	243.3	0.4	0.3	555
			Sep 26 1997	7.8	17.2	720				
PZ-802	1.14	peat	Mar 07 1998	6.96	4.8	250	222.1	3.3	9.5	203
			Sep 26 1997	6.85	15.3	340				
PZ-902	1.06	clay	Mar 05 1998	6.04	6.1	270	264	3.5	7.5	88
Mraz well	100	bedrock	Mar 05 1998	8.2	6.4	1010	92	0.8	0.4	732
			Sep 25 1997	7.83	17.2	940				
Prairie Creek at E			Mar 04 1998	8.09	7.8	400	377		0.0	283
			Sep 24 1997							
Prairie Creek at A			Mar 04 1998	7.89	7.7	540	380		0.0	345
			Sep 25 1997	7.57	15.4	360				
Shaughnessy Springs			Mar 04 1998	7.25	12.8	560	437	0.0	0.0	317
			Sep 24 1997							
Cowan Springs			Mar 06 1998	7.68	7	670	368.5	0.0	0.0	488
Indian Springs			Mar 06 1998	7.3	7.4	120	393	0.0	0.0	83

Table 4-5 Continued Geochemical sampling results from September, 1997 and March, 1998

Location	TC mg/L	IC mg/L	OC mg/L	NO$_3$ mg/L	PO$_4$ mg/L	SO$_4$ mg/L	Cl mg/L	Ca mg/L	Mg mg/L	Na mg/L	K mg/L	U ug/L
PZ-101	31	30	1	0.3	0.9	28.9	19.0	46	10.7	11.9	2.25	12
				0.1								14
PZ-401	103	59	44	0.4	0.8	222.9	18.7	116	46.2	64.0	1.86	743
	89	50	39	0.6								7
PZ-601	91	74	17	0.4	1.7	42.9	31.9	104	35.7	30.0	2.30	36
				0.4								57
PZ-701	70	69	1	6.7	0.8	50.1	60.6	43	41.3	70.0	4.75	81
												166
PZ-102	97	72	25	14.5	1.1	229.5	48.9	116	42.4	61.0	3.05	74
				1.4								31
PZ-202	250	93	157	43.2	0.7	2490.3	265.2	381	165.5	630.0	10.10	3961
PZ-302	42	39	3	3.6	1.7	15.2	38.6	85	17.7	16.1	3.03	120
PZ-402	142	87	55	5.0	0.9	788.3	24.8	201	99.0	126.0	2.86	566
	99	67	32	1.9				346	40.0	47.0	0.37	967
PZ-502	76	62	14	14.5	ND	29.5	21.1	95	27.0	34.8	2.10	154
												338
PZ-602	106	83	23	21.5	1.1	82.8	51.0	113	39.4	37.2	2.45	208
				0.6								63
PZ-702	81	79	2	13.0	0.7	20.6	72.7	56	48.8	69.0	4.30	75
												151
PZ-802	41	30	11	6.0	0.9	8.9	74.1	47	6.4	6.7	2.00	14
												19
PZ-902	50	23	27	33.2	0.7	10.8	81.9	16	7.3	27.9	1.42	9
Mraz well				1.2	1.2	121.4	68.1	7	4.8	267.0	2.08	1
				0.1								2
Prairie Creek at E				3.3	0.8	23.5	67.7	54	17.2	19.0	3.72	34
												22
Prairie Creek at A				3.7	1.0	62.7	93.4	46	18.2	27.1	2.86	117
				0.5								34
Shaughnessy Springs				0.0	0.9	41.9	262.0	35	7.0	10.6	1.49	10
				4.7								24
Cowan Springs				4.3	0.9	40.6	368.7	84	34.5	37.5	5.60	106
Indian Springs				1.0	ND	5.1	23.8	16	3.6	4.2	1.33	1
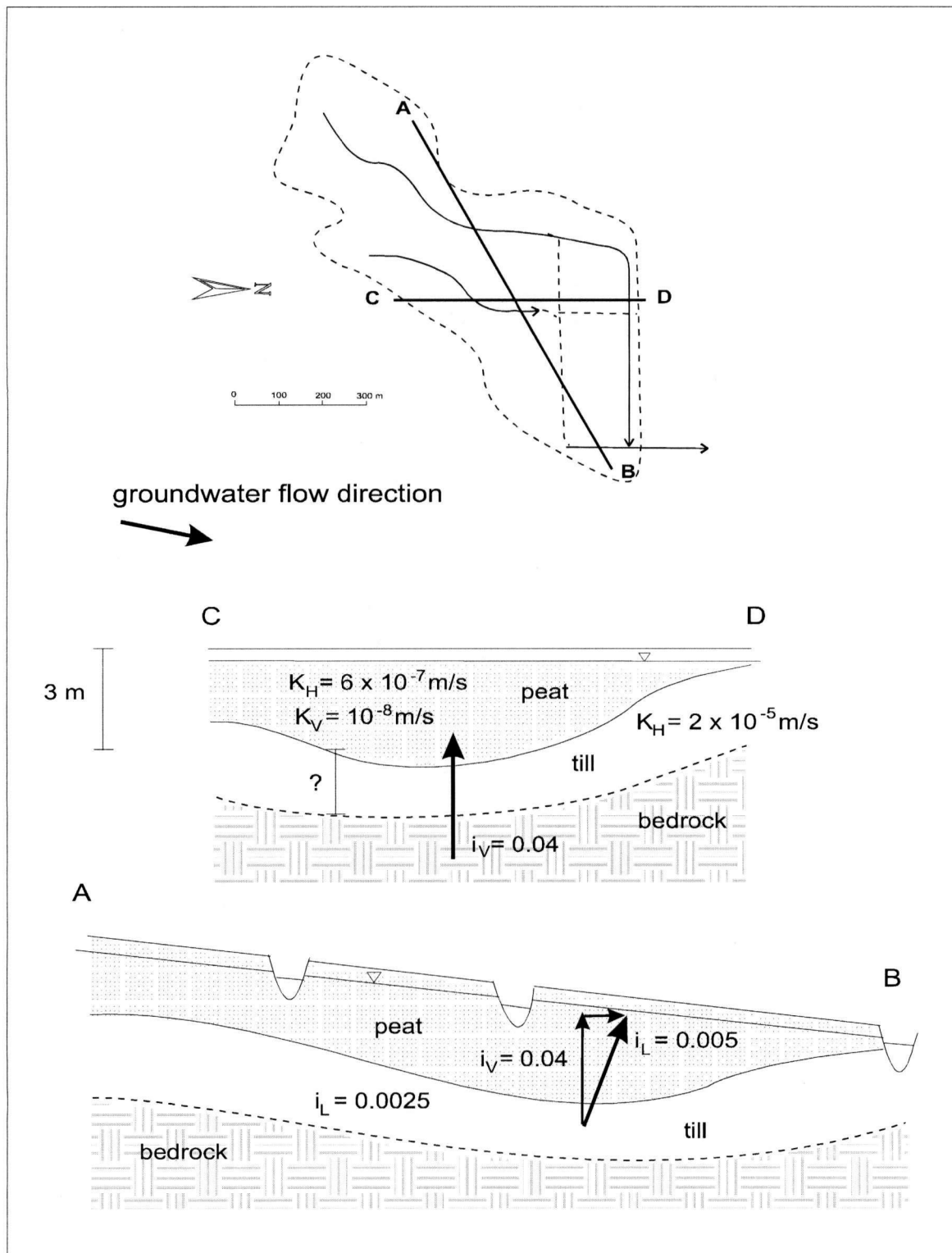
Figure 4-10 Summary diagram of Prairie Flats hydrostratigraphy and groundwater flow patterns during summer months

5 DISCUSSION OF SOURCE AND QUANTITY OF GROUNDWATER DISCHARGE

This section uses the hydrogeological and geochemical field data presented in Chapter 4 to formulate hypotheses on the origins and quantities of groundwater discharge into the Prairie Flats. The first section presents geochemical arguments that the flats are a discharge zone for locally-recharged groundwaters. Next, groundwater sources and sinks are quantified within the framework of a simplified hydrologic budget and used to estimate the current uranium deposition rate, thereby providing some insight into the history of the deposit.

5.1 SOURCE OF PRAIRIE FLATS GROUNDWATERS

Both the groundwater geochemistry and physical flow regime indicate that the Prairie Flats is a groundwater discharge zone. The accumulation of uranium in this area is an obvious proof, since it was leached from the surrounding rocks rather than coming from atmospheric sources. In most wetland areas, the decomposition of organic matter generates carbonic and organic acids which lower groundwater pH. In groundwater-fed areas, these acids are neutralized by mineral bases (eg. $CaCO_3$) dissolved in the discharging groundwaters (Shotyk, 1988). This results in a groundwater pH of between 6 and 8 rather than between 4 and 6, as is the case in the Prairie Flats. The measurement of upward flow gradients across the peat unit, as well as the immediate change in head in the till unit after a rainstorm (**Figure 4-9**) confirm that groundwaters are discharging here. Infiltrating rainwater could not have caused such a fast response in the underlying till owing to the low hydraulic conductivity of the peat & clay unit.

Further geochemical analysis indicates that the current source of these discharging groundwaters is local rather than regional. A Piper diagram of Prairie Flats groundwaters is given in **Figure 5-1**, which closely resembles the Piper diagram of other local

Figure 5-1 Piper plot of Prairie Flats groundwaters and nearby springs and surface waters. Shaughnessy springs data is taken from Piteau & Associates (1984)

groundwaters (**Figure 3-4**), as opposed to that of regional groundwaters (**Figure 3-3**). Prairie Flats groundwaters are relatively fresh (TDS < 1000 mg/L), neutral in pH, and are dominated by Ca and HCO_3, which is characteristic of shallowly circulating groundwaters in glacial sediments (Freeze and Cherry, p. 284). Summertime irrigation activity further up Prairie Valley is a major source of recharge to this shallow groundwater flow system. If regional groundwaters are discharging here, they are diluted beyond recognition by local groundwaters.

Water samples from the Mraz well, Indian Springs, Shaughnessy springs, and Cowan springs add further argument to the local origin of Prairie Flats groundwaters, and have been added to **Figure 5-1.** Indian springs is the freshest of the springs sampled (TDS < 100 mg/L) and plots close to Prairie Flats groundwaters on the Piper plot. The Mraz well groundwater sample shows a predominance of Na and K, plotting close to samples taken from the deep bedrock wells in the White Lake basin (**Figure 3-3**). This, plus its low uranium content (< 2 µg/L) and reducing redox conditions (Eh = –172 mV) suggest that deep bedrock groundwaters have a negligible role in the formation of this deposit.

High uranium concentrations measured at Cowan and Shaughnessy springs (106 µg/L and 10-24 µg/L, respectively) suggest that shallow groundwaters carry significant quantities of uranium. Mass balance calculations for a similar surficial uranium deposit in Nevada (Zephyr Cove) proved that modest losses of uranium from near-surface bedrock within the 1.75 km^2 drainage basin could supply the 40 000 kg of uranium present in the deposit (Otton et. al, 1989). Therefore, the uranium underlying the Prairie Flats need not have migrated great distances, but rather may have come from local bedrock sources within the Summerland basin.

5.2 QUANTIFYING GROUNDWATER DISCHARGE

A Simplified Hydrologic Budget

A hydrologic budget balances the inflow and outflow components of a given drainage system. With respect to the groundwater flow regime, it is divided into areas of recharge (usually at higher elevation) and discharge (usually at lower elevation), as is illustrated in **Figure 5-2** (Freeze and Cherry, 1979, pp. 3, 205-207). In a recharge zone, precipitation that is not lost to surface runoff (ie. streamflow) or to evapotranspiration infiltrates the ground surface and recharges the groundwater regime:

$$R = P - ET_R - Q \qquad\qquad (5.1)$$

where R is the groundwater recharge (m^3/yr)

      P is the precipitation (m^3/yr)

      ET_R is the evapotranspiration rate over the recharge area (m^3/yr)

      Q is the surface runoff (m^3/yr)

Some of the groundwater recharge goes into storage while the rest moves down the hydraulic gradient as groundwater flow until reaching a groundwater discharge zone. At the groundwater discharge zone, this water may go into storage, evaporate, or exit as stream baseflow (ie. the groundwater contribution to stream flow):

$$D = B + ET_D + S_D \qquad\qquad (5.2)$$

where D is the groundwater discharge (m^3/yr)

      B is the baseflow component of streamflow (m^3/yr)

      ET_D is the groundwater lost to evapotranspiration over the discharge area (m^3/yr)

      S_D is the groundwater that is stored (m^3/year)

Precipitation can be neglected from the above equation because discharge areas usually cover only a small fraction of the total area of the drainage basin, as is illustrated in **Figure 5-2**. Similarly, the approximate area of Prairie Valley, from the reservoir to the base of Giant's head, is 6 km^2, and that of the Prairie Flats is about 0.75 km^2. The insignificance of precipitation is particularly true during the summer months when high temperatures cause most of the precipitation to evaporate before infiltration.
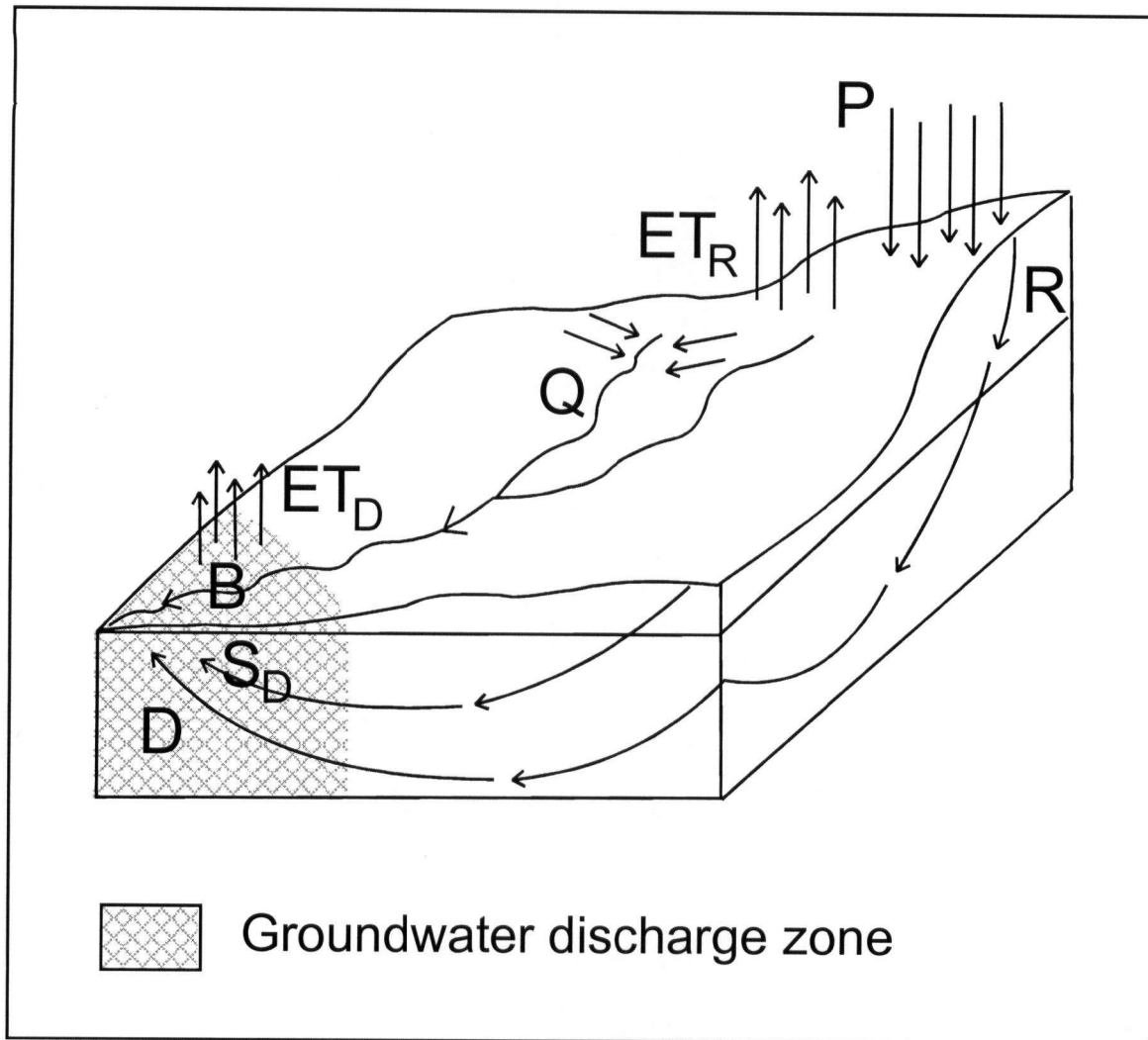
Figure 5-2 Components of recharge zones and discharge zones in a hydrologic budget, modified from Freeze and Cherry (1979, p. 3)

Piteau & Associates (1984) estimated that the groundwater recharge rate for shallow groundwater flow systems in the Trout Creek basin (which they defined as being recharged in local upland areas and having flow depths in the order of 10 to 50m) is approximately 4% of the precipitation. An average annual shallow groundwater recharge rate of 20.2 mm was calculated by dividing the total annual baseflow to Trout Creek by the catchment area, then multiplying by a factor of 1.3 to account for flow into the creek alluvium and evapotranspiration losses. This is assumed to be equivalent to the average annual shallow groundwater discharge rate in the basin.

Estimating Groundwater Discharge into the Prairie Flats

This section estimates the current rate of shallow groundwater discharge into the Prairie Flats by calculating the discharge rate into the peat & clay unit. ·

The above approach used by Piteau & Associates (1984) could not be used to calculate the shallow groundwater discharge rate into the Prairie Flats because flow rate data for Prairie Creek during the winter months (when irrigation is effectively turned off) is unavailable. Instead, the average annual groundwater discharge into the flats was estimated using Darcy's law, which is written

$$Q = K \, i \, A \qquad\qquad (5.3)$$

where Q is the flow rate (m^3/year)

  K is the hydraulic conductivity of the porous medium (m/sec)

  A is the cross-sectional area of flow (m^2)

As discussed in Chapter 4 and illustrated in **Figure 4-10**, the horizontal component of the groundwater flux into the flats is negligible compared to the vertical component, therefore total discharge (D) can be approximated using

$$D = K_V \, i_V \, A \qquad\qquad (5.4)$$

where D is the total discharge into the flats (m^3/year)

K_V is the vertical hydraulic conductivity of the peat and clay units (m/sec)

i_V is the vertical hydraulic gradient across the peat and clay units

A is the approximate surface area of the known extent of the uranium deposit (m^2)

From Chapter 4, K_V is approximately 10^{-8} m/s, the average annual i_V is approximately 0.04, and A is about 0.75 km^2. Substituting these values into equation 5.4 gives a total discharge rate of 9450 m^3/year, which is equivalent to about 13 mm/year over the area of the flats. This is of the same order of magnitude as Piteau & Associate's (1984) estimate of 20.2 mm/year for the Trout Creek basin.

During the summer months, most of the groundwater discharge exits the flats as evapotranspiration across the shallow water table (E_D). Evapotranspiration can also be calculated from shallow water table fluctuations (White, 1932, Meyboom 1967) but this method requires estimates of groundwater inflow and specific yield, as well as a continuous record of water levels over several days. Using potential evapotranspiration to estimate E_D would yield too high a value since potential evapotranspiration includes water lost from all surfaces (surface water, soil, vegetation, etc.) and not just from the water table.

Relative to evapotranspiration, other sinks such as groundwater storage, S_D, and baseflow to Prairie Creek, B, are negligible during the summer months. Losses to storage can be ignored since water levels are at an annual low. Groundwater exiting the flats as baseflow to Prairie Creek is relatively small since the surface area of the streambed (1700 m^2 excluding culverted sections) represents less than one percent of the total area of the flats (750 000 m^2). This statement assumes that the creek bed is also peat (K_V approximately 10^{-8} m/s) and that the vertical hydraulic gradient across it is the same as that across the rest of the flats. Also, measurements of hydraulic gradient and seepage rate along Prairie Creek offer no discernable pattern of groundwater discharge or recharge to or from the creek.

During the winter months however, evapotranspiration across the water table is effectively turned off due to low temperatures and snow accumulation on ground surface. At this time, most of the discharging groundwater goes into storage, causing a rise in the water table. For example, in March 1997, average water levels in the shallow piezometers were 45 cm higher than in August, 1996. Flow rate measurements in Prairie Creek at this time of year, when irrigation is ceased, would yield better estimates of the fraction of groundwater discharge contributing to baseflow of Prairie Creek.

Given the limited amount of field data collected at the Prairie flats, the above calculations provide only rough estimates of the various components of the hydrologic budget. Seasonal climate changes and irrigation practices significantly affect this budget and therefore require further consideration. More stream and groundwater measurements at different locations and at different times of year are needed to improve these estimates.

5.3 NEW INSIGHTS ON DEPOSITIONAL HISTORY

Using the calculated discharge rate and measured uranium concentrations of Prairie Flats groundwaters, the current flux of uranium into Prairie Flats was calculated. Next, this was compared with former estimates to gain new insights on the depositional history.

It has been established by Levinson (1984) that the Prairie flats uranium deposit is less than 10,000 years old, based on U^{238}/Th^{230} isotope ratios. This is a maximum value, as minimum uranium ages on two soil cores were 2,000 and 8,000 years (Levinson, 1984). Based on a soil survey done by Culbert (1979), there is an estimated 230 000 kg of uranium underlying the flats. Dividing this by the maximum age of the deposit gives a minimum average uranium deposition rate of about 23 kg/yr.

The current flux of uranium into Prairie Flats is calculated using the equation:

$$C = D[U] \tag{5.3}$$

where C is flux of uranium into the flats (kg/yr)

   D is the average groundwater discharge (m^3/yr)

   [U] is the average incoming uranium concentration (kg/m^3)

Uranium concentrations in water samples taken from the deep piezometers, which represent incoming groundwaters, were between 10 and 100 $\mu g/L$. This range of uranium concentrations is consistent with other stream and groundwater measurements in the Okanagan area (Boyle, 1982, Ministry of Health B.C., 1981). Uranium concentrations on the order of 1000 $\mu g/L$ have been measured only at a number of hydrologically isolated, highly alkaline ponds that are subject to high rates of evaporation, which does not represent conditions at the flats. Therefore, 100 $\mu g/L$ is assumed to be the maximum uranium concentration in groundwaters discharging into the Prairie Flats. When multiplied by the estimated discharge rate of 9450 m^3/yr (section 5.2), the estimated current maximum flux of uranium into the Prairie Flats is 0.95 kg/yr.

$$C = (9450 \ m^3/year)(1 \times 10^{-4} \ kg/m^3)$$
$$= 0.95 \ kg/yr$$

This calculation assumes that the amount of uranium entering or leaving the flats via Prairie Creek is negligible. Instead, all of the uranium is assumed to come from discharging groundwaters, most of which probably evaporates during the summer months and goes into storage during the winter months, according to the budget presented in section 5.2. Ignoring uranium losses or gains from groundwater-surface water interaction is reasonable because:

1. The drainage ditches relaying Prairie Creek across the flats were excavated in the later part of this century whereas the deposit is thousands of years old. Prior to agricultural development the flats were a marshland,

2. There is no visual correlation between the distribution of uranium and the courses of drainage ditches across the flats,

3. There is minimal topographic relief around the drainage ditches that would direct groundwater into them. Similarly, the hydraulic head distribution in the vicinity of the drainage ditches does not suggest significant groundwater-surface water interaction (see **Figure 4-7**).

Therefore, the current maximum uranium flux into the flats is at least an order of magnitude lower than the minimum rate estimated by Culbert and Leighton (1988). This discrepancy suggests that a deposit of this size could not have been created if the uranium deposition rates were the same in the past as they are today. At some point they were much higher, either due to increased groundwater discharge rates and/or higher uranium concentrations in the groundwater. For example, rocks that were scoured, fractured, and granulated by glacial processes were probably stripped of most of their labile uranium thousands of years ago. Furthermore, the Okanagan Valley was probably wetter and cooler at this time and not the dry, hot, semi-desert that it is today. Other past climatic events such as flooding may have enhanced uranium leaching and deposition. This uranium may have initially been deposited in the silt and clay deposits left by the meltwater lake that covered Prairie Valley, and then subsequently redeposited in the overlying peat layers by upward flowing groundwaters.

Another hypothesis is that the Prairie Flats uranium deposit is a more recent phenomenon associated with agricultural development in Prairie Valley. Cultivation and construction activity may have prompted a release of uranium from rocks and sediments, which were flushed down Prairie Valley by increased volumes of groundwater and surface runoff from irrigation and reservoir leakage. Upon arrival at the Prairie Flats, this water maintained the marshy conditions and which are responsible for the accumulation of peat. Still, this theory can be disputed by the facts that:

1. Analyses of the U^{238}/Th^{230} activity ratios by Levinson (1984) of peat cores taken from the flats conclude that the uranium has been in place for at least 2000 years.

2. Many other surficial uranium deposits analogous to the Prairie Flats deposit have
   been discovered in the Okanagan Valley, many in isolated areas unaffected by
   agricultural development.

Obviously, further research is required to better define the timing of uranium deposition
at the Prairie Flats. Further isotopic analysis of the uranium and carbon dating of the peat
layer would help to resolve whether they accumulated simultaneously or at different
times. A more thorough historical analysis of glacial and anthropogenic activity in this
valley would also be useful.

SUMMARY

This chapter provides evidence that Prairie Flats is a discharge zone for groundwaters
recharged within or just outside the Summerland basin. These groundwaters encounter
carbonate minerals along short, shallow flow paths to the site, which upon discharge
neutralize the acids generated in the peat. Piper plots show that Prairie Flats
groundwaters and other local groundwaters are similar in chemical composition.

A simple hydrologic budget for the Prairie Flats suggests that evapotransporation in the
summer, and groundwater storage in the winter are the prevalent sinks for discharging
groundwaters. Also, the rate of uranium deposition appears to be much smaller today
than in the past. Today's estimated discharge rates are on the order of 9450 m^3/year,
which when combined with maximum incoming uranium concentrations of 100 μg/L,
give an incoming uranium flux of 0.95 kg/year, at least ten times less than the average
rate estimated from the size and age of the deposit. It is proposed that uranium
deposition rates were higher in the past than they are today, however further scientific
investigation is needed to confirm this hypothesis.

6 URANIUM GEOCHEMISTRY

This chapter summarizes the geochemical behaviour of uranium in natural groundwater environments. This information is used to form hypotheses on the nature of uranium fixation at the Prairie Flats based on the geochemical data collected in this thesis. The first section looks at how uranium mobility is enhanced by complexation with soluble species, especially carbonate. The next section presents processes that fix uranium, such as adsorption, reductive precipitation, evaporative precipitation, and microbial assimilation. Most of this material is taken from laboratory studies with peat.

6.1 MOBILE URANIUM

Uranium exists in two valence states in nature: U^{6+} and U^{4+}. U^{4+} exists in primary ore-forming uranium minerals such as uraninite (UO_2), pitchblende (amorphous UO_2) and coffinite ($USiO_4$). These minerals are highly insoluble in reducing groundwaters. However, upon contact with relatively oxygenated waters, U^{4+} is oxidized to U^{6+} and is released into solution as the uranyl (UO_2^{2+}) ion.

Uranyl readily forms soluble complexes with oxygen-bearing ligands (eg. CO_3^{2-}, SO_4^{2-}, PO_4^{2-}, F^{2-}, OH^-), thereby enhancing its mobility in aqueous environments. In the pH range of most groundwaters (5 to 7), uranyl carbonate complexes are the most important. Uranyl dicarbonate ($UO_2(CO_3)_2^{2-}$) and uranyl tricarbonate ($UO_2(CO_3)_3^{4-}$) form at pH 4.5 and well into the alkaline range. They are also highly stable, with stability constants on the order of 10^{17} and 10^{22}, respectively (Langmuir, 1997, p. 552). This stability and their negative charge make them highly mobile and resistant to processes like adsorption. The stability constant (or formation constant) of a complex is the equilibrium constant, K, for the reaction of a metal with its ligands to form a metal-ligand complex. For example, the equilibrium constant for the reacton $UO_2^{2+} + 2CO_3^{2-} = UO_2(CO_3)_2^{2-}$, is equal to $A_{UO2(CO3)2}/(A_{UO2})(A_{CO3})^2$, where A is the activity of each species.

Uranyl phosphate complexes are also highly stable in the pH range of 4 to 9, with stability constants on the order of 10^{14} for $UO_2PO_4^-$ and 10^8 for $UO_2HPO_4^0$ (Langmuir, 1997, p. 552). Phosphate can compete with carbonate only when phosphate concentrations are significantly enriched (ie. $[PO_4^{3-}]_T/[CO_3^{2-}]_T > 0.1$), which is unlikely in most natural groundwater environments (Sandino and Bruno, 1992).

6.2   IMMOBILE URANIUM

In the absence of solubilizing ligands such as carbonate, uranyl can be removed from solution by a variety of mechanisms:

(1) adsorption onto organics

(2) adsorption onto inorganics

(3) reduction and precipitation of uranium minerals

(4) precipitation by evaporation

(5) microbial assimilation

Each of these is discussed in detail in the following sections:

Adsorption onto Organics

Field and laboratory studies present many examples of uranium adsorption onto organic-rich soils (Owen and Otton, 1995; Shotyk, 1988; Lopatkina, 1967; Szalay, 1964). The superior ability of organic molecules to adsorb uranium is attributable to their large surface area and abundance of negatively charged ligands which attract UO_2^{2+}. The term "adsorption" as it is used here implies a chemical complexation or ion exchange process as opposed to purely physical adsorption on molecular surfaces.

Organics are concentrated in the humus layer of soils, which is a dark material made up of decaying plant and animal matter. Humus has three main constituents: humic acid,

fulvic acid, and humin, which are defined behaviourally. Fulvic acid is soluble at all pH values, and humin is insoluble at all pH values. Humic acid is insoluble under acid conditions (pH < 6) but soluble under alkaline conditions.

During adsorption to organics, most of the uranium is retained by humic acid (Kochenov et al, 1965; Shanbhag and Choppin, 1981), which exchanges H^+ ions on its carboxyl groups for UO_2^{2+} ions (Szalay, 1964; Borovec et al., 1979; Idiz et. al, 1986). Published stability constants for uranyl-humic acid complexes are on the order of 10^5 to 10^8 for 1:1 complexes and 10^9 to 10^{12} for 1:2 complexes (Kribek and Podlaha, 1980; Shanbhag and Choppin, 1981).

Conditions affecting Uranium Adsorption onto Organics

The optimum pH for uranium adsorption onto humic acids is between 4 and 6 (Manskaya et. al 1956; Shanbhag and Choppin, 1981). In sorption experiments with peat, Lopatkina (1967) noted a sharp decline in uranium retention under more alkaline conditions. Between pH 6 and 7.2, nearly all the uranium was adsorbed; at pH 7.8 about one half was adsorbed, and at pH 8.3, none was absorbed. This loss of sorptive capacity at alkaline pH is attributable to the peptization or dissolution of humic acids (Titayeva, 1967) and to the appearance of other complexing agents that scavenge uranium (eg. hydroxides and carbonates).

Uranium sorption rates decrease with increasing dissolved uranium concentration according to a Langmuir adsorption isotherm (Borovec et al, 1979; Szalay, 1964). The Langmuir isotherm relates quantities sorbed to quantities in solution by means of the expression:

$$X/C = bX_m/(1 + C_b) \tag{6.1}$$

where X is the quantity adsorbed (mol/g), C is the quantity in solution at equilibrium (mol/L), b is the binding constant of the substrate (L/mol), and X_m is the sorption

capacity of the substrate (mol/g). Another constant, called the geochemical enrichment factor (G.E.F.), is the slope of the tangent of the isotherm (X/C) at low dissolved U concentrations. These are all shown graphically in **Figure 6-1**.
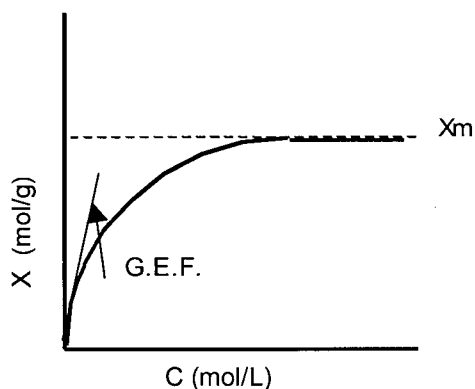
Figure 6-1 A Langmuir Adsorption Isotherm

The sorption capacity for uranium on peat is around 2 to 3 meq/g (Szalay, 1964), and "near perfect" G.E.F.'s on the order of 10,000:1 have been reported (Szalay,1964; Idiz et al.1986; Owen and Otton, 1995).

Adsorption onto Inorganics

Studies of uranyl adsorption onto iron oxides and iron oxyhydroxides generally conclude that adsorption increases with increasing pH between pH 5 and 8.5 (Langmuir, 1997, p. 509). Typical G.E.F.'s for uranyl on amorphous Fe oxyhydroxides and on goethite are on the order of 10^6 and 10^3 respectively (Langmuir, 1978). Uranyl adsorption onto clays is weak at best, for example montmorillonite and kaolinite have G.E.F.'s of only 6 and 2 (Langmuir, 1978).

Where organics and inorganics are present together, organics will dominate and adsorb most of the uranium. Lopatkina (1967) collected both organic and inorganic material from a uranium-rich peatland and found the sorptive capacity of the organic material to

be 10 to 100 times greater. Idiz et al. (1986) found uranium to be preferentially sorbed to the organic fraction in bog sediments despite the presence of Fe and Mn oxides.

Reductive Precipitation of Uranium Minerals

The oxidation of organic matter during peat diagenesis creates oxygen depleted, relatively reducing conditions that are ideal for the reductive precipitation of uranium to coffinite ($USiO_4$), uraninite (UO_2), or pitchblende (amorphous UO_2). Reducing agents can be the organic matter itself, Fe^{2+} minerals such as pyrite or marcasite, or mobile H_2S, CH_4, or Fe^{2+} in the peat (Langmuir, 1997, p.509). This reduction of U^{6+} to U^{4+} is a two step process. The reaction $UO_2^{2+} \rightarrow UO_2^{+}$ is instantaneous, whereas $UO_2^{+} \rightarrow U^{4+}$ is slower because a U-O bond is broken (DeVoto, 1978, p.4). Therefore reductive precipitation of uranyl is a slower and less reversible process than adsorption.

In peatland environments it has been suggested that adsorption and reduction work together in fixing uranium (Andreqev & Chumanchenko, 1964), with adsorption serving to preconcentrate the uranium so that the slower process of reductive precipitation can proceed. Langmuir (1978) states that "whereas mineral solubilities limit only maximal uranyl concentrations, sorption limits uranyl concentrations at all levels below saturation with the least soluble mineral in a given water." Furthermore, if reduction does not follow adsorption, uranyl can be desorbed by an increase in alkalinity at constant pH, or by raising the pH (Langmuir, 1997, p 509).

Most naturally-occurring uraninites have chemical formulas between $UO_{2.00}$ and $UO_{2.67}$ (Langmuir, 1997, p. 505) due to partial oxidation after precipitation (Langmuir, 1978). **Figure 6-2** shows the stability fields of these species, which overlap with those conditions commonly found in groundwater.

71
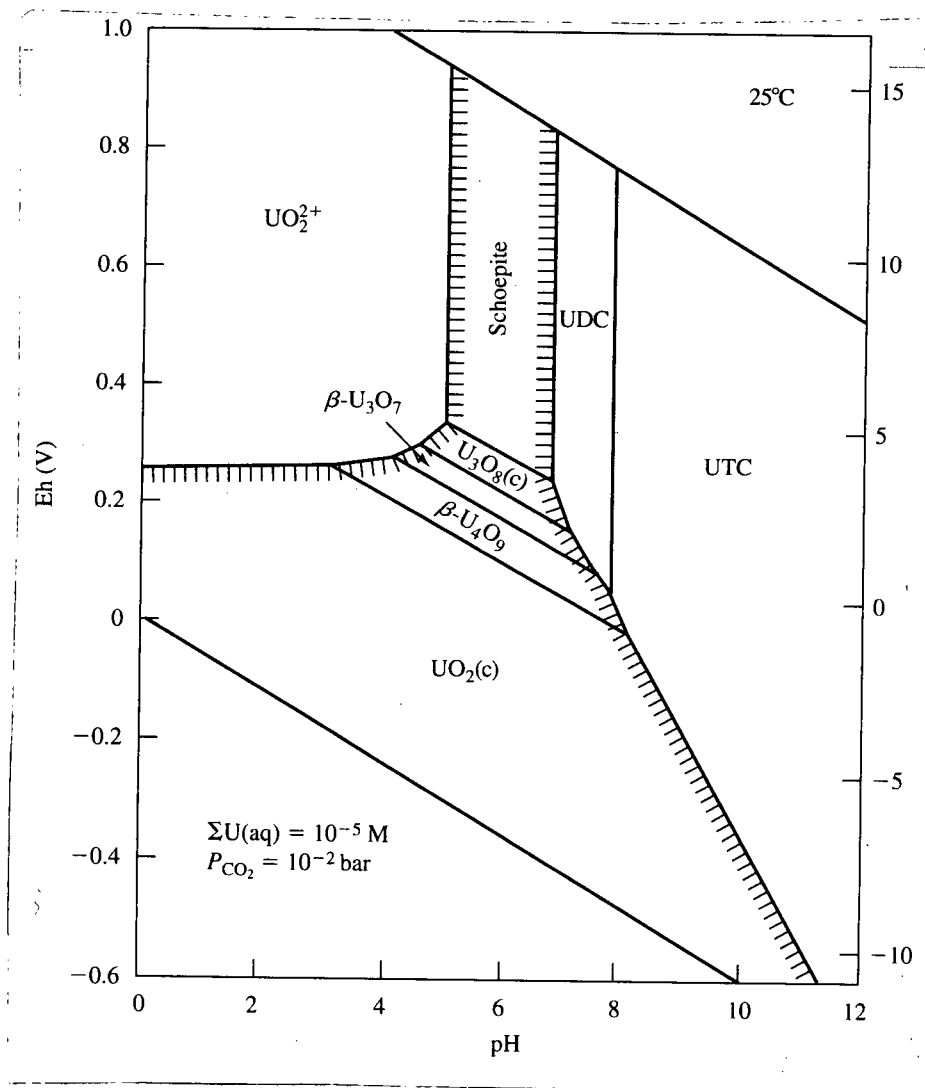
Figure 6-2 Eh-pH diagram for aqueous species and solids in the system $U\text{-}O_2\text{-}CO_2\text{-}H_2O$ at 25 °C and 1 bar total pressure. Solid/aqueous boundaries (stippled) are drawn for $\Sigma U = 10^{-5}$ M. UDC and UTC are $UO_2(CO_3)_2^{2-}$ and $UO_2(CO_3)_3^{4-}$ respectively. From Langmuir, 1997, p. 505.

Evaporative Precipitation

Uranyl minerals (U^{6+}) can be formed by evaporative concentration of uranyl under arid conditions. Some of the most common minerals, in order of decreasing solubility, are schoepite (β-$UO_3 \cdot 2H_2O$), autinite ($Ca(UO_2)_2(PO_4)_2$), carnotite ($K_2(UO_2)_2(VO_4)_2$) and tyuyamunite ($Ca(UO_2)_2(VO_4)_2$). While carnotite and tyuyamunite precipitate at concentrations in the ppb range, shoepite requires concentrations in the ppm range. Except for carnotite and tyuyanmunite, uranyl minerals are not known to form extensive deposits and are limited to very arid environments and low-CO_2 waters (Langmuir, 1997, p. 497).

Microbial Assimilation of Uranium

Microbes play a part in retaining uranium both directly and indirectly. Indirectly, they help to degrade plant material to produce peat, whose high surface area and high organic content enhance uranium adsorption (Robbins et. al 1990). Humic material also provides carbon energy sources for sulfate-reducing bacteria. These organisms take SO_4 dissolved in groundwater and produce H_2S, which in turn reduces U^{6+} to U^{4+}.

Further studies have shown that sulfate-reducing bacteria, such as the *Desulfovibrio desulfuricans* can also directly assimilate uranium. Mohagheghi et al. (1984) postulated that this may be due to the ability of their cell walls to adsorb uranium, thereby holding it in place during the more sluggish reduction step. In work with marine sediments, Lovely et al. (1993) later demonstrated that the *Desulfovibrio desulfuricans* can precipitate uraninite directly from solution through enzymatic mechanisms.

SUMMARY

The speciation and mobility of uranium is controlled by many factors: redox, pH, its concentration in solution, and the presence of complexing ligands. Uranium is most mobile in oxygen-rich, carbonate-bearing waters having a neutral to alkaline pH. Under these conditions uranium as U^{6+} is complexed with carbonate as uranyl dicarbonate and uranyl tricarbonate.

In peaty groundwater environments where the pH is between 4 and 6, organics can overcome the uranyl-carbonate complex and thereby immobilize uranium. Organics contribute humic acid ligands which adsorb uranium, and also foster a reducing environment. Uranyl which is initially adsorbed may be reduced to a U^{4+} mineral by the organic matter itself, by mobile reductants such as H_2S and Fe^{2+}, or by microbial processes. Other fixation mechanisms such as adsorption on colloidal iron oxides and evaporite formation are less important in such organic-rich environments.

7 DISCUSSION OF GROUNDWATER GEOCHEMISTRY AND URANIUM DEPOSITIONAL CONTROLS

This chapter begins with a discussion of key processes which control the geochemistry of Prairie Flats groundwaters, based on the aqueous geochemical data collected on site. These controls include carbonate mineral-solution equilibria, redox reactions, and evapotranspiration. Next, their role in uranium retention via adsorption, reductive precipitation, and evaporative precipitation is addressed. Redox conditions may further explain uranium concentration near ground surface, and the hydrogeology offers new insights on its lateral distribution. Finally, the issue of uranium remobilization due to cultural inputs is addressed using two field observations.

7.1 CONTROLS ON THE GROUNDWATER GEOCHEMISTRY

Carbonate Mineral-Solution Equilibria

Chemical analyses of Prairie Flats groundwaters show that carbonate mineral-solution equilibria exert a major control on the groundwater chemistry. Bicarbonate concentrations are relatively high, averaging between 500 and 650 mg/L. This maintains the pH in a neutral range of 6.0 to 7.8, and accounts for the high acid-neutralizing capacity. Bicarbonate likely comes from the incorporation of soil CO_2 in groundwater recharge zones and the subsequent dissolution of carbonate minerals during groundwater migration to the site.

Of these carbonate minerals, calcite is a likely source of HCO_3. In a plot of HCO_3 vs pH (see **Figure 7-1**), most samples plot on or slightly above the saturation line with respect to calcite. Similarly, PHREEQC calculations give saturation indices with respect to calcite of between -0.5 and +0.5 (see **Appendix F**). The linear relationship between HCO_3 and Ca also suggests that calcite is the main source of HCO_3 (see **Figure 7-2**).

Calcite is preferred over dolomite since the Ca to Mg ratios are consistently 2 or more, whereas in equilibrium with dolomite they would be closer to unity (Langmuir, 1997, p. 209).
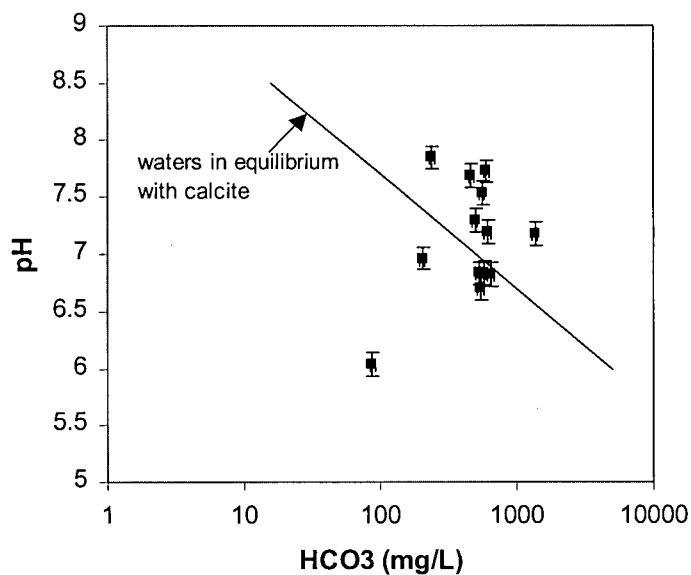
Figure 7-1 Plot of Prairie Flats groundwaters in relation to waters undergoing open system dissolution of calcite with P_{CO2} of $10^{-1.5}$ atm
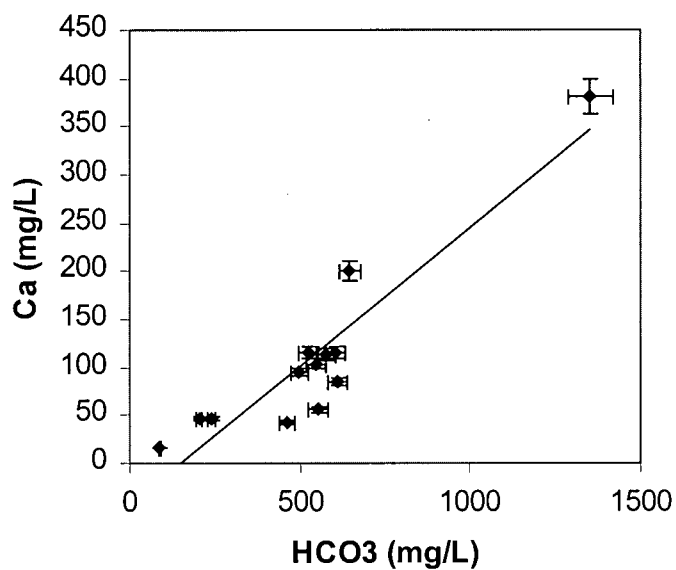
Figure 7-2 Relationship between HCO_3 and Ca in Prairie Flats groundwaters, suggesting calcite as a source of HCO_3

Redox Conditions

Three methods were used to interpret redox conditions in Prairie Flats groundwaters. First, Eh was measured directly using a redox probe. Second, concentrations of redox-sensitive species, namely NO_3, SO_4 and Fe^{2+} were compared with the redox reaction sequences introduced by Froelich et al. (1978). Lastly, measured pH's and Fe^{2+} concentrations were used to calculate Eh assuming equilibrium with ferrihydrite, $Fe(OH)_3$, also referred to as hydrous ferric oxide, $Fe(OH)_3 \cdot nH_2O$ or HFO.

Eh measurements

Meaningful measurements of Eh using platinum electrode redox probes have been obtained for groundwaters enriched in iron (Langmuir, 1997 p. 411). However, since no correlation was found between measured Eh and dissolved Fe^{2+} concentrations (see **Figure 7-3**) the Eh measurements were discarded due to suspected fouling of the platinum electrode by organics.
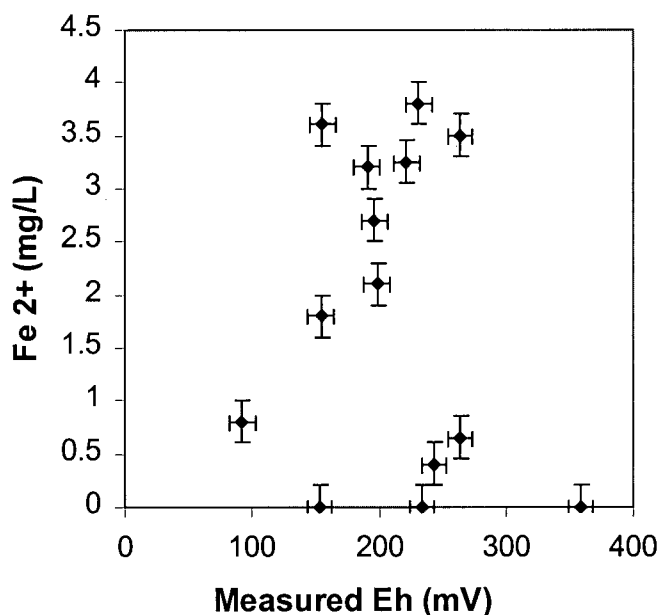
Figure 7-3 Inconsistency between measured Eh and Fe^{2+} concentrations in Prairie Flats groundwaters

Redox Reaction Sequences

Froelich et al. (1978) indroduced a series of redox reactions that occur during organic diagenesis in upper marine sediments. Assuming that organic matter is the principal electron-donor, O_2, followed by NO_3, Fe_2O_3 or $FeOOH$, MnO_2, SO_4 are subsequently reduced in order of greatest free energy yield. Thus under equilibrium conditions, each redox-sensitive species is expected to exist only within a particular Eh range. The same applies to microorganisms that act as mediators or catalysts in these redox reactions, including aerobic heterotrophs, denitrifiers, sulfate-reducers, and so on (Stumm and Morgan, 1981, p. 458).

Based on Froelich's redox reaction series, Berner (1981, p. 359-365) illustrates how concentrations of various redox-sensitive species are expected to vary within the sediment column, from oxic conditions near the surface to anoxic conditions at depth. Stumm and Morgan (1981, p. 460) assigned an Eh scale to the same sequence of reactions (see **Figure 7-4a**). Thus, by replacing Berner's "depth" axis with Stumm and Morgan's "Eh" scale, we can assign an approximate Eh range to a water sample based on the subset of redox-sensitive species present. This is illustrated in **Figure 7-4b**.

At the Prairie Flats, NO_3, SO_4, and Fe^{2+} concentrations were measured at each of the four nested piezometer pairs, and plotted versus depth in **Figure 7-5**. SO_4, NO_3, and Fe^{2+} were found together just below the water table, which from **Figure 7-4** is possible only between roughly -150 and +50 mV. About one metre below that, Fe^{2+} has disappeared and only SO_4 and NO_3 remain, corresponding to an Eh of between +50 and 250 mV. Dilution by incoming groundwaters can not account for the disappearance of iron in the till unit because measurable amounts of SO_4 and NO_3 are still present.
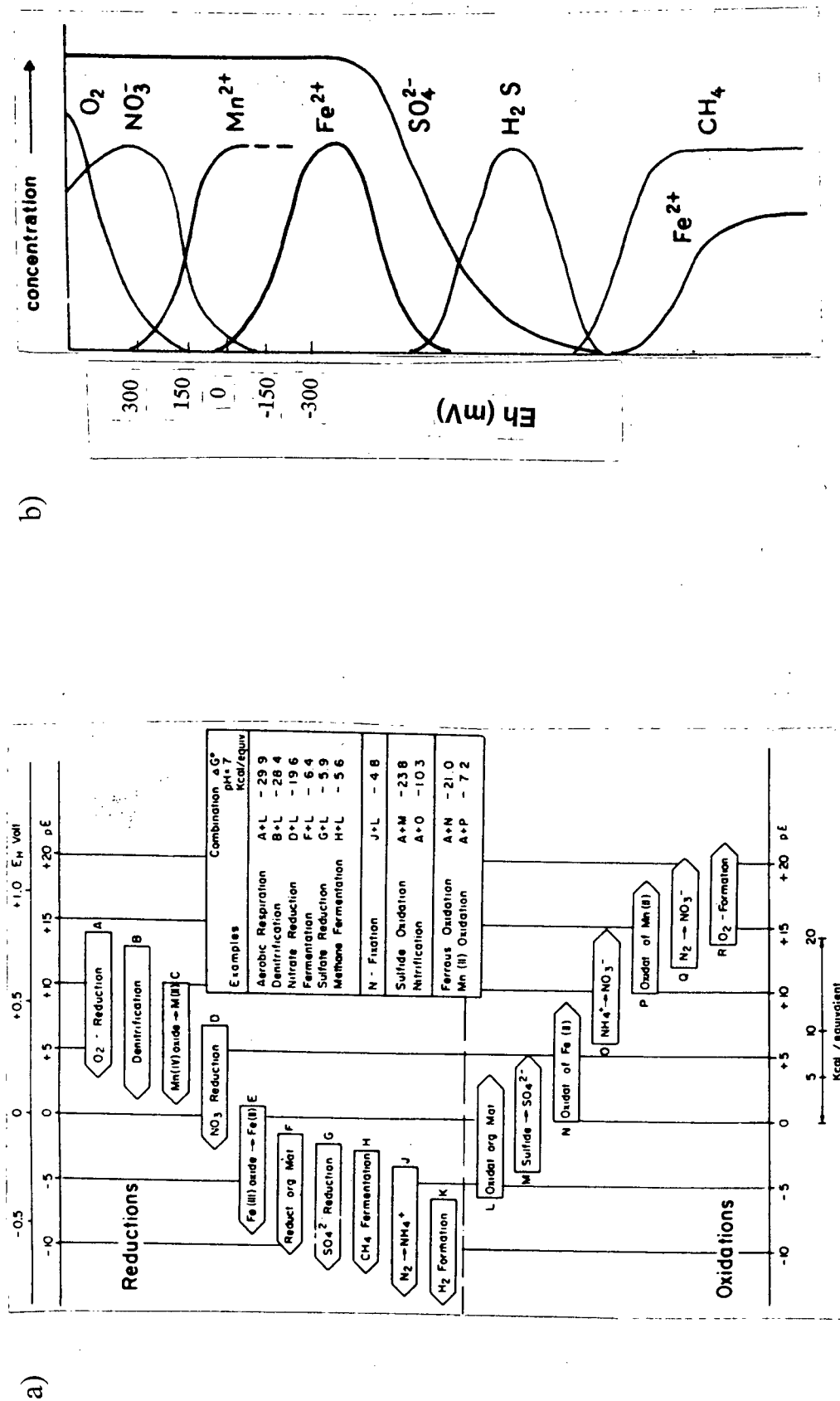
Figure 7-4 a) Sequences of important redox processes at pH 7 in natural systems, from Stumm and Morgan, 1981 and b) Berner's (1971) plot of changes in groundwater composition with depth, with depth scale replaced by an Eh scale according to a)

a)

b)
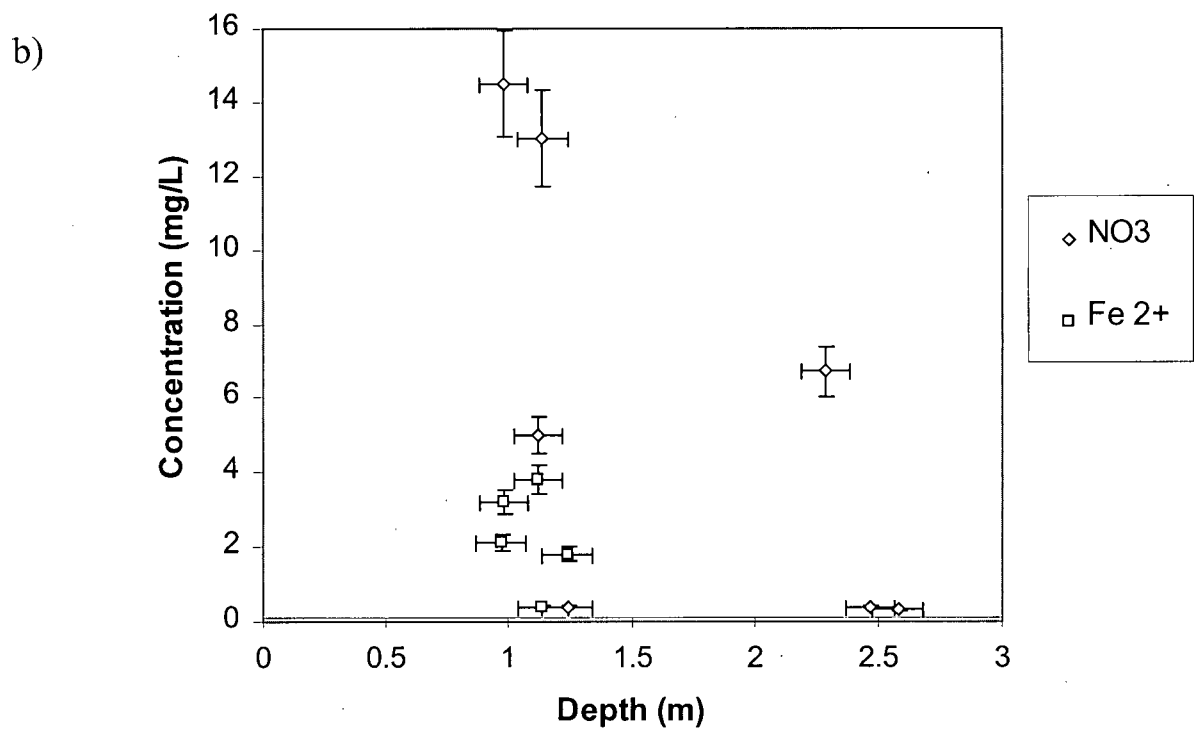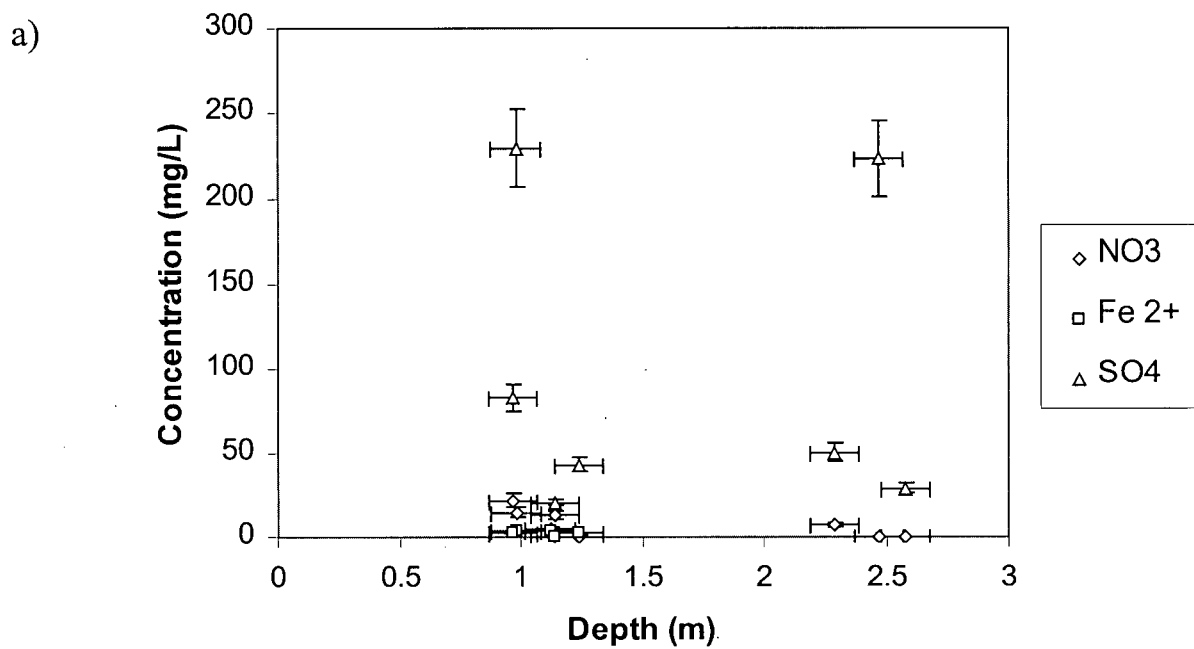
Figure 7-5 Change in concentration of a) NO_3, Fe^{2+}, and SO_4 with depth in Prairie Flats groundwaters and b) showing NO_3 and Fe^{2+} only at a smaller vertical scale

Still, it is unusual to find NO_3 and Fe^{2+} together since NO_3 is a strong oxidant capable of oxidizing Fe^{2+} according to the reaction:

$$10Fe^{2+} + 2NO_3^- + 14H_2O \rightarrow 10FeOOH + N_2 + 18H^+ \qquad (7.1)$$
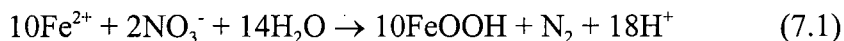
One explanation for the persistence of NO_3 is its introduction at ground surface in amounts that exceed the immediate reducing capacity of the soil. Nitrate concentrations in the 10's of mg/L (as measured at piezometers 202, 502, 602 and 902) are much greater than the 0.1 mg/l typical of peat environments (Shotyk, 1988), pointing to fertilizer and manure application up Prairie Valley as likely sources of NO_3. The formation of intermediates like NO_2^-, NO and N_2O before N_2 may also slow this reduction step. At the same time, Fe^{2+} may be continuously regenerated by the dissolution of Fe^{2+} bearing minerals and the reduction of Fe-oxyhydroxides in the soil.

Fe^{2+} / Ferrihydrite Equilibria

Langmuir (1997, p. 436) states that in aquatic environments, the oxidation of Fe^{2+} forms ferric hydroxides and oxyhydroxides that are mixtures of amorphous material and goethite (α-FeOOH). The amorphous material is most commonly ferrihydrite - $Fe(OH)_3$. Iron-oxidizing bacteria can catalyze its production (Steinmann and Shotyk, 1997), and soil horizons rich in carbon will preferentially precipitate ferrihydrite before goethite, hematite, and lepidocrocite (Schwertmann et al, 1986). Colloidal mixtures of ferrihydrite and organic matter produce a thin "oily" film on puddles of water at ground surface, as was observed by the author at the Prairie Flats (see **Plate 7-1**).

10cm _____

Plate 7-1   Oily film on puddled water on the flats, thought to be a mixture of ferrihydrite and organic matter

Therefore ferrihydrite is believed to be in equilibrium with the redox environment of the Prairie Flats peats according to the reaction:

$$Fe^{2+} + 2H_2O \leftrightarrow Fe(OH)_{3(am)} + 3H^+ + e^- \qquad (7.2)$$
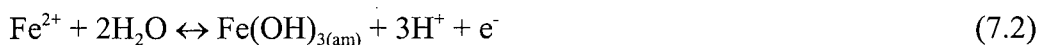
Eh was calculated using:

$$Eh = E_0 - 0.18pH - 0.0592 \log a(Fe^{2+}) \quad E_0 = 0.975 \text{ V to } 1.06 \text{ V}$$

(Langmuir, 1997, pp. 417,437,482) $\qquad (7.3)$

The value of E_0 is difficult to pinpoint since it depends on the mass ratio of ferrihydrite to other species in the precipitate (eg. goethite), and on its degree of crystallization. The solubility product (K_{sp}) of a mineral is defined as the equilibrium constant for the dissolution of a solid salt to give its ions in solution. For the reaction $M_mN_{n(s)} \leftrightarrow mM^{n+} + nN^{m-}$, the K_{sp} is equal to $(A_M)^m(A_N)^n$ where A is the activity of each species. The K_{sp} for ferrihydrite can range from 10^{-37} to 10^{-39} M (moles/L), higher for fresh precipitates and lower for more crystallized forms. A K_{sp} of 10^{-37} corresponds to an E_0 of 1.06, and for a K_{sp} of 10^{-39}, E_0 is 0.975 (Langmuir, 1997, pp. 417, 437, 482). Since the water chemistry data offer no means of distinguishing the crystal nature of ferrihydrite, a mean E_0 of 1.02 was used to calculate the Eh value of each water sample. These were assigned error bars of $\pm$ 0.0425 V, which correspond to the maximum and minimum E_0 values. For those showing no detectable iron, the default Eh of 240 mV was chosen, which corresponds to relatively oxygenated waters (Langmuir, 1997, p. 411).

Calculated Eh values are plotted against depth in **Figure 7-6**. Redox potentials in the peat unit just below the water table generally lie between -100 and 200 mV, and in the till unit underlying the peat, between 50 and 250 mV. This gives an overall Eh range of between −100 mV and 250 mV, which is the same as that inferred from the redox reaction sequences.
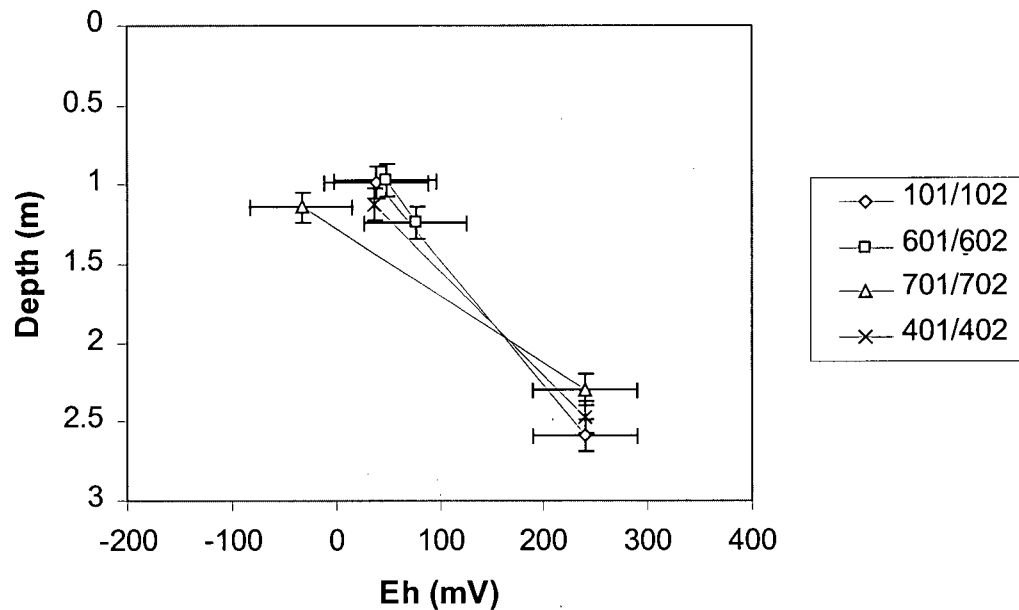
Figure 7-6 Depth-Eh plot showing relatively reducing groundwater conditions in the peat unit and relatively oxidizing conditions in the underlying till unit

In summary, both methods of determining redox conditions indicate conditions to be relatively more reducing near surface than at depth. This is due to a combination of two processes: 1) the intense degradation of organic matter in the root zone and just below the water table which sets up an oxygen-poor and relatively reducing environment, and 2) the upward discharge of relatively oxygenated groundwaters from the till unit below the peat. Consistent upward hydraulic gradients measured at the piezometers pairs together with the consistent absence of dissolved Fe^{2+} in the deep piezometers confirm the second process. Eh values probably continue to decrease with depth below the water table, but at some point undergo a redox reversal upon encountering the zone of influence of the discharging groundwaters.

Evapotranspiration

At all piezometer pairs the major ions were found to generally increase in concentration towards ground surface, as shown in **Figure 7-7** and **Figure 7-8**.

If evapotranspiration were the cause of this upward increase in ion concentration, these ions would show the same rate of enrichment as Cl, which is a conservative species. Thus, a histogram of the percent increase in concentration over depth, normalized by that of Cl was constructed (see **Figure 7-9**). From the histogram, it is evident that HCO_3, Ca, Mg, Na, and K are being concentrated by evapotranspiration. The fact that HCO_3 shows the same pattern as these other ions further proves that the Prairie Flats is a groundwater discharge zone. If this were a recharge zone, a more dramatic increase in HCO_3 would be expected due to the incorporation of CO_2 during infiltration, which is produced by root respiration and the oxidation of organics.

Upward increases in NO_3, SO_4, and Fe^{2+} concentrations are more acute than for Cl due to the change in redox environment between the peat unit and the underlying till. Also, the fact that NO_3 and Fe^{2+} underwent more drastic declines than SO_4 indicates that conditions just below the water table are not more reducing than -250 mV, since this is the point at which SO_4 reduction is initiated. Greater changes in dissolved U concentration relative to Cl may be explained by desorption or redissolution of fixed U.
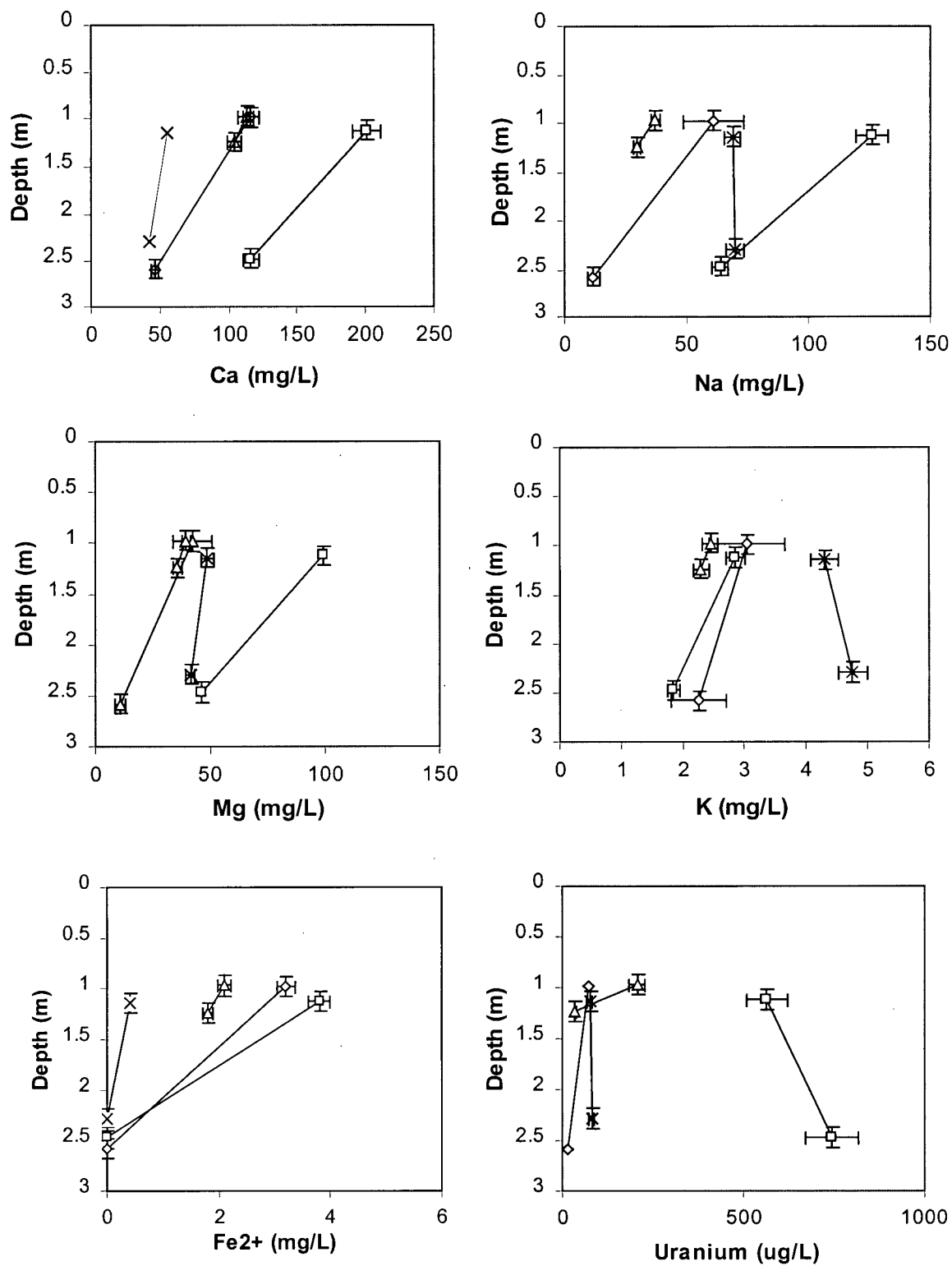
Figure 7-7 Increase in concentrations of Ca, Na, Mg,K, Fe$_{TOT,}$ and U towards ground surface in Prairie Flats groundwaters
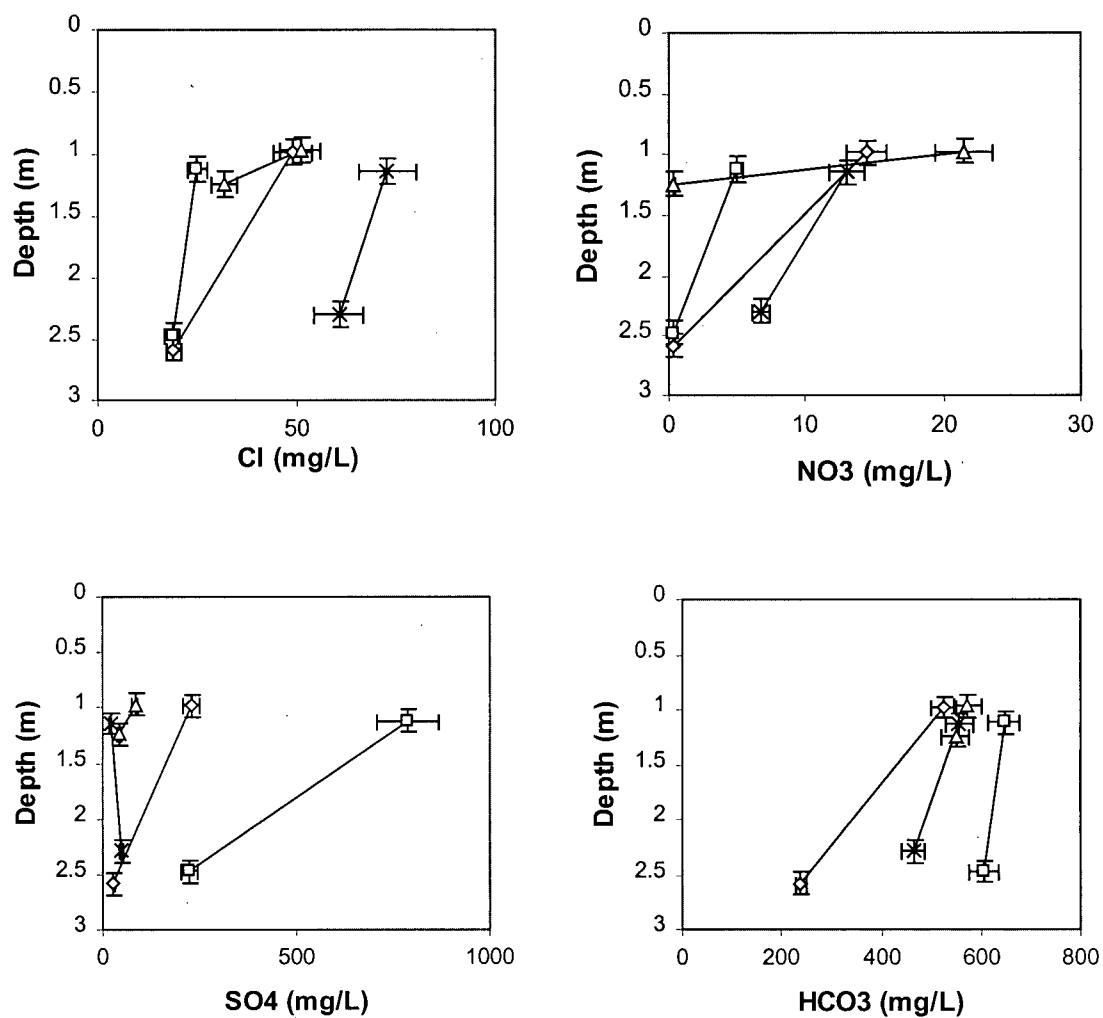
Figure 7-8 Increase in concentrations of Cl, NO3, SO4, and HCO3 towards ground surface in Prairie Flats groundwaters
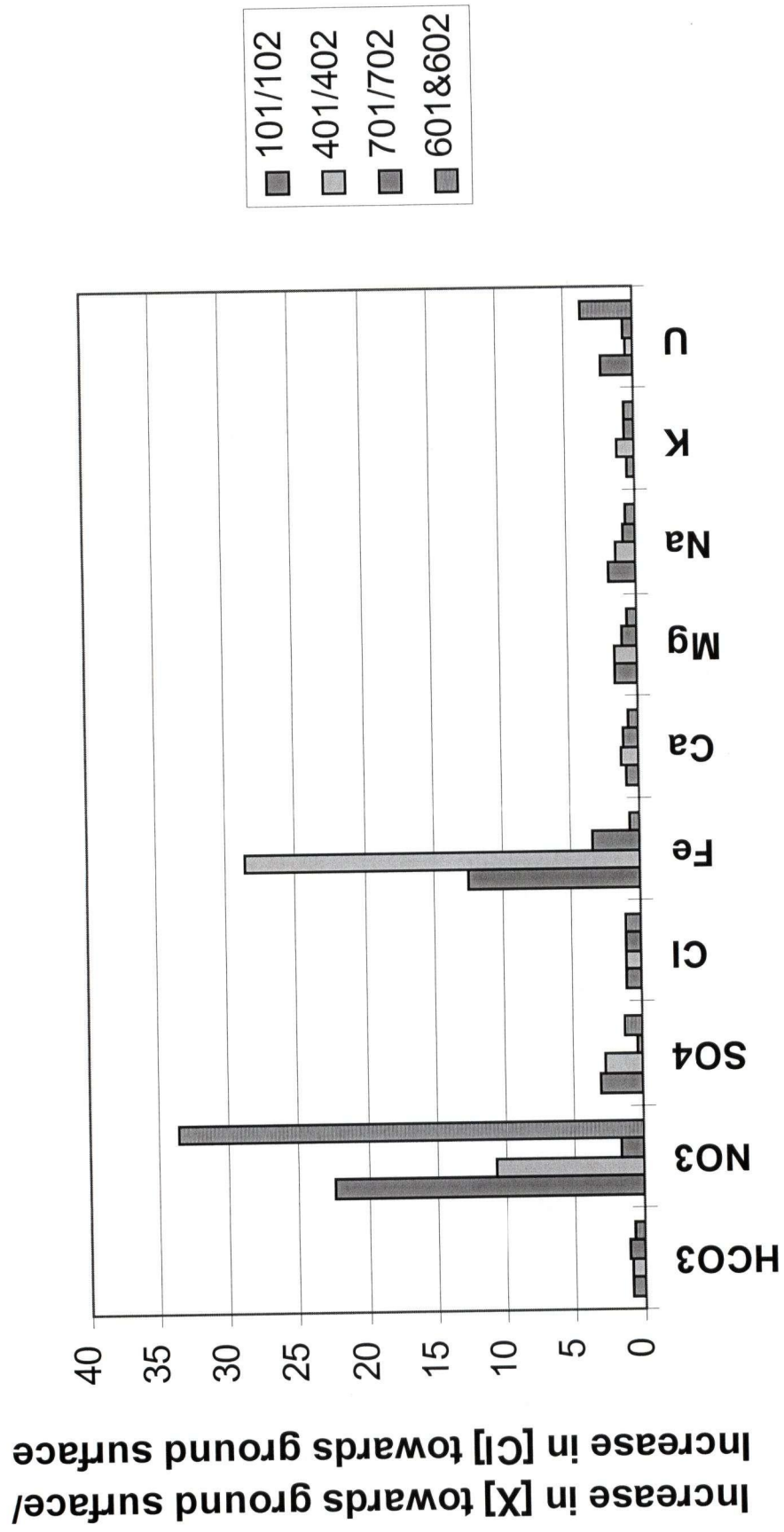
Figure 7-9 Upward concentration of dissolved groundwater species in relation to Cl

Legend:
- 101/102
- 401/402
- 701/702
- 601&602

Y-axis: Increase in [X] towards ground surface/ Increase in [Cl] towards ground surface

X-axis categories: HCO3, NO3, SO4, Cl, Fe, Ca, Mg, Na, K, U

7.2 CONTROLS ON URANIUM FIXATION

Adsorption

Uranium adsorption refers to the replacement of a proton or other cation on a humic acid molecule by the uranyl ion, UO_2^{2+}. Adsorption is a relatively quick process, but not permanent, as UO_2^{2+} can later be desorbed from the exchange site. Indirect proof that U adsorption is occurring at this site comes from evidence of desorption. In brief, these observations include:

1) the detection of dissolved U in amounts that exceed background levels of ≈ 10 μg/L
2) increasing U levels in Prairie Creek from entrance (E) to exit (A) of the flats
3) a relationship between dissolved U and carbonate
4) a relationship between dissolved U and soil U

A review of the data presented in **Table 4-5** confirms the first two points. The last three require further explanation.

Dissolved U and Bicarbonate

Figure 7-10a plots dissolved U against HCO_3 concentrations measured in Prairie Flats groundwaters in March '98. Here, U values exponentially increase with increasing HCO_3, due to the high stability and poor sorptive behaviour of uranyl-carbonate complexes. Points falling below the line of best fit may denote U that is not easily desorbed, but rather is precipitated as a U^{4+} mineral.

The same relationship between dissolved U and HCO_3 can be inferred from the Sept '97 data set where U and conductivity were measured but HCO_3 was not. **Figure 7-10b** shows an exponential relationship between dissolved U and conductivity. The March

data set shows that conductivity is proportional to the HCO_3 concentration (see **Figure 10c**).
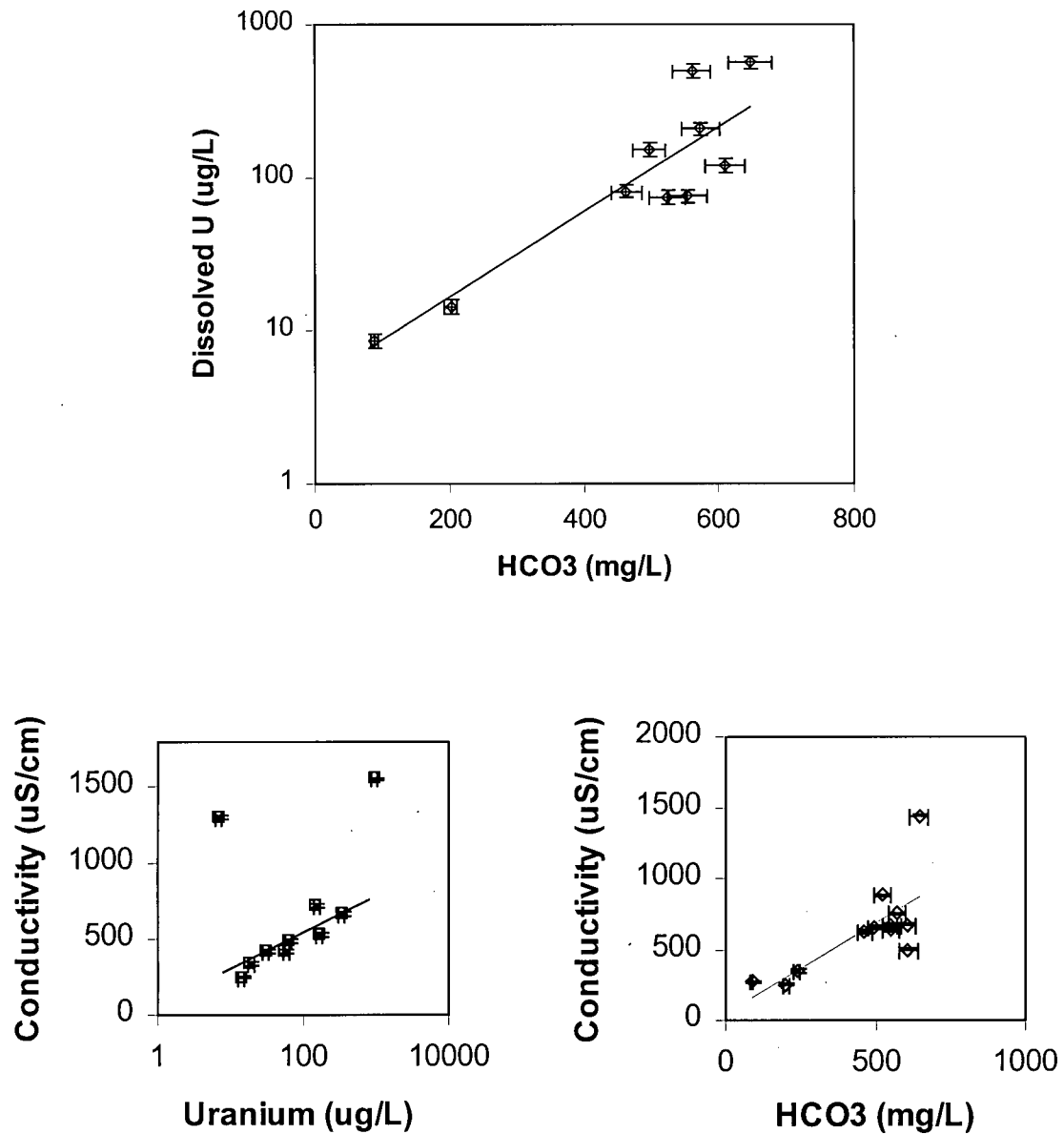
Figure 7-10 Evidence of uranyl-bicarbonate complexation in Prairie Flats groundwaters in (a) March '98 and (b) September '97, inferred from the (c) HCO_3- conductivity relationship found in March data

The relationship between dissolved U and HCO_3 is even more apparent when all of the field data, including spring and surface waters, is plotted (see **Figure 7-11**). Furthermore, speciation calculations using PHREEQC and a corrected version of the WATEQ4F database found dissolved U to be complexed predominantly with carbonate (see **Appendix F**). In these calculations, uranyl-carbonate complexes outnumbered uranyl-phosphate complexes by more than 10^3. Therefore other complexing agents, such as phosphate and dissolved organic acids play a negligible role in enhancing U mobility.
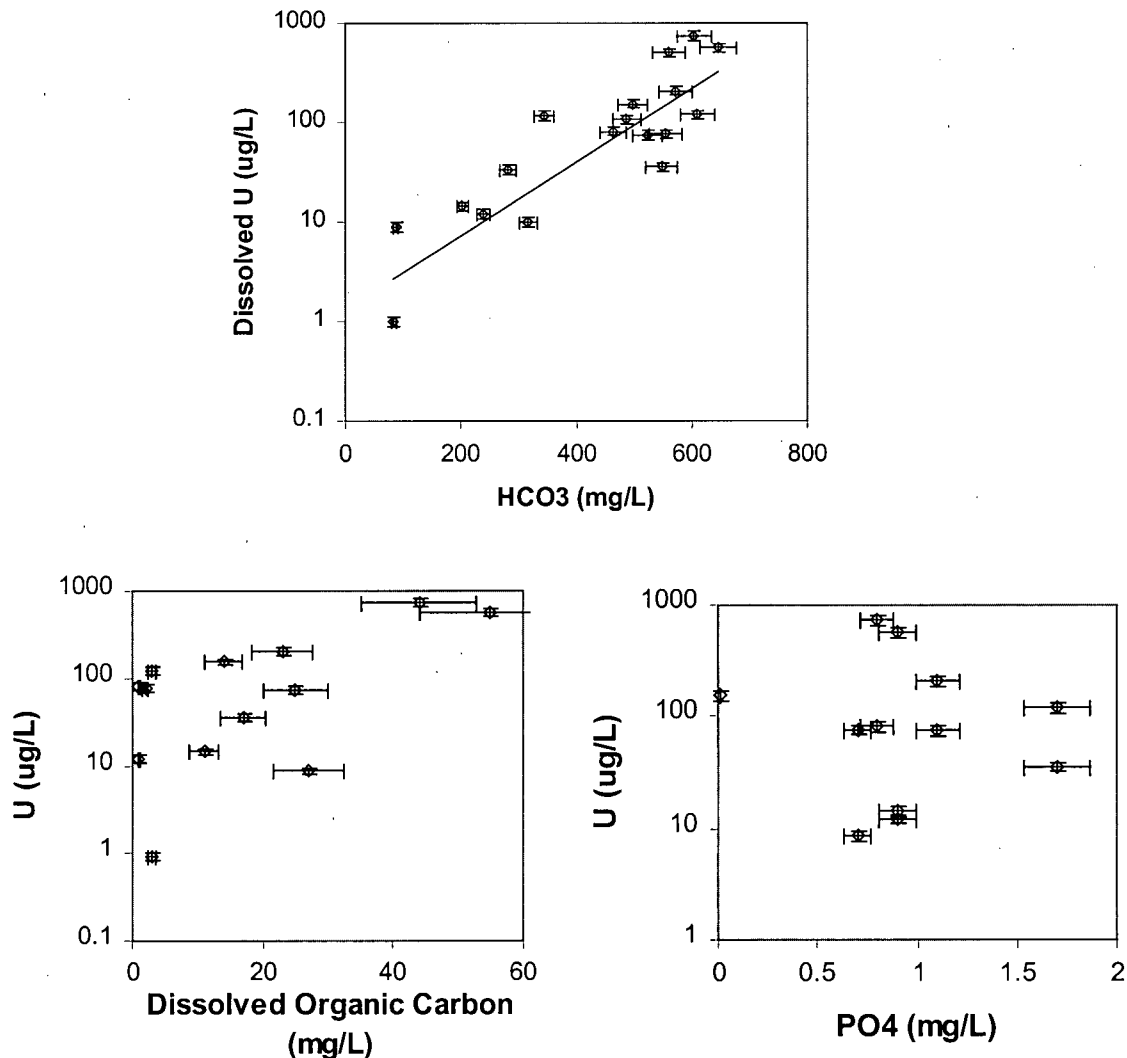
Figure 7-11 Evidence of uranyl-carbonate complexation in waters in and around Prairie Flats as opposed to complexation with dissolved organic carbon and PO_4

Dissolved U and Soil U

Carbonate-bearing groundwaters in prolonged contact with high concentrations of sorbed U would be expected to have higher concentrations of dissolved U. In this study, soil U concentrations nearest to the shallow piezometers were obtained from a soil survey of Prairie Flats by Culbert (1979). Graphs of soil U versus dissolved U for the Sept '97 and March '98 sampling rounds is shown in **Figure 7-12**. Both resemble Langmuir adsorption isotherms. The same relationship between soil U and dissolved U is illustrated in the contour plots of dissolved U concentrations shown in **Figures 7-13** and **7-14**. Dissolved U concentrations in Sept '97 are higher than those measured in March '98, probably because evapotranspiration rates are higher in late summer than in early spring. Like the soil U distribution shown in **Figure 1-3a**, the highest values are centred around piezometers 401/402 (**Figure 4-1**).

a)

b)
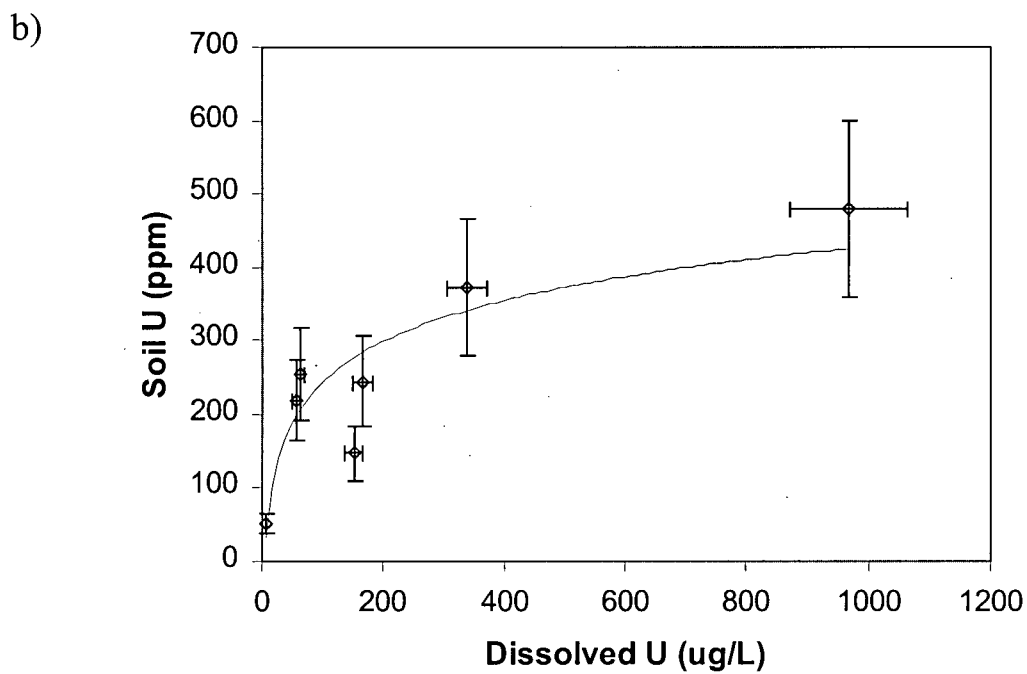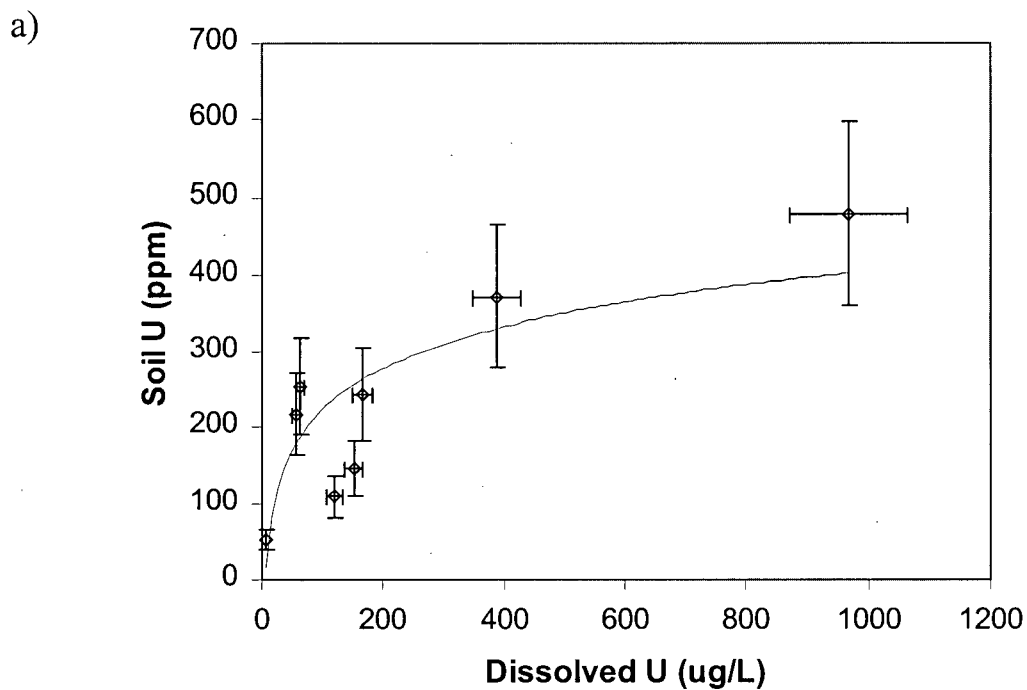
Figure 7-12 Relationship between soil U and dissolved U in a) March '98 and b) September '97
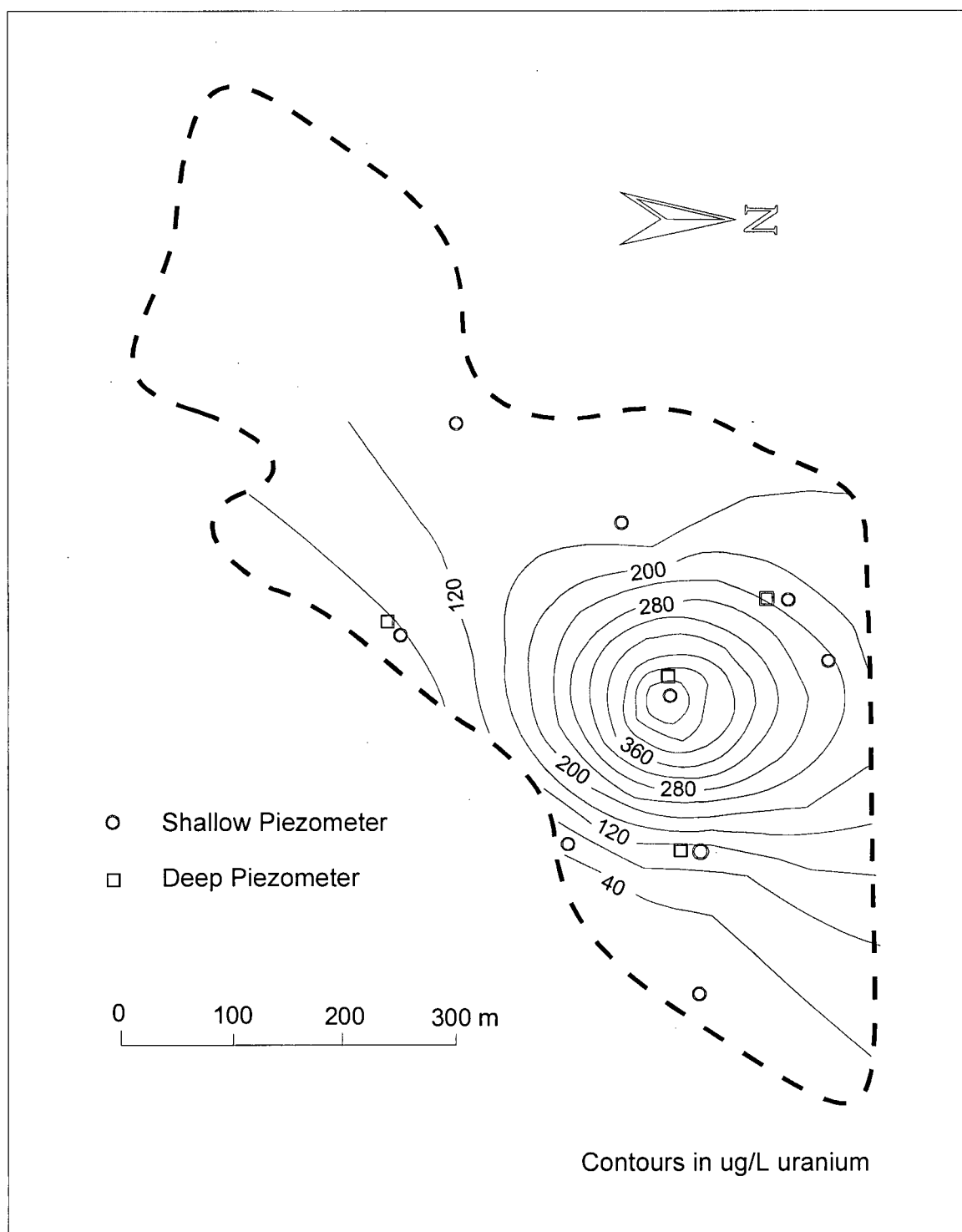
Figure 7-13 Contour plot of dissolved U concentrations (in µg/L) in shallow groundwaters underlying Prairie Flats (March '98)
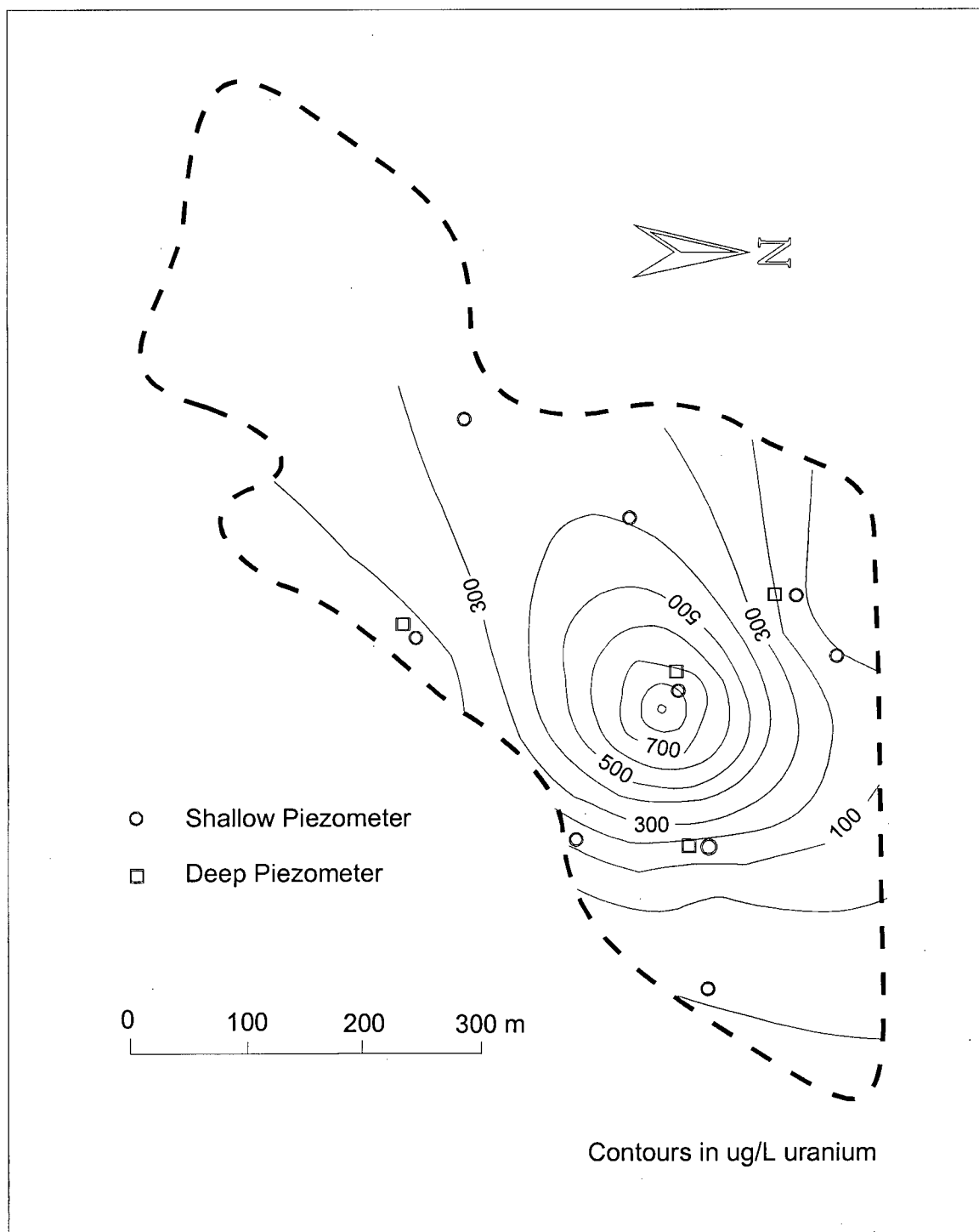
Figure 7-14 Contour plot of dissolved U concentrations (in μg/L) in shallow groundwaters underlying Prairie Flats (September '97)

Reductive Precipitation

In a reducing environment, the UO_2^{2+} ion may be reduced to U^{4+} and precipitate uraninite $(UO_{2(c)})$, pitchblende $(UO_{2(am)})$, or coffinite $(USIO_4)$, which usually occurs after adsorption. Reoxidation and resolubilization of U is impeded by sluggish reaction kinetics, thereby making it a more "permanent" means of U fixation than adsorption. Evidence of reductive precipitation can be drawn from an analysis of the aqueous geochemical data collected on site. These interpretive methods are detailed below.

Eh-pH Diagrams

Figure 7-15 is an Eh-pH diagram for the $U-O_2-CO_2-H_2O$ system that incorporates the mean dissolved U and HCO_3 concentrations of Prairie Flats groundwaters. Measured pH and calculated Eh values are used to plot the shallow groundwater data. Compared to **Figure 6-2**, the $UO_2(CO_3)_2^{2-}/U_3O_{7(c)}$ and $UO_2(CO_3)_2^{2-}/U_4O_{9(c)}$ solid-solution boundaries have been shifted down because of the higher levels of dissolved carbonate. This causes a collapse of the $U_3O_{8(c)}$, $U_4O_{9(c)}$ and $U_3O_{7(c)}$ stability zones, thereby making $UO_{2(c)}$ the more likely initial precipitate.

Uranium mineral saturation indices

The aqueous geochemical data for each water sample were entered into PHREEQC to give saturation indices with respect to various U mineral phases (see **Appendix F**). Saturation indices for $UO_{2(c)}$ and $U_4O_{9(c)}$ are plotted in **Figure 7-16**. In all of the shallow piezometers, conditions are saturated to supersaturated with respect to $UO_{2(c)}$. Saturation indices with respect to $U_4O_{9(c)}$ are even greater, although whether or not this means $UO_{2(c)}$ is being oxidized to $U_4O_{9(c)}$ is unclear. Saturation indices for $U_3O_{8(c)}$ and $UO_{2(am)}$ are consistently negative, and the database does not include $U_3O_{7(c)}$. Therefore, the most probable initial U precipitate is uraninite, $UO_{2(c)}$.
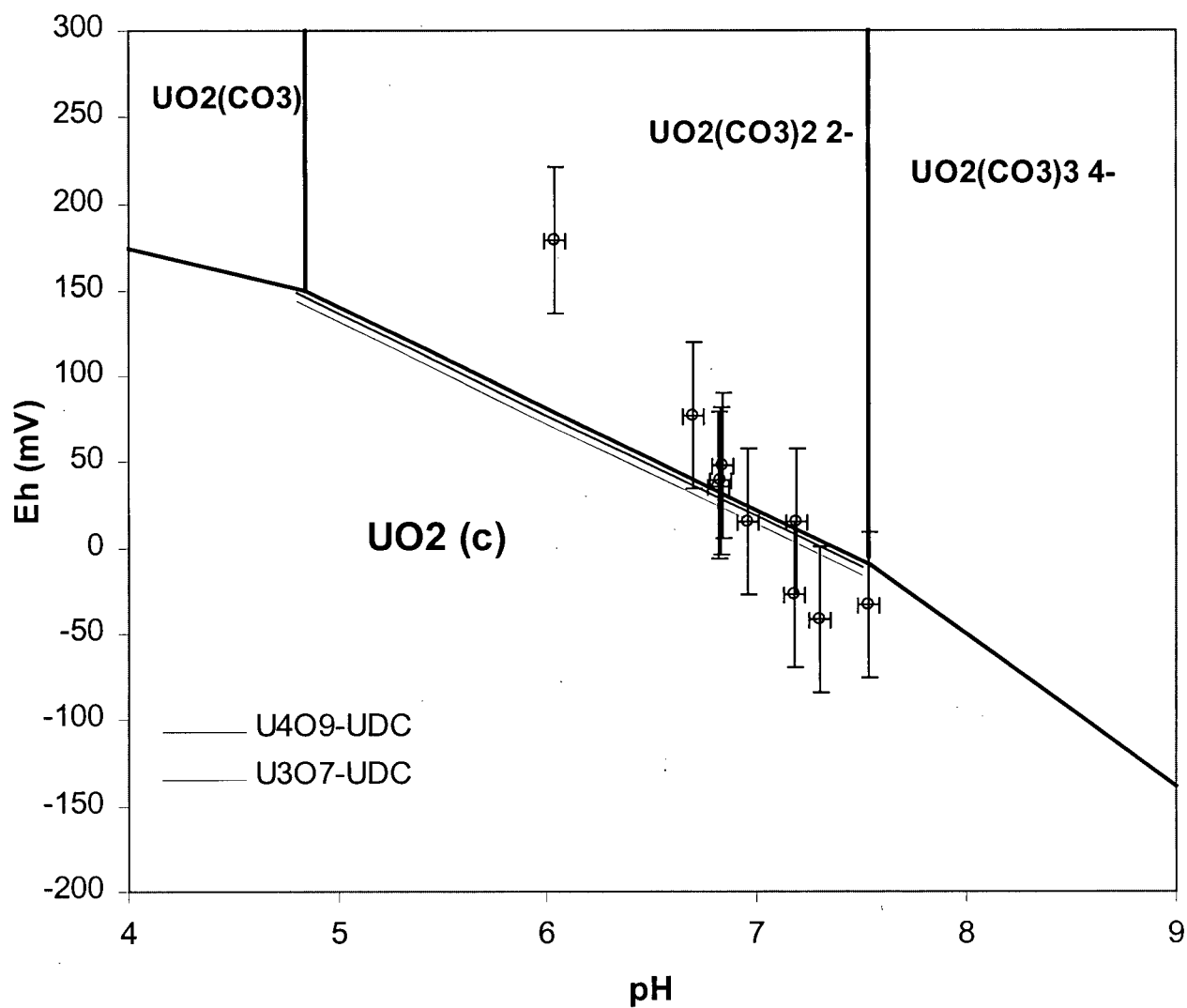
Figure 7-15 Eh-pH diagram showing calculated Eh and measured pH in shallow groundwaters underlying Prairie Flats. Also shown are the collapsed stability zones of $U_3O_{8(c)}$, $U_4O_{9(c)}$ and $U_3O_{7(c)}$

Effect of Eh, pH, and HCO$_3$ on U-Mineral Saturation

To test the sensitivity of reductive precipitation of U to changes in Eh, pH, HCO$_3$ and dissolved U, a number of PHREEQC simulations were made on a representative sample. PZ-702 was chosen for its proximity to the average U, HCO$_3$ and redox conditions, and for its good charge balance. All relevant analytical data was entered into the model and pH, Eh, and HCO$_3$ values were varied in turn across the measured range. Saturation indices of UO$_{2(c)}$ and U$_4$O$_{9(c)}$ are plotted against these parameters in **Figure 7-17**.

Of these variables, Eh and pH were found to have the greatest effect on U mineral saturation. UO$_{2(c)}$ and U$_4$O$_{9(c)}$ saturation is reached at Eh's below 0 mV and at pH's below 7.5. Under these conditions, U can precipitate at dissolved U concentrations as low as 100 µg/L. Increasing HCO$_3$ concentrations slightly increases UO$_{2(c)}$ solubility because of its tendency to form soluble uranyl-carbonate complexes.

Although PHREEQC simulations gave both UO$_{2(c)}$ and U$_4$O$_{9(c)}$ as possible U mineral phases, these plots show UO$_{2(c)}$ to be the more stable U-precipitate. As Eh conditions become more reducing, UO$_{2(c)}$ is the first to attain supersaturation. At Eh values around 0 mV, it maintains supersaturation up to pH's of 7.7, whereas U$_4$O$_{9(c)}$ can precipitate only up to pH 7.5. UO$_{2(c)}$ saturation is less affected by HCO$_3$, precipitating at HCO$_3$ concentrations up to 700 mg/L, unlike the 500 mg/L for U$_4$O$_{9(c)}$. Also, UO$_{2(c)}$ can precipitate at much lower dissolved U concentrations than U$_4$O$_{9(c)}$. Therefore, although partial oxidation to U$_4$O$_{9(c)}$ is possible, it is likely to be limited.
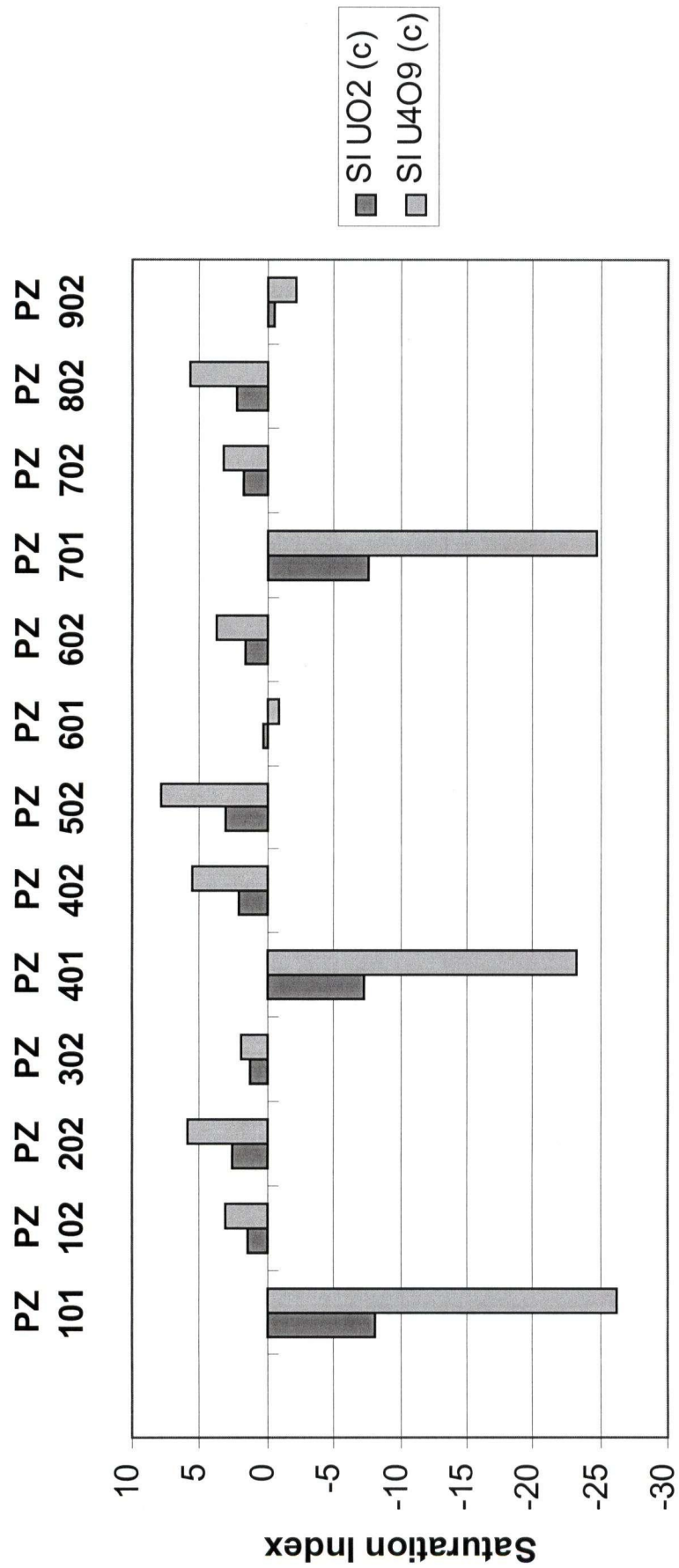
Figure 7-16 Plot of saturation indices with respect to $UO_2(c)$ and $U_4O_9(c)$ at each piezometer location

99
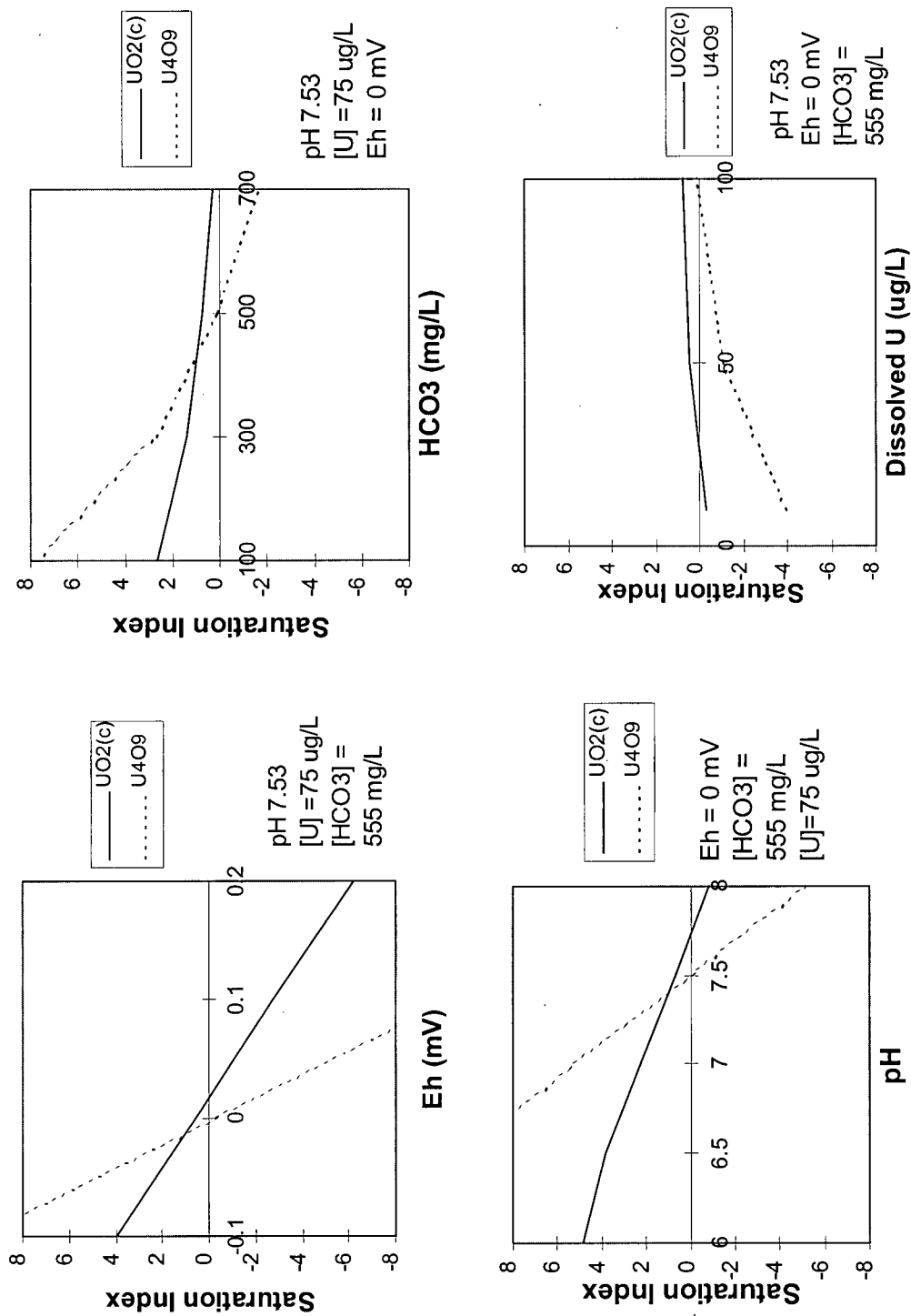
Figure 7-17 Effect of Eh, pH, HCO₃ concentration and dissolved U concentration on saturation indices with respect to UO₂(c) and U₄O₉(c)

100

<u>Evidence from Analogous Deposits</u>

Studies of other surficial U deposits in the United States have made similar conclusions about the role of adsorption and reductive precipitation in retaining U. Those that have been researched in sufficient detail are the *Zephyr Cove* deposit on Lake Tahoe (Zielinski et al. 1988, Johnson et al. 1987, Otton et al. 1989, Owen and Otton 1995) and the *Flodelle Creek* deposit in Stevens County, NE Washington state (Zielinski et al. 1987, Zielinski et al. 1986, Owen and Otton 1995). Geochemical studies carried out at these two sites concluded that where Eh conditions in the saturated zone are above 100 mV, U is fixed by adsorption onto humic acids. Where Eh conditions fall below 100 mV, reductive precipitation occurs, either directly or indirectly following the burial and diagenesis of previously sorbed U.

Evaporative Precipitation

Geochemical analyses of shallow and deep groundwaters suggest that evaporation may increase concentrations of dissolved constituents near the top of the peat unit, but not enough to precipitate U^{6+} minerals. According to PHREEQC simulations, saturation indices for U^{6+} minerals such as schoepite (β-$UO_3 \cdot 2H_2O$), autinite ($Ca(UO_2)_2(PO_4)_2$), carnotite ($K_2(UO_2)(VO_4)_2$ and tyuyamunite ($Ca(UO_2(VO_4)_2$) never rise above 0. This can be explained by the high solubilities of these minerals (most in the mg/L range), which are enhanced in high-CO_2 waters due to uranyl-carbonate complexation (Langmuir, 1997, p. 497).

7.3   CONTROLS ON SOIL URANIUM DISTRIBUTION

Vertical Distribution

One puzzling feature of the Prairie Flats deposit is that the highest concentrations of U exist near the ground surface (see **Figure 1-3b**), which is also true of the organic content of the soils. Simply put, the organics provide 1) sorption sites for the initial entrapment of U, and 2) prolonged reducing conditions which facilitate U reduction and precipitation to a more stable mineral form.

PHREEQC simulations show that the near-surface environment is more conducive to the reductive precipitation of $UO_{2(c)}$ than at depth, as shown in **Figure 7-18**. This is very different from most groundwater environments where conditions tend to be more reducing at depth. The cause of this redox reversal is the relatively oxygenated waters discharging into the peat unit from the till unit below. This causes a continual refreshening of the base of the peat and resolubilization of U.
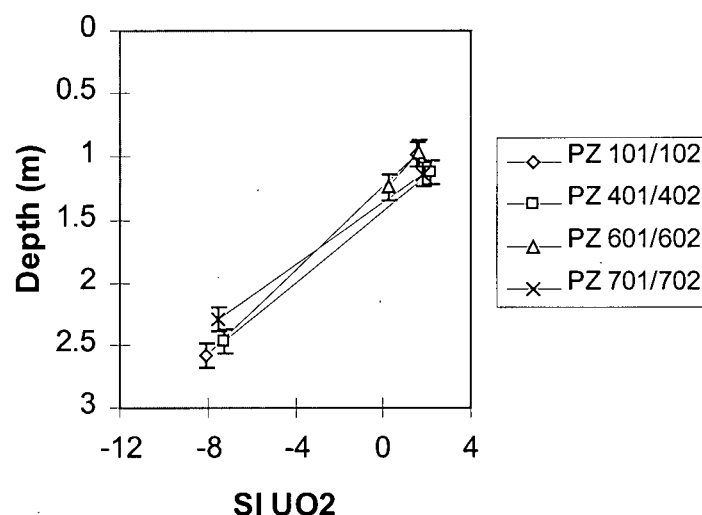
Figure 7-18 Change in $UO_{2(c)}$ saturation indices with depth in Prairie Flats groundwaters, showing more favourable precipitation conditions near-surface

Lateral Distribution

With respect to the lateral distribution of U across Prairie Flats, it is interesting to note that the highest soil U concentrations (see **Figure 1-3a**) coincide with the thickest sections of peat and clay (see **Figure 4-3**). Both sets of contours encircle PZ 401/402 and have the same kidney-bean shape. Groundwaters discharging from the till into the peat would be slowed down due to the drop in hydraulic conductivity, thereby allowing ample time for U entrapment. Therefore, the peat unit not only provides the right chemistry for U retention, but also the right flow conditions.

7.4 POTENTIAL FOR URANIUM REMOBILIZATION

Evidence presented in this study and by Culbert (1980) shows that a major proportion of the U in the Prairie Flats is loosely retained by adsorption and could potentially be remobilized under the right geochemical conditions. Once remobilized, substantial amounts may enter Prairie Creek and discharge into Lake Okanagan.

In 1981, concentrations of dissolved U in runoff waters around Summerland were at or above the drinking water standard of 20 μg/L, possibly indicating some leaching of the Prairie Flats deposit (Ministry of Health, 1981). In the water sampling results from this thesis, two other possible pieces of evidence are highlighted, namely;

· remarkably anomalous dissolved U concentrations near a household septic field and
· a marked increase in dissolved U concentration at the exit point of Prairie Creek during sewer system installation in the spring of 1998.

Septic Field

Piezometer 202 is located adjacent to a private septic field, as shown in **Figure 7-19**. The groundwater sampled here in March '98 had a highly anomalous U value (nearly 4

mg/L!), as shown in **Table 7-1**. It also had high concentrations of NO_3, PO_4, SO_4, and dissolved organic carbon, as is characteristic of septic effluent.

Table 7-1: Water chemistry data at piezometer 202 (March, 1998)

pH	Eh(V)	HCO3	OC	NO3	PO4	SO4	Cl	Ca	Mg	Na	K	U (µg/L)
							26	38				
7.1	-0.027	1354	157	43	0.7	2490	5	1	166	630	10.1	3961

* all values given in mg/L unless otherwise specified

This water sample exemplifies the potential impact of increased septic discharge into the flats. The assortment of oxidants and complexing agents in septic effluent comprises a strong leach solution that can strip U from the peat. Such high dissolved U concentrations at PZ 202 may be due to reoxidation and desorption working together, wherein NO_3 reoxidizes UO_2 to uranyl, which then complexes with HCO_3. Therefore, it is important that mixing of septic effluent with Prairie Flats groundwaters be avoided as residential development continues to expand up Prairie Valley and Cartwright mountain.

Prairie Creek

Results from both water sampling rounds show an increase in U levels in Prairie Creek from entrance (E) to exit (A) of the flats. In Sept '97 concentrations increased from 22 to 34 µg/L, and in March '98 from 34 to 117 µg/L. One explanation for the dramatic increase in March is the expansion of the town's sewer system on the property adjacent to the flats (see **Figure 7-19**). Here the excavation of ditches exposed the peat unit to air and thereby caused oxidization of any UO_2 present to uranyl, which subsequently be washed into Prairie Creek by rainstorms and other runoff events. Further field evidence is required at this point to support this claim.
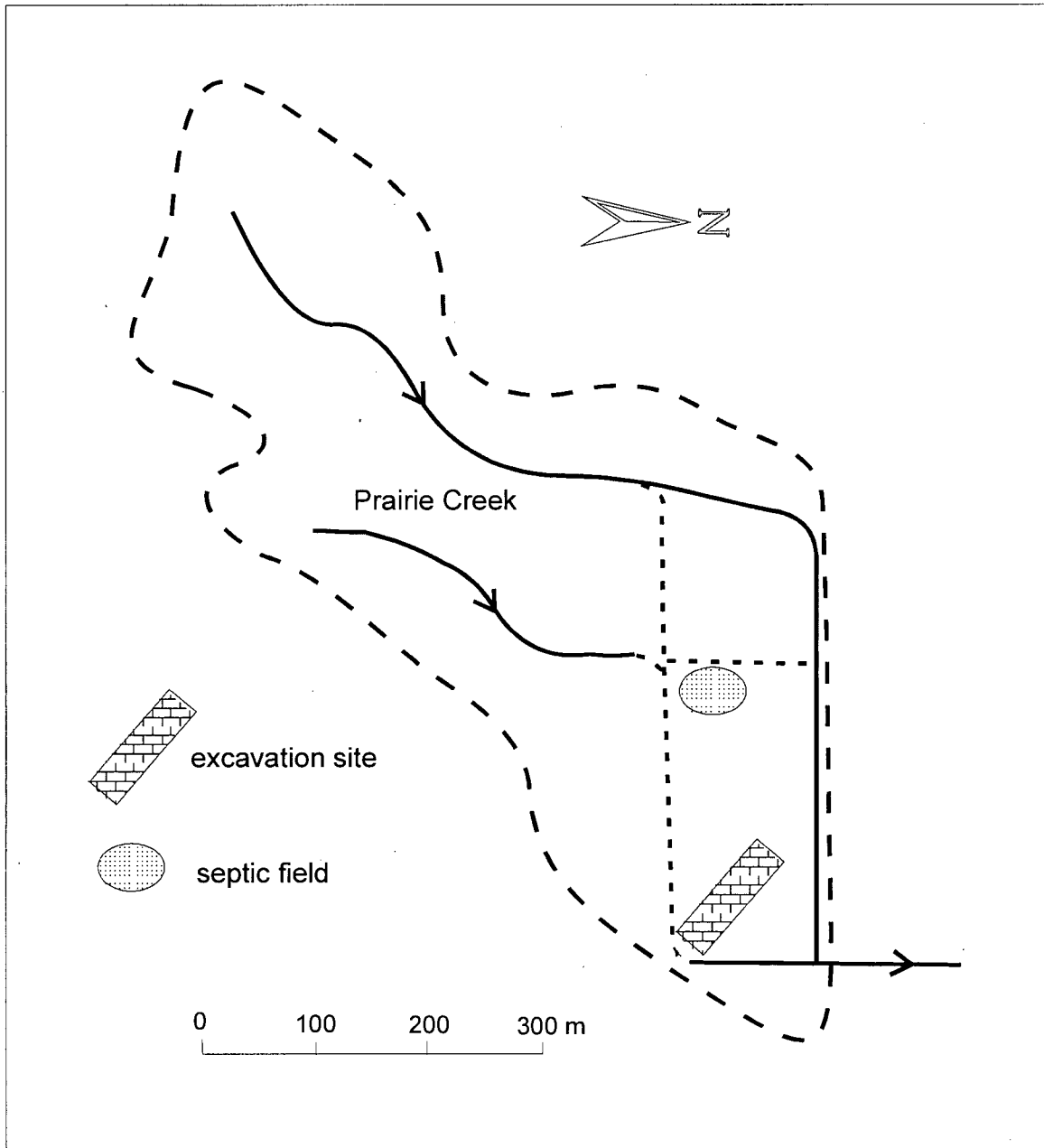
Figure 7-19 Location of septic field and excavation pit for sewage system installation

Since the Prairie Flats U deposit has been around for thousands of years already, the likelihood of natural remobilization is low. However, this section points out that cultural disturbances such as fertilizer use, septic discharge, and soil excavation may increase the chances of such an event.

SUMMARY

This chapter identified the principle controls of the aqueous geochemistry of Prairie Flats groundwaters and demonstrated how these affect the mobility and distribution of U in the deposit. Calcite mineral-solution equilibria control the HCO_3 concentrations, and redox conditions reflect the near-surface oxidation of organic material and the discharge of fresh, relatively oxygenated groundwaters from below. After initial adsorption to the organics, U is likely reduced and precipitated as $UO_{2(c)}$ in this near-surface reducing environment. This is shown by Eh-pH diagrams and PHREEQC simulations, which also indicate that evaporative precipitation of U to some U^{6+} mineral is unlikely. Remobilization of U and subsequent migration to Okanagan Lake via Prairie Creek could occur if agricultural and residential activities continue to intensify in the area, but at this point the likelihood and consequences of such an event require further consideration.

8 GENERAL CONCLUSIONS AND SUGGESTIONS FOR FUTURE WORK

This thesis further characterizes the hydrogeology and aqueous geochemistry of the Prairie Flats uranium deposit. When combined with the soil and surface water studies already carried out at the site and surrounding region, it offers a more complete picture of how the uranium deposit was formed, and in what condition it lies today.

The hydrostratigraphy of the Prairie Flats consists of a low-permeability peat & clay unit overlying a well-drained till unit, followed by bedrock. The peat unit is up to 3m thick and has a horizontal hydraulic conductivity of about 6×10^{-7} m/s and vertical hydraulic conductivity on the order of 10^{-8} m/s. The till unit has a horizontal hydraulic conductivity on the order of 10^{-5} m/s. Further augering or drilling in and around the Prairie Flats would help to delineate the vertical and lateral extent of the till unit and clarify its connection to the neighbouring glaciofluvial deposits.

Physical measurements of the groundwater flow regime underlying the flats indicate that groundwaters are discharging upwards into the uranium-bearing peat unit. During the summer months, the average lateral component of the hydraulic gradient through the peat is around 0.005, whereas the average vertical component is 0.04. This upward flow is topographically-driven since the flats lie at the base of Prairie Valley and are encircled by a number of small mountains. More frequent monitoring of water levels in the piezometers is needed to identify the effects of seasonal climate change, rainfall events, irrigation practices and other anthropogenic activities on the groundwater hydrology of the flats.

Darcy's law and a simplified hydrologic budget were used to estimate the amount of groundwater entering and leaving the Prairie Flats, respectively. The estimated total groundwater discharge rate is approximately 9450 m³/year, assuming that recharge to

groundwater from Prairie Creek are negligible. During the summer months, most of this discharge leaves the flats as evapotranspiration, and in the winter months, it goes into storage. The limited understanding of groundwater-surface water interaction across the flats could be improved with more frequent and extensive measurements of seepage rates, hydraulic gradients, flow rates, etc. in the drainage ditches (Prairie Creek).

Combining the groundwater discharge rate and average incoming uranium concentration gives an estimate of the current uranium deposition rate in the Prairie Flats of 0.95 kg U per year. This is an order of magnitude smaller than the rate predicted given the estimated tonnage and age of the uranium in the deposit. Therefore, uranium deposition rates were probably much higher in the past than they are today. For example, recently-scoured and fractured rock surfaces combined with a colder, wetter climate would result in greater amounts of uranium leaching and deposition in this region. Radiocarbon dating of the peat unit that hosts the uranium may help to determine whether the deposit was formed thousands of years ago closer to deglaciation, or more recently as a consequence of the onset of agricultural activity in Prairie Valley.

Water chemistry analyses confirm that the Prairie Flats are a groundwater discharge zone for local groundwaters. By definition, local groundwaters are recharged within the Summerland basin and flow at shallow depths ($<$ 100m) in the glacial sediments and shallow bedrock. Incoming groundwaters are relatively oxidizing and have a $Ca-HCO_3$ chemistry with low concentrations of dissolved solids. Piper plots show a match between Prairie Flats groundwaters and other local groundwaters. If regional waters are discharging at this site, dilution by local groundwaters prevents their identification. Assuming that groundwater flow paths are unchanging in time, it is possible that the uranium in this deposit came from source rocks within the Summerland basin.

The chemistry of Prairie Flats groundwaters indicates that both adsorption and reductive precipitation of uranium are dominant fixation mechanisms. Both processes are facilitated by organic molecules in the peat which initially adsorb uranium and whose

oxidation sets up an oxygen-poor, relatively reducing environment suited to the reductive precipitation of $UO_{2(c)}$. Given the high competition for uranium by dissolved carbonate species, neither process is fully efficient, therefore both were probably involved in generating a deposit of this size. Further analysis of soil samples by Scanning Electron Microscopy or X-ray diffraction may better identify uranium minerals on these soils and distinguish how much of the uranium is adsorbed, and how much is reduced.

Combining the geochemistry with the groundwater flow patterns offers further insight on the uranium distribution. Highest uranium values correspond to a thick mound of peat in the centre of the deposit because flow is slowed and contact times are higher. Uranium is concentrated near the ground surface because of the reducing environment set up by the oxidation of organics. Retention at depth is inhibited by the discharge of relatively oxygenating waters from the till unit below the peat. A multilevel piezometer would offer more resolution on the changes in groundwater chemistry with depth.

Anomalous counts of uranium near a septic field and during excavation of the peat warn that remobilization could occur if the chemistry of Prairie Flats groundwaters is significantly changed. Leaching tests with septic discharge, for example, would help to further evaluate this risk.

REFERENCES

Ahonen, Lasse, Ervanne, H., Ruskeeniemi, Jaakkola, T., and Blomqvist, R. 1993. Uranium mineral - groundwater equilibration at the Palmottu natural analogue study site, Finland. *Mat. Res. Soc. symp. proc.* 294: 497-504..

Andreyev and Chumachenko. 1964. Reduction of uranium by natural organic substances. *Geochemistry International.* 1: 3-7.

Appelo, C.A.J. and Postma, D. 1994. *Geochemistry, Groundwater and Pollution.* Rotterdam, The Netherlands: A.A. Balkema. ISBN 90 5410 105 9

Bates, David V., Murray, James W., and Raudsepp, Valter. 1980. *Royal Commission of Inquiry, Health and Environmental Protection, Uranium Mining, Comissioner's Report, Volume 1.* Oct 30, 1980.

Berner, R.A. 1971. *Principles of Chemical Sedimentology.* New York: McGraw-Hill Book Company. 209 p.

Borovec, Z., Kribek, B. and Tolar, V. 1979. Sorption of Uranyl by Humic Acids. *Chemical Geology.* 27: 39-46.

Bouwer, Herman and Rice, R.C. 1976. Slug Test for Determining Hydraulic Conductivity of Unconfined Aquifers With Completely or Partially Penetrating Wells. *Water Resources Research.* 12: 423-428.

Boyle, Dan R. 1982. The Formation of Basal-Type Uranium Deposits in South Central British Columbia. *Economic Geology.* 7: 176-1209.

Butler, James J. Jr., McElwee, Carl D., and Liu, Wenzhi. 1996. Improving the Quality of Parameter Estimates Obtained from Slug Tests. *Groundwater.* May/June: 480-490.

Church, B.N., Jessop, A.M., Bell, R., and Pettipas, G.S.B. 1991. Tertiary Outlier Studies: Recent Investigations in the Summerland Basin, South Okanagan Area, B.C. *Geological Fieldwork 1990, Paper 1991-1.* pp.163-170.

Church, B.N. 1982. Geology of the Penticton Tertiary Outlier, B.C. Ministry of Energy, Mines and Petroleum Resources B.C. Revised Preliminary Map 35.

Church, B.N. 1980. Anomalous Uranium in the Summerland Caldera. *Geological Fieldwork 1979, Paper 1980-1.* pp. 11-15.

Church, B.N. 1973. Geology of the White Lake Basin. *B.C. Department of Mines & Petroleum Resource Bulletin No. 61.* 120 p.

Cooper, H. H. Jr., Bredehoeft, J.D., and Papadopulos, I.S. 1967. Response of Finite-Diameter Well to an Instantaneous Charge of Water. *Water Resources Research.* 3: 263-269.

Culbert, R.R. and Leighton, D.G. 1988. Young Uranium. *Ore Geology Reviews.* 3: 313-330.

Culbert, R.R., Boyle, D.R., and Levinson, A.A. 1984. Surficial Uranium Deposits in Canada. *Surficial Uranium Deposits.* Vienna: International Atomic Energy Agency. 252 p.

Culbert, R.R. 1980. Report on Post-Glacial Uranium Concentrations in the Southern Okanagan Valley. *For* Ministry of Health B.C. June 4, 1980.

Culbert, R.R. 1980b. *Proceedings of Royal Commission of Inquiry, Health and Environmental Protection, Uranium Mining, Volume 69.* p. 12662.

Culbert, R.R. 1980c. *Proceedings of Royal Commission of Inquiry, Health and Environmental Protection, Uranium Mining, Volume 69.* p. 12626.

Culbert, R.R. 1979. Post-Glacial Uranium Concentration in South Central British Columbia. *For* Royal Commission of Inquiry, Health and Environmental Protection, Uranium Mining. October 24, 1979.

Culbert, R.R. and Leighton, D.G. 1978. Uranium in Alkaline Waters - Okanagan Area, British Columbia. *CIM Bulletin.* May: 103-110.

DeVeto, Richard H. 1978. *Uranium Geology and Exploration – Lecture Notes and References.* Golden, Colorado: Colorado School of Mines.

Demir, Z. and Narasimhan, T.N. 1994. Improved Interpretation of Hvorslev Tests. *Journal of Hydraulic Engineering.* 120: 477-495.

Drever, James I. 1988. *The Geochemistry of Natural Waters.* Englewood Cliffs, New Jersey: Prentice-Hall Inc. 437 p.

Freeze, R.A. and Cherry, John A. 1979. *Groundwater.* Englewood Cliffs, New Jersey: Prentice-Hall Inc. 589 p.

Froelich, P.N., Klinkhammer, G.P., Bender, M.L., Luedtke, N.A., Heath, G.R., Cullen, Doug, Dauphin, Paul, Hammond, Doug, Hartman, Blayne, and Maynard, Val. 1978. Early oxidation of organic matter in pelagic sediments of the eastern equatorial Atlantic: suboxic diagenesis. *Geochimica et Cosmochimica Acta.* 43: 1075-1090.

Giridhar, J. and Langmuir, D. 1991. Determination of E^0 for the UO_2^{2+}/U^{4+} Couple from Measurement of the Equilibrium: $UO_2^{2+} + Cu_{(s)} + 4H^+ = U^{4+} + Cu^{2+} + 2H_2O$ at 25° C and some Geochemical Implications. *Radiochimica Acta.* 54: 133-138.

Golder Associates Ltd. 1994. Groundwater Monitoring Program - Summerland Landfill, Summerland, BC. *For* The Corporation of the District of Summerland. March 20, 1995.

Golder Associates Ltd. 1980. Geotechnical Investigation, proposed injection well, proposed hotel development, College Road Summerland, B.C. *For* 5005 Holdings Ltd., c/o P. Avard, Naramata, B.C. April 7, 1980.

Grant, M.B. and F.A. Michel. 1983. Study of the Hydrogeology of the White Lake Basin, British Columbia. *For* B.C. Department of Energy, Mines, and Resources. March, 1983. Contract Serial No. OSB83-00223.

Hunkin Enginers, Inc. 1979. Preliminary Metallurgical Test Results and Conceptual Production Processes for Young Uranium Deposits with Construction and Operating Cost Estimates. *For* D.G. Leighton & Associates, Ltd., Vancouver, B.C.

Hvorslev, M.J. 1951. Time lag and soil permeability in groundwater observations. *U.S. Army Corps Engrs. Waterways Exp. Sta. Bull. 36.* Vicksburg, Miss.

Idiz, Erdem F., Carlisle, Donald and Kaplan, I.R. 1986. Interaction between organic matter and trace metals in a uranium rich bog, Kern County, California, U.S.A. *Applied Geochemistry.* 1: 573-590.

Jessop, A.M. and Church, B.N. 1991. Geothermal Drilling in the Summerland Basin, British Columbia, 1990. *Geological Survey of Canada Open File 2348.* 14p.

Johnson, S.Y., Otton, J.K., and Macke, D.L. 1987. Geology of the Holocene surficial uranium deposit of the north fork of Flodelle Creek, northeastern Washington. *Geological Society of America Bulletin.* 98: 77-85.

Kochenov, A.V., Zinev'yev, and Lovaleva, S.A. 1965. Some Features of the Accumulation of Uranium in Peat Bogs. *Geochemical International.* 2: 65-70.

Kribek, Bohdan and Podlaha, Jaroslav. 1980. The Stability Constant of the $U_2O_2^{2+}$ - humic acid complex. *Organic Geochemistry.* 2: 93-97.

Kvill, Donald Raymond. 1976. *Glacial History of the Trout Creek Basin, Summerland, British Columbia.* Master of Science Thesis, Dept of Geography, University of Alberta.

Langmuir, D. 1997. *Aqueous Environmental Geochemistry.* Upper Saddle River, New Jersey: Prentice Hall Inc. 590 p.

Langmuir, D. 1978. Uranium Solution-Mineral Equilibria at Low Temperatures with Applications to Sedimentary Ore Deposits. *Geochimica et Cosmochimica Acta.* 42: 547-569.

Lawson, D.W. 1968. Groundwater flow systems in the crystalline rocks of the Okanagan Highland, British Columbia. *Canadian Journal of Earth Sciences.* 5: 813-824.

Lee, David R. and Cherry, John A. 1978. A Field Exercise on Groundwater Flow Using Seepage Meters and Mini-Piezometers. *Journal of Geological Education.* 27: 6-10.

Leenheer, J.A., Malcolm, R.L., and White, W.R. 1974. Investigations of the reactivity and fate of certain organic components of an industrial waste after deep-well injection. *Environmental Science and Technology.* 10: 445-451
Levinson, A.A., Bland, C.J. and Dean, J.R. 1984. Uranium Series Disequilibrium in Young Surficial Uranium Deposits in Souther British Columbia. *Canadian Journal of Earth Sciences.* 21: 559-566.

Lewis, Trevor. 1984. Geothermal energy from Penticton Tertiary outlier, British Columbia: an initial assessment. *Canadian Journal of Earth Sciences.* 21: 181-188.

Little, 1961. Geology of the Kettle River (West Half) area, British Columbia. Canadian Geological Survey Map 15-1961.

Lopatkina, A.P. 1967. Conditions of accumulation of uranium in peat. *Geochemistry International.* 4: 577-588.

Lovely, Derek R., Roden, Eric El, Phillips, E.J.P. and Woodward, J.C. 1993. Enzymatic iron and uranium reduction by sulfate-reducing bacteria. *Marine Geology.* 113: 41-53.

Manskaya, S.M, Drozdova, T.V. and Emelianova, M.P. 1956. Association of uranium with humic acids and melanoidins. *Geokhimiya.* 4: 339-347.

Meyboom, P. 1967. Groundwater studies in the Assiniboine River Drainage Basin: II. Hydrologic characteristics of phreatophytic vegetation in south-central Saskatchewan. *Geol. Surv. Can. Bull 139.* 64 p.

Ministry of Environment, Lands and Parks, B.C. 1998. Groundwater Section website: http://wtrww.env.gov.bc.ca/wat/gws.

Ministry of Environment, Lands and Parks, B.C. 1997. *Memo to* Mark Siemens, Summerland Trout Hatchery, Summerland, B.C. May 8, 1997.

Ministry of Environment, Lands and Parks, B.C. 1986. *Assessment of Water Resources at the Summerland Trout Hatchery, Report and Recommendations.*

Ministry of Health, B.C. 1981. *Interim Report by the working group on Post-Glacial Uranium Deposits.*

Ministry of Health, B.C. and Ministry of Energy, Mines and Petroleum Resources, B.C. 1981. *Variations in Uranium and Radioactivity Levels in Surface and Groundwater at Selected Sites in British Columbia, April 1980-March 1981.* 45 p.

Ministry of Health, B.C. and Ministry of Energy, Mines, and Petroleum Resources, B.C. 1980. *Variations in the Uranium and Radioactivity Levels of Potable Surface and Groundwater in the Okanagan and West Kootenay Regions of British Columbia.* 63 p.

Mohagheghi, Ali, Updegraff, David M., and Goldhaber, Martin B. 1984. The Role of Sulfate-Reducing Bacteria in the Deposition of Sedimentary Uranium Ores. *Geomicrobiology Journal.* 4: 153-173.

Nasmith, Hugh. 1962. Glacial History and Surficial Deposits of the Okanagan Valley, BC. *B.C. Department of Mines and Petroleum Resources Bulletin No. 46.*

Owen, D.E. and Otton, J.K. 1995. Mountain wetlands: efficient uranium filters - potential impacts. *Ecological Engineering.* 5: 77-93.

Otton, J.K., Zielinski, R.A. and Been, J.M. 1989. Uranium in Holocene Valley-fill Sediments and Uranium, Radon, and Helium in Waters, Lake Tahoe-Carson Range Area, Nevada and California, U.S.A. *Environ. Geol. Water Sci.* 13(1): 15-28.

Pacific Hydrology Consultants Ltd. 1983. Groundwater Resources in the Faulder-Meadow Valley Area. *For* Regional District of Okanagan-Similkameen. Nov 4, 1983.

Piteau & Associates. 1984. Summerland Basin Hydrogeological Study. *For* Physics Branch, Energy, Mines and Resources Canada. January, 1984. Open File #85-29.

Robbins, E.I., Zielinski, R.A., Otton, J.K., Owen, D.E., Schumann, R.R., and McKee, J.P. 1990. Microbially Mediated Fixation of Uranium, Sulfur, and Iron in a Peat-Forming Montane Wetland, Larimer County, Colorado. *U.S.G.S. Research on Energy Resources – 1990, Programs and Abstracts*: pp. 70-71.

Sandino, Amai and Bruno, Jordi. 1992. The solubility of $(UO_2)_3(PO_4)_2 \cdot 4H_2O_{(s)}$ and the formation of U(VI) phosphate complexes: Their influence in uranium speciation in natural waters. *Geochimica et Cosmochimica Acta.* 56: 4135-4145.

Schwertmann, U., Kodama, H., and Fischer, W.R. 1986. Mutual Interactions Between Organics and Iron Oxides. *Interactions of Soil Minerals with Natural Organics and Microbes.* Soil Science Society of America Spec. Pub. no 17. pp. 223-250.

Shanbhag, P.M. and Choppin, G. 1981. Binding of uranyl by humic acid. *J. Inorg. Nucl. Chem.* 43: 3369-3372.

Shotyk, William. 1988. Review of the Inorganic Geochemistry of Peats and Peatland Waters. *Earth Science Reviews.* 25: 95-176.

Steinmann, Philip, and Shotyk, William. 1997. Chemical composition, pH, and redox state of sulfur and iron in complete vertical porewater profiles from two *Sphagnum* peat bogs, Jura Mountains, Switzerland. *Geochimica et Cosmochimica Acta.* 61(6): 1143-1163.

Stumm, Werner and Morgan, James J. 1981. *Aquatic Chemistry – An Introduction Emphasizing Chemical Equilibria in Natural Waters, 2nd Edition.* New York: John Wiley & Sons Inc.

Szalay, A. 1964. Cation exchange properties of humic acids and their importance in the geochemical enrichment of UO_2^{2+} and other cations. *Geochimica et Cosmochimica Acta.* 28: 1605-1614.

Titayeva, N.A. 1967. Association of radium and uranium with peat. *Geochemistry International.* 4: 1168-1174.

White, W.N. 1932. A method of estimating groundwater supplies based on discharge by plants and evaporation from soil. *U.S. Geol. Surv. Water-Supply Paper 659-A.*

Zielinski, R.A., Otton, J.K. Wanty, R.B. and Pierson, C.T. 1988. The Aqueous Geochemistry of Uranium in a Drainage Containing Uraniferous Organic-rich Sediments, Lake Tahoe area, Nevada, U.S.A. *Uranium.* 4(4): 281-305.

Zielinski, Robert A., Otton, James K., Wanty, Richard B. and Pierson, Charles. 1987. The geochemistry of Water Near a Surficial Organic-Rich Uranium Deposit Northeastern Washington State, USA. *Chemical Geology.* 62: 263-289.

Zielinski, Robert A., Bush, C.A. and Rosholt, J.N. 1986. Uranium series disequilibrium in a young surficial uranium deposit, northeastern Washington, U.S.A. *Applied Geochemistry.* 1: 503-511.

Zielinski, Robert A. 1981. *Experimental Leaching of Volcanic Glass: Implications for Evaluation of Glassy Volcanic Rocks as Sources of Uranium.* pp. 1-10

A   HYDROGEOLOGICAL FIELD METHODS

This appendix describes the installation of the Prairie Flats piezometer network and the hydrogeological tests carried out in July, August, and September '97. It is divided into three main sections: 1) piezometer installation, 2) hydrogeological tests, and 3) stream measurements.

PIEZOMETER INSTALLATION

Soil Sampling

During borehole excavation for piezometer installation, soil samples were taken to characterize the peat, clay and till units underlying the Prairie Flats. Grab samples of borehole cuttings were put in sealed plastic bags at piezometer locations 101/102, 302, 401/402, and 701/702. A list of the samples collected and their descriptions is found in **Table A-1.**

Table A-1 Grab sample descriptions

Unit	Sample Location	Description
Till	101/102 401/402	Coarse sand and gravel fining downward with rounded, pebble-sized clasts Grey Free of fines except at peat interface
Peat	101/102 701/702	Fine, powdery near surface, more decaying plant material at depth Dark brown to black 0.5 to 2.5m thick
Clay	302 402	clay with some silt blue-grey

Piezometer Construction

Piezometers were made from sections of 1¼-inch diameter, schedule 40 PVC pipe. The shallow and deep piezometers were roughly 1.5m and 3m in length, respectively. The deep piexometers were constructed from 1-metre flush-threaded sections, thereby allowing flexibility in length.

An alternating pattern of one-eighth-inch holes was drilled into the pipe and covered with landscape filter fabric to make screens for the piezometers. The screened interval was 15cm long. The filter fabric was secured using plastic ties, and a plastic slip cap was fitted to the bottom. For piezometers 302 and 401, a fine nylon mesh was used in place of the filter fabric. A photo of these piezometers is shown in **Plate A-1**.

Plate A-1   A 1.5m-long piezometer with other 1m-long piezometer sections in background

Borehole Digging

Various digging tools were used to make boreholes for the piezometers. Choices depended on the desired depth of borehole and the type of material encountered. A description of each method is given below:

Rotating Dutch Auger

A hand-held rotating dutch auger with a cutter head 4 inches in diameter and 25 cm long was used to drill shallow boreholes into the peat and clay for piezometers 102, 202, 302 and 602 (see **Plate A-2**). With extensions, it could attain a depth of 3 metres. Pebble-sized clasts prevented the auger from penetrating the till unit beneath the peat, and lifting such water-logged, cohesionless material without losing it on its way up was impossible.

Plate A-2 Rotating dutch auger used to dig boreholes, 3m long with extensions

Post-hole Digger

A two-man, gas-powered, post-hole digger with 4-inch solid stem was used to drill shallow boreholes into the peat and clay for piezometers 402, 702 and 502 (see **Plate A-3**). A 1-foot extention was fitted to a 4 foot flighted section to attain the desired depth of one metre.

Plate A-3 Gas-powered post-hole digger

Sand bailer

The sand bailer (see **Plate A-4**) was the only effective means of removing the cohesionless till material beneath the peat unit, and was used at piezometers 101, 401, 601 and 701. A 3-inch diameter PVC casing (see **Plate A-5**) kept the formation open. The sand bailer consisted of a hollow aluminum cylinder 80 cm long and 8 cm in diameter with a one-way flap at its base. At its top an aluminum rod extended to a length of 4 metres. When pounded up and down inside the borehole, material became lodged inside the cylinder. Once full, it was brought up to surface, dumped out, and reinserted.

Plate A-4 Sand bailer with 1m-long extensions

Plate A-5 3-inch internal diameter PVC casing used during deep piezometer installation. The apparatus used to remove the casing lies on top of it.

Piezometer Insertion

Appendix B contains construction and stratigraphic details for each piezometer. Shallow piezometers were inserted deep enough so that their screened interval was below the water table, and deep piezometers were inserted as deep as possible.

Some piezometers were installed using a 3-inch diameter PVC casing and others not due to time and resource constraints. A 3-inch casing was used for piezometers 101, 102, 202, 302, 401, 601, 602 and 701 to prevent collapse of the peat around the borehole and to serve as a chute for sand, bentonite, and cuttings. First, the piezometer was slid into the open casing and allowed to fill with water. Next, clean, sorted silica filter sand was added to just above the screen. Bentonite chips were added to the top to create a 10cm seal, thereby isolating this depth interval for head measurements. This was especially important for the deep piezometers, but not so much for the shallow since these were completed just below the water table. The rest of the hole was filled with cuttings in the approximate order that they were removed, and more bentonite was added at the ground surface to create a final seal. With each filling step, the casing was pulled up to meet the new base of the hole and finally to remove it.

Piezometers installed without the use of casing include 402, 502, 702, 802 and 902. These were dropped into the open borehole and pushed into the soft saturated zone. No filter sand or bentonite seal was added around the screen. The borehole was filled with cuttings and sealed with bentonite at the ground surface.

Capping

The final step in piezometer installation was capping. Excess standpipe was cut off with a hack saw, leaving about 10 cm above ground surface. A mark was made with a black marker on the top edge of the standpipe to indicate where water level measurements would be read and where the elevation of the piezometer would be surveyed in. A slip cap was put on and a 1/8-inch hole was drilled through the pipe and cap on each side. A piece of plastic-coated wire was threaded through these two holes and the ends were fastened with an electrical connector. This allowed air to move in and out of the standpipe with fluctuating water levels.

Surveying

Two level surveys (the second as a check) were conducted using a Wild Heerbrugg No. 1 dumpy level to measure the elevations of the tops of the piezometers. A local benchmark was chosen and assigned an elevation of 10.000m, and all elevations were assigned relative to it. Angles and distances between piezometers were also measured to place them accurately on a map. Short distances were chained using a 30-metre nylon tape and chaining pins and horizontal angles were measured using a Pentax GT-48 transit. Range poles were positioned at each piezometer for easy sighting.

HYDROGEOLOGICAL TESTS

Head Measurements

Several rounds of head measurements were made to draw piezometric contour maps of the site and to measure vertical hydraulic gradients. This data is presented in **Table A-2**. Depths to water were read relative to a black mark on the side of the piezometer standpipe using a water level tape, and relative head values were calculated using elevations from the level survey.

Slug Tests

Slug tests were used to measure horizontal hydraulic conductivities of the peat and till units at most piezometer locations. For this method, a known volume of water is either withdrawn or added to the piezometer to cause an instantaneous change in head. Head recovery with time is recorded until it returns to its initial value. Head recovery data for the slug tests can be found in **Appendix C**.

Two rounds of slug tests were carried out over two visits to the site. On the first visit in July/August '97, injection tests were done at piezometers 202, 302, 402, and 902 using either tap water or a 1-inch diameter, 50cm long slug made of solid nylon. It is unlikely that this water affected the water chemistry results since ample time was allowed for re-equilibration before sampling (two and seven months), and some of the highest uranium concentrations were found at 402 only two months later. More slug tests were performed in September '97 on piezometers 102, 602, 802, 902, 101, and 601, this time as withdrawal tests because of high water levels in the piezometers. For these a nylon bailer made from a 50cm length of 1-inch diameter nylon pipe was used.

124

Table A-2 Head measurements taken between July '97 and May '98

Location	Jul-23	Jul-24	Aug-01	Aug-02	Aug-03 (am)	Aug-03 (pm)	Sep-24	Sep-26	Sep-28	Mar-03	Mar-05	Mar-06	May-11	May-12
PZ 101	8.935	8.805	8.738	8.754	8.752	8.729	8.955	9.023	8.972	9.133	9.141	9.142	8.685	8.692
PZ 102	8.870	8.766	8.692	8.696	8.683	8.654	8.915	8.967	8.944	9.135	9.118	9.116	8.616	8.634
PZ 202		9.05	9.021	9.015	9.032	8.994	9.24	9.432	9.266	9.472	9.435	9.408	8.942	8.94
PZ 302			9.269	9.275	9.279	9.255	9.904	9.947	9.91	9.943	10.092	9.946	9.336	9.25
PZ 401			8.895	8.877	8.868	8.85	9.192	9.256	9.252	9.48			8.838	8.838
PZ 402		8.955	8.861	8.847	8.832	8.822	9.395	9.446	9.488	9.57	9.585	9.58	8.857	8.845
PZ 502		11.13	11.126	11.086	11.074	11.069	11.359	11.291	11.39	11.698	11.655	11.679	10.966	10.972
PZ 601			9.059	9.05	9.054	9.025	9.399	9.575	9.456	9.602	9.591	9.584	8.969	8.965
PZ 602			9.059	9.042	9.047	9.02	9.404	9.585	9.461	9.62	9.602	9.598	8.974	8.972
PZ 701		9.535	9.715	9.712	9.705	9.701	9.735	9.240	9.695	9.99	9.894	10.068	9.771	9.781
PZ 702		10.34	9.652	9.645	9.64	9.635	9.682	9.397	9.6	9.87	9.708	9.894	9.676	9.687
PZ 802			8.917	8.897	8.932	8.885	9.043	9.149	9.059	9.262	9.19	9.185	8.82	8.819
PZ902			8.652	8.645	8.635	8.633		8.764	8.79	8.94	8.952	8.949	8.544	8.559

* all head measurements in metres

Recent work by Butler and others (1996) recommends that three or more slug tests be carried out at a well during a particular test period, and using at least two different initial head displacements. This is to identify any evolving "skin effects" or dependence on initial head displacement. Therefore, three withdrawal tests with two different initial displacements were done at piezometer 602.

Borehole Infiltration tests in peat

The vertical hydraulic conductivity of the peat was measured by means of an infiltration test. A 30 cm deep hole was bored into the peat using the dutch auger, into which a section of 3-inch diameter PVC casing was inserted to the bottom of the hole. The open cross-section at the bottom of the casing permits vertical flow only. An initial head displacement of 28cm was made by pouring water into the casing, and falling head measurements were made over a two-day period.

STREAM MEASUREMENTS

Vertical hydraulic gradient

The vertical component of the hydraulic gradient between Prairie Creek and the underlying groundwater at points B, C, and D was measured using a miniature piezometer inserted in the streambed (see **Figure A-1**). The piezometer was made of a 0.3 cm diameter polyethylene tube with a perforated end (screen) wrapped with fine nylon mesh to prevent sediment intrusion. It was 2.20 m long to the midpoint of the screen. To install it, a 2 cm diameter steel pipe was driven into the streambed with a sledge hammer, the base of which was plugged with a steel bolt. The piezometer was inserted into the steel pipe and then the pipe removed, leaving the piezometer in place. For further details on the use of mini-piezometers see Lee and Cherry (1978).
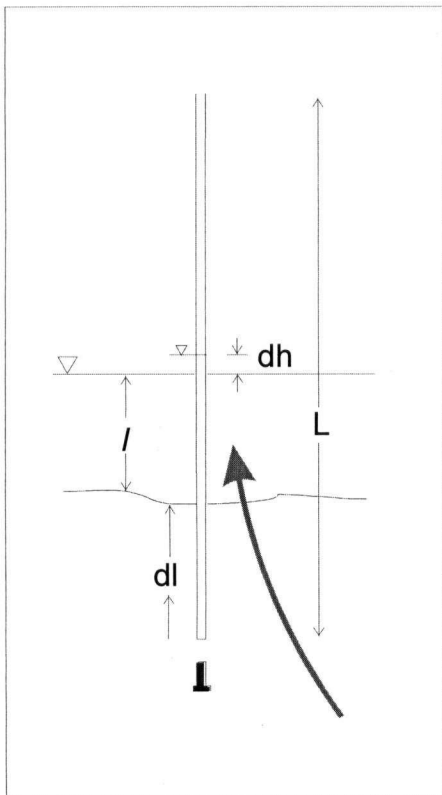
Figure A-1   Diagram of mini-piezometer installation in a streambed

The distance over which the vertical component of the hydraulic gradient was measured (dl) was calculated by subtracting the exposed length of piezometer above the streambed (*l*) from the total length of the piezometer (L). The head difference (dh) was the difference in elevation between the stream water level and that inside the piezometer. Hydraulic gradient (i) was calculated as dh/dl, as shown in **Table A-3**.

Table A-3 Measurement of the vertical component of the hydraulic gradient in Prairie Creek

Location	Date	Time	L (m)	*l* (m)	dl (m)	dh (m)	i
B	July 19/97	17:00	2.20	0.88	1.33	0.12	0.13
C	July 22/97	12:50	2.20	0.60	1.60	-0.04	-0.06
D	July 20/97	17:00	2.20	0.44	1.76	-0.14	-0.32

Seepage Rate

A seepage meter measures the seepage rate between groundwater and a stream bed (see **Figure A-2**). The base of the seepage meter consists of a 57 cm diameter metal drum with a 3 cm diameter hole drilled on the top and side. The base is pushed into the sediment about 10 cm and allowed to fill with water. Next, a one-hole stopper fitted with a 40 cm-long polyethylene tube is inserted into the top hole to serve as a vent. Another stopper is inserted into the side hole to which a plastic bag is attached with electric tape, taking care that it is well-sealed and completely submerged (thereby maintaining the same head as the stream). Where hydraulic gradients indicated groundwater discharge into the stream, the plastic bag was inserted empty and allowed to fill over a set time period. Where the opposite flow direction was measured, the bag was filled with a known quantity of water and allowed to drain. This technique is described in Lee and Cherry (1978).

Seepage rate was calculated as dV/dtA, where dV is the volume of water gained or lost, dT is the total time elapsed and A is the cross-sectional area of the seepage meter, as is tabulated below:
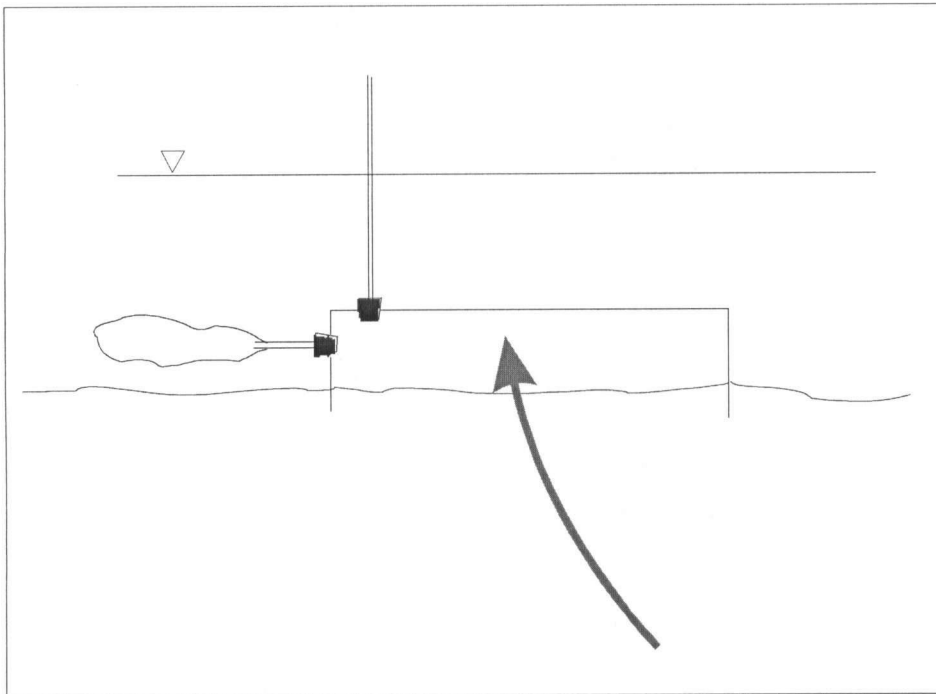
Figure A-2 Diagram of seepage meter installation in a streambed

Table A-4 Seepage meter measurements in Prairie Creek

Location	B	C
Date	July 19/97	July 21/97
Time of insertion	16:40	14:15
Time of removal	17:50	14:55
Elapsed time (hrs) (dT)	1.17	0.67
Change in volume (mL) (dV)	870	-190.00
Flow rate (mL/hr)	745.71	-285.00
area of seepage meter (cm^2) (A)	2570	2570
Seepage rate (mL/hr/cm^3)	0.29	-0.11

B PIEZOMETER LOGS

PIEZOMETER 101
completed in **sandy till**

Depth(m)   Lithology

Elevation of standpipe (w/o cap) (m)	9.250	
Total depth of piez. (m)	2.730	
Depth to eff. midscreen (m)	2.585	
Avg depth to water (m)	0.300	
Inside diameter (cm)	3.4	
Cross-sectional area (cm2)	9.1	
Purge volume (mL)	7435.9	
Screen length (cm)	15.0	
Effective screen length (cm)	15.0	
Length of piezometer (m)	2.950	
Z = elevation head (m)	6.665	
Completion Date	Jul 22 97	
Drilling method	auger & bailer	

Depth(m):
0.0
0.1
0.2
0.3
0.4
0.5
0.6
0.7
0.8
0.9
1.0
1.1
1.2
1.3
1.4
1.5
1.6
1.7
1.8
1.9
2
2.1
2.2
2.3
2.4
2.5
2.6
2.7
2.8
2.9
3

peat

peat

peat and clay

pebbly sand fining up

PIEZOMETER 102

completed in **peat**

		Depth(m)	Lithology
Elevation of standpipe (w/o cap) (m)	9.250	0.0	
		0.1	
Total depth of piez. (m)	1.120	0.2	
Depth to eff. midscreen (m)	0.975	0.3	
Avg depth to water (m)	0.300	0.4	see 101
		0.5	
Inside diameter (cm)	3.4	0.6	mostly peat
Cross-sectional area (cm2)	9.1	0.7	some clay
Purge volume (mL)	3050.6	0.8	
		0.9	
Screen length (cm)	15.0	1.0	screen
Effective screen length (cm)	15.0	1.1	
Total length of piezometer (m)	1.545	1.2	
Z = elevation head (m)	8.275		
Completion Date	Jul 22 97		
Drilling Method	Hand Auger		

sand pack

clay and peat cuttings

bentonite seal
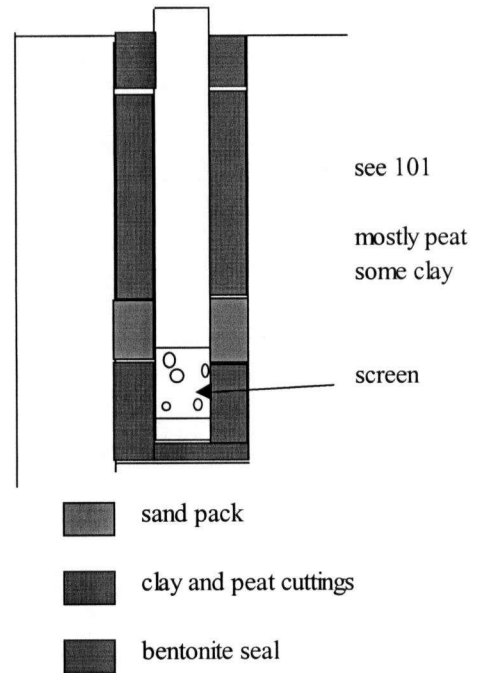
PIEZOMETER 202

completed in **sandy till** w/ sand pack

Elevation of standpipe (w/o cap) (m)	9.745
Total depth of piez. (m)	1.022
Depth to eff. midscreen (m)	0.877
Avg depth to water (m)	0.700
Inside diameter (cm)	3.4
Cross-sectional area (cm2)	9.1
Purge volume (mL)	2783.7
Screen length (cm)	15.0
Effective screen length (cm)	?
Total length of piezometer (m)	1.540
Z = elevation head (m)	8.868
Completion Date	Jul-23-97
Drilling method	auger,
	bailer,
	posthole digger

Depth(m)

0.0
0.1
0.2
0.3
0.4
0.5
0.6
0.7
0.8
0.9
1.0
1.1
1.2

Lithology

peat

pebbly
sand

 sand pack

 clay and peat cuttings

 bentonite seal
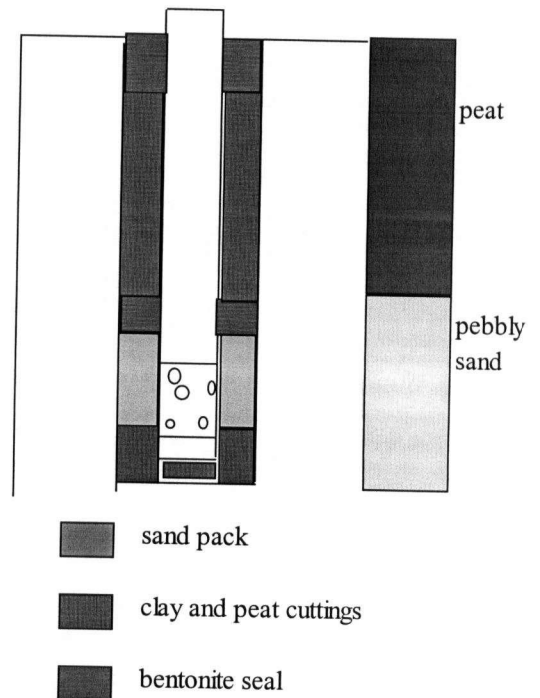
PIEZOMETER 302

completed in **clay** w/ sand pack

Elevation of standpipe (w/o cap) (m)	10.450
Total depth of piez. (m)	1.845
Depth to eff. midscreen (m)	1.700
Avg depth to water (m)	1.100
Inside diameter (cm)	3.4
Cross-sectional area (cm2)	9.1
Purge volume (mL)	5025.3
Screen length (cm)	15.0
Effective screen length (cm)	40.0
Total length of piezometer (m)	2.050
Z = elevation head (m)	8.750
Completion Date	31-Jul-97
Drilling method	auger only

Depth(m)

0.0
0.1
0.2
0.3
0.4
0.5
0.6
0.7
0.8
0.9
1.0
1.1
1.2
1.3
1.4
1.5
1.6
1.7
1.8
1.9
2

Lithology

peat

clay

clay grading to sand

sand pack

clay and peat cuttings

bentonite seal
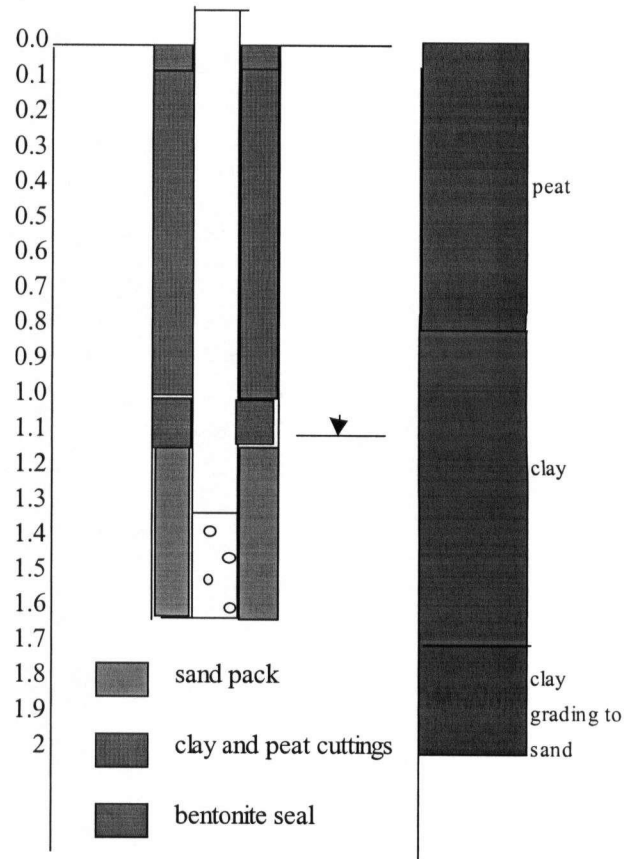
PIEZOMETER 401

completed in **pebbly sand** w/ sand pack

Elevation of standpipe (w/o cap) (m)	9.580
Total depth of piez. (m)	2.611
Depth to eff. midscreen (m)	2.466
Avg depth to water (m)	0.900
Inside diameter (cm)	3.4
Cross-sectional area (cm2)	9.1
Purge volume (mL)	7111.7
Screen length (cm)	15.0
Effective screen length (cm)	?
Length of piezometer (m)	2.938
Z = elevation head (m)	7.114
Completion Date	Jul-97
Drilling method	auger,
	bailer

Depth(m)

Lithology

peat

170 cm

mostly clay

240 cm

pebbly sand

134
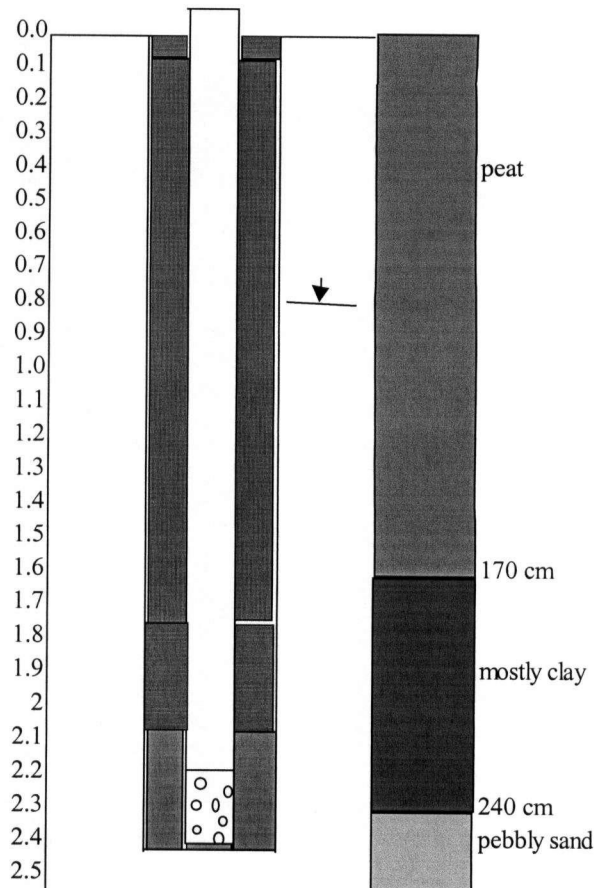
PIEZOMETER 402

completed in **peat**

Elevation of standpipe (w/o cap) (m)	9.630
Total depth of piez. (m)	1.262
Depth to eff. midscreen (m)	1.117
Avg depth to water (m)	0.700
Inside diameter (cm)	3.4
Cross-sectional area (cm2)	9.1
Purge volume (mL)	3437.4
Screen length (cm)	15.0
Effective screen length (cm)	?
Total length of piezometer (m)	1.540
Z = elevation head (m)	8.513
Completion Date	Jul-23-97
Drilling method	posthole digger

Depth(m)

0.0
0.1
0.2
0.3
0.4
0.5
0.6
0.7
0.8
0.9
1.0

Lithology

see 401

sand pack

clay and peat cuttings

bentonite seal
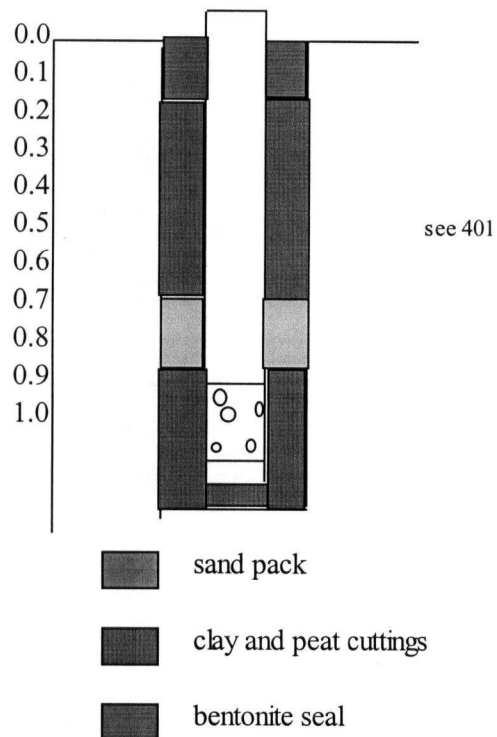
PIEZOMETER 502

completed in **peat**

Depth(m)

Lithology

Elevation of standpipe (w/o cap) (m)	11.900
Total depth of piez. (m)	1.305
Depth to eff. midscreen (m)	1.160
Avg depth to water (m)	77.000
Inside diameter (cm)	3.4
Cross-sectional area (cm2)	9.1
Purge volume (mL)	3554.5
Screen length (cm)	15.0
Effective screen length (cm)	?
Total length of piezometer (m)	1.540
Length of cutoff	0.235
Z = elevation head (m)	10.740
Completion Date	Jul-23-97
Drilling method	post-hole
	digger

0.0
0.1
0.2
0.3
0.4
0.5
0.6
0.7
0.8
0.9
1.0

peat

sand pack

clay and peat cuttings

bentonite seal
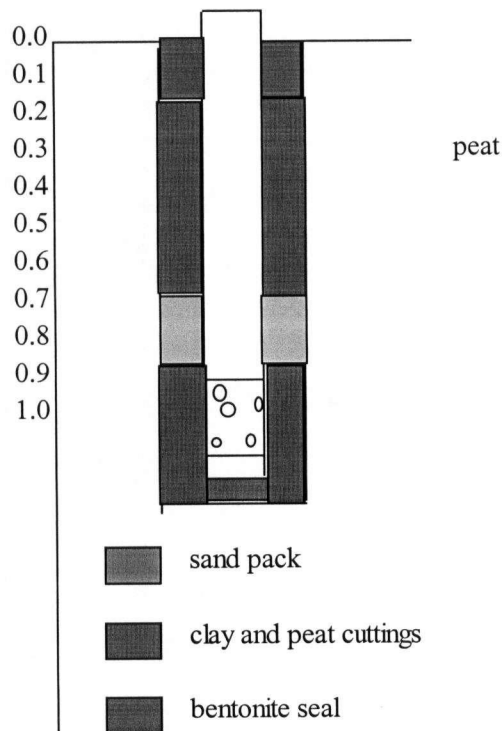
PIEZOMETER 601

completed in **sand** w/ sand pack

Depth(m)

Lithology

Elevation of standpipe (w/o cap) (m)	9.720
Total depth of piez. (m)	1.385
Depth to eff. midscreen (m)	1.240
Avg depth to water (m)	0.690
Inside diameter (cm)	3.4
Cross-sectional area (cm2)	9.1
Purge volume (mL)	3772.4
Screen length (cm)	15.0
Effective screen length (cm)	26.5
Length of piezometer (m)	1.540
Z = elevation head (m)	8.480
Completion Date	July 30'97
Drilling method	auger,
	bailer

Depth scale: 0.0, 0.1, 0.2, 0.3, 0.4, 0.5, 0.6, 0.7, 0.8, 0.9, 1.0, 1.1, 1.2, 1.3, 1.4, 1.5, 1.6, 1.7

Lithology labels:
- peat
- 65cm
- clay and peat
- 88cm
- sand (fining up)
- sand with pebbles

Legend:
- sand pack
- clay and peat cuttings
- bentonite seal

PIEZOMETER 602

completed in **sandy till/clay** w/ sand pack

Depth(m)

Lithology

Elevation of standpipe (w/o cap) (m)	9.725
Total depth of piez. (m)	1.115
Depth to eff. midscreen (m)	0.970
Avg depth to water (m)	0.690
Inside diameter (cm)	3.4
Cross-sectional area (cm2)	9.1
Purge volume (mL)	3037.0
Screen length (cm)	15.0
Effective screen length (cm)	
Total length of piezometer (m)	1.965
Length of cutoff (m)	0.850
Z = elevation head (m)	8.755
Completion Date	Jul-97
Drilling method	auger

see 601
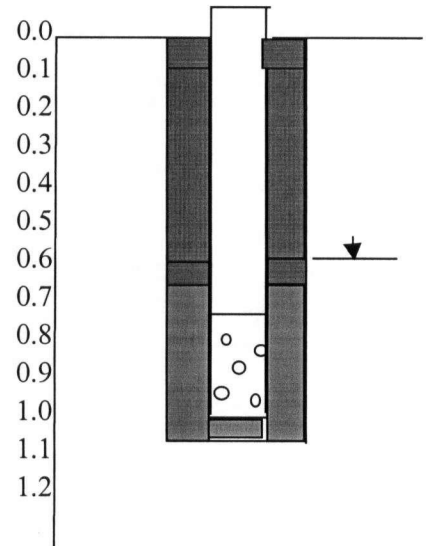
sand pack

clay and peat cuttings

bentonite seal

PIEZOMETER 701

completed in **sandy till** w/ sand pack

Elevation of standpipe (w/o cap) (m)	10.485
Total depth of piez. (m)	2.437
Depth to eff. midscreen (m)	2.292
Avg depth to water (m)	1.000
Inside diameter (cm)	3.4
Cross-sectional area (cm2)	9.1
Purge volume (mL)	6637.8
Screen length (cm)	15.0
Effective screen length (cm)	?
Length of piezometer (m)	2.950
Z = elevation head (m)	8.193
Completion Date	Jul 23 97
Drilling method	auger,
	bailer

Depth(m)

0.0
0.1
0.2
0.3
0.4
0.5
0.6
0.7
0.8
0.9
1.0
1.1
1.2
1.3
1.4
1.5
1.6
1.7
1.8
1.9
2
2.1
2.2
2.3
2.4
2.5
2.6
2.7
2.8
2.9
3

Lithology

peat

volcanic ash

clay

peat

peat&clay
1.50m

1.80m
clayey sand

coarser
sand
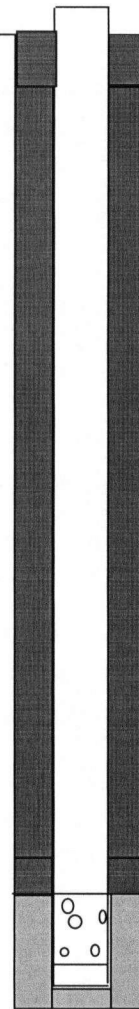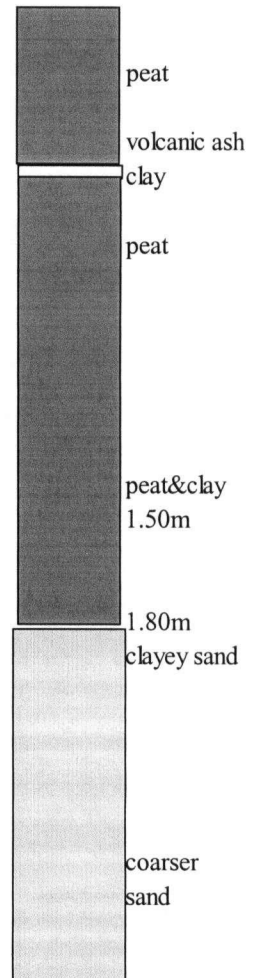
PIEZOMETER 702

completed in **peat**

Depth(m)

Lithology

Elevation of standpipe (w/o cap) (m)	10.465
Total depth of piez. (m)	1.287
Depth to eff. midscreen (m)	1.142
Avg depth to water (m)	1.000
Inside diameter (cm)	3.4
Cross-sectional area (cm2)	9.1
Purge volume (mL)	3505.5
Screen length (cm)	15.0
Effective screen length (cm)	?
Total length of piezometer (m)	1.540
Z = elevation head (m)	9.323
Completion Date	Jul 23 97
Drilling method	post-hole digger

0.0
0.1
0.2
0.3
0.4
0.5
0.6
0.7
0.8
0.9
1.0

see 701
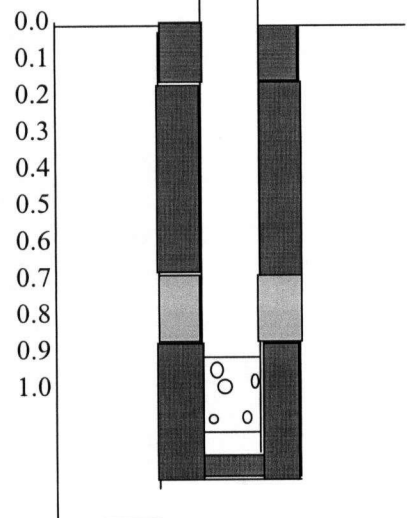
sand pack

clay and peat cuttings

bentonite seal

PIEZOMETER 802

Completed in **peat**   **Depth(m)**   **Lithology**

Elevation of standpipe (w/o cap) (m)	9.580
Total depth of piez. (m)	1.285
Depth to eff. midscreen (m)	1.140
Avg depth to water (m)	0.700
Inside diameter (cm)	3.4
Cross-sectional area (cm2)	9.1
Purge volume (mL)	3500.0
Screen length (cm)	15.0
Effective screen length (cm)	15.0
Total length of piezometer (m)	1.540
Z = elevation head (m)	8.440
Completion Date	31-Jul-97
Drilling method	auger

sand pack

clay and peat cuttings

bentonite seal
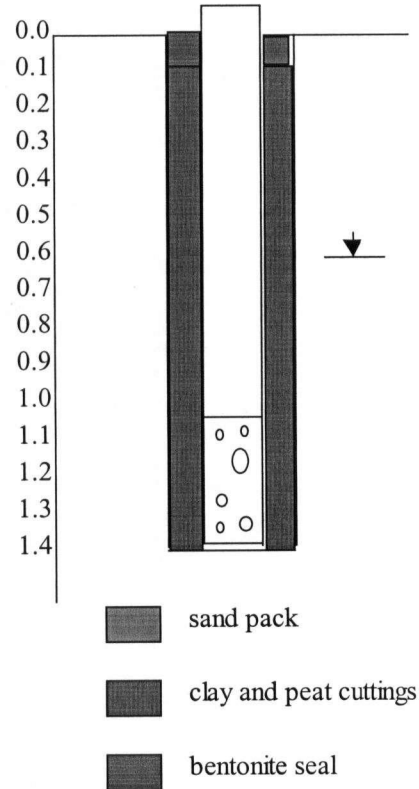
PIEZOMETER 902

completed in **peat**

Depth(m)

Lithology

Elevation of standpipe (w/o cap) (m)	9.122
Total depth of piez. (m)	1.201
Depth to eff. midscreen (m)	1.056
Avg depth to water (m)	0.650
Inside diameter (cm)	3.4
Cross-sectional area (cm2)	9.1
Purge volume (mL)	3271.2
Screen length (cm)	15.0
Effective screen length (cm)	15.0
Total length of piezometer (m)	1.540
Z = elevation head (m)	8.066
Completion Date	31-Jul-97
Drilling method	auger
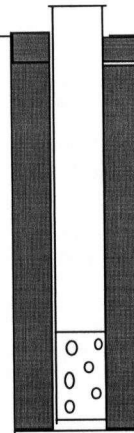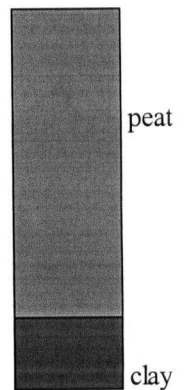
sand pack

clay and peat cuttings

bentonite seal

C HYDRAULIC CONDUCTIVITY TEST DATA

BAIL TEST   PIEZOMETER 101

Date	Actual Time	Elapsed Time	Elapsed Time (s)	Depth to Water (m)	Total Head Water (m)
Aug2/97	9:50:00	0:00		0.496	8.754
	10:00:00	0		2.540	6.710
	10:02:00	0:02:00	120	2.352	6.898
	10:04:00	0:04:00	240	2.230	7.020
	10:06:00	0:06:00	360	2.115	7.135
	10:15:00	0:15:00	900	1.680	7.570
	10:21:00	0:21:00	1260	1.406	7.844
	10:26:00	0:26:00	1560	1.290	7.960
	11:06:00	1:06:00	3960	0.642	8.608
	11:10:00	1:10:00	4200	0.601	8.649
	11:16:00	1:16:00	4560	0.542	8.708
	11:24:00	1:24:00	5040	0.513	8.737
	11:45:00	1:45:00	6300	0.487	8.763
	13:13:00	3:13:00	11580	0.494	8.756
	14:03:00	4:03:00	14580	0.498	8.752
	16:30:00	6:30:00	23400	0.509	8.741
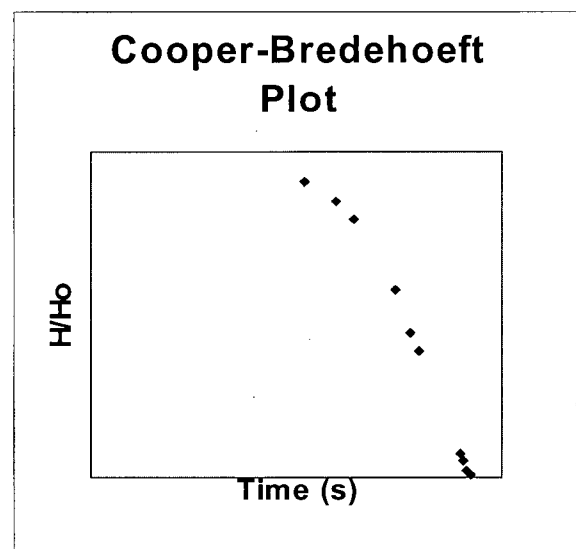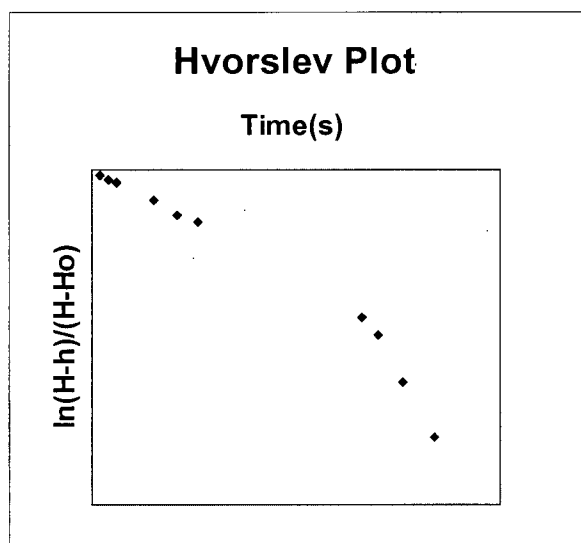
Hvorslev Plot

Time(s)

ln(H-h)/(H-Ho)

Cooper-Bredehoeft Plot

H/Ho

Time (s)

BAIL TEST   **PIEZOMETER 101**

Date	Actual Time	Elapsed Time	Elapsed Time (s)	Depth to Water (m)	Total Head Water (m)
Sep27/97	1:50:00	0:00		0.258	8.992
	1:51:30	0:00	0:00	0.606	8.644
	1:52:00	0:30	30	0.415	8.835
	1:53:00	0:01:30	90	0.333	8.917
	1:54:00	0:02:30	150	0.282	8.968
	1:54:30	0:03:00	180	0.271	8.979
	1:55:00	0:03:30	210	0.266	8.984
	1:55:30	0:04:00	240	0.264	8.986
	1:56:00	0:04:30	270	0.263	8.987
	1:57:00	0:05:30	330	0.263	8.988
	1:58:00	0:06:30	390	0.262	8.990
	2:00:00	0:08:30	510	0.260	8.991
	2:10:00	0:18:30	1110	0.259	8.991
	2:20:00	0:28:30	1710	0.259	8.984
	3:07:00	1:15:30	4530	0.266	9.250

Hvorslev Plot
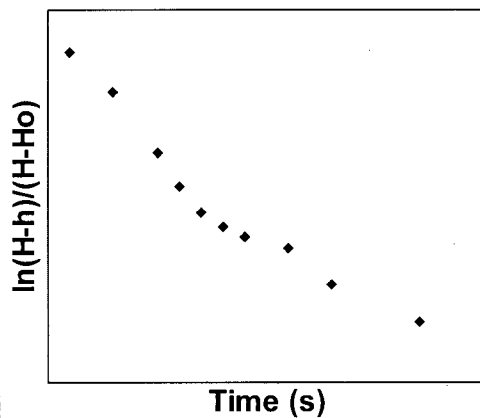
Cooper-Bredehoeft Plot
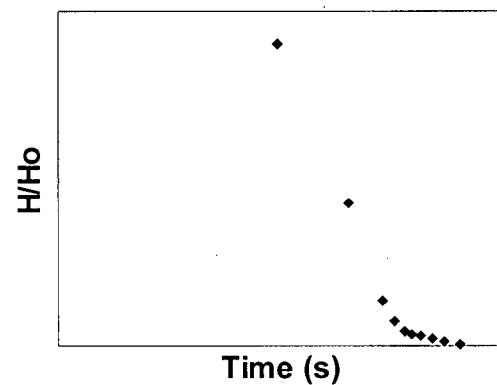
BAIL TEST PIEZOMETER 102

Date	Actual Time	Elapsed Time	Elapsed Time (s)	Depth to Water (m)	Total Head Water (m)
Sep27/97	1:30:00	0:00		0.274	8.976
	1:30:30	0:00:00	0:00	0.622	8.628
	1:31:00	0:00:30	30	0.528	8.722
	1:32:00	0:01:30	90	0.526	8.724
	1:33:00	0:02:30	150	0.522	8.728
	1:34:00	0:03:30	210	0.520	8.730
	1:35:00	0:04:30	270	0.517	8.733
	1:40:00	0:09:30	570	0.506	8.744
	1:45:00	0:14:30	870	0.498	8.752
	1:50:00	0:19:30	1170	0.490	8.776
	2:00:00	0:29:30	1770	0.474	8.791
	2:10:00	0:39:30	2370	0.459	8.805
	2:20:00	0:49:30	2970	0.445	8.851
	3:09:00	1:38:30	5910	0.399	8.887
	4:10:00	2:39:30	9570	0.363	9.250

Hvorslev Plot
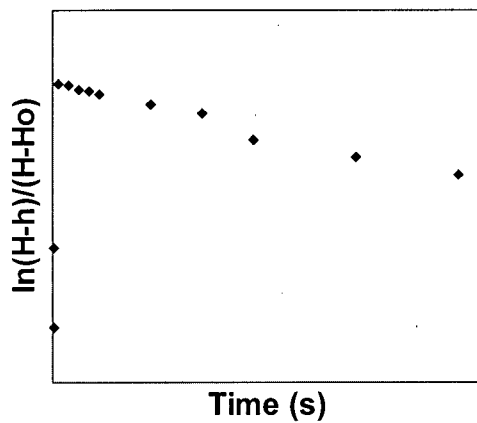
Cooper-Bredehoeft Plot
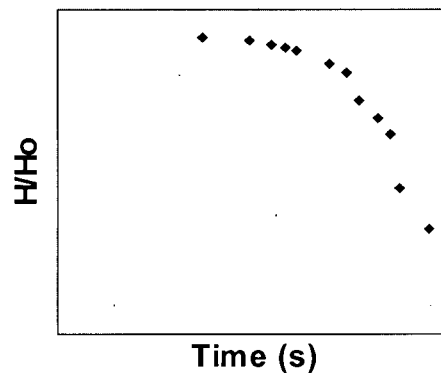
SLUG TEST   PIEZOMETER 202

Date	Actual Time	Elapsed Time	Elapsed Time (s)	Depth to Water (m)	Total Head Water (m)
Aug3/97	19:38:00		0	0.755	8.990
	19:38:00	0:00	0	0.285	9.460
		0:00:15	15	0.320	9.425
		0:00:25	25	0.398	9.347
		0:00:40	40	0.498	9.247
		0:00:50	50	0.470	9.275
		0:01:00	60	0.486	9.259
		0:01:10	70	0.494	9.251
		0:01:20	80	0.500	9.245
		0:01:40	100	0.503	9.242
		0:02:05	125	0.510	9.235
		0:02:40	160	0.515	9.230
		0:03:00	180	0.519	9.226
		0:03:15	195	0.520	9.225
		0:03:45	225	0.524	9.221
		0:04:15	255	0.528	9.217
		0:05:00	300	0.533	9.212
		0:06:00	360	0.538	9.207
		0:08:00	480	0.550	9.195
		0:10:00	600	0.559	9.186
	20:03:00	0:25:00	1500	0.616	9.129
	20:13:00	0:35:00	2100	0.643	9.102
	20:15:00	0:37:00	2220	0.649	9.096
	20:37:00	0:59:00	3540	0.682	9.063
	21:01:00	1:23:00	4980	0.704	9.041

Hvorslev Plot

y-axis: ln(H-h)/(H-Ho)
x-axis: Time (s)

Cooper-Bredehoeft Plot

y-axis: H/Ho
x-axis: Time (s)
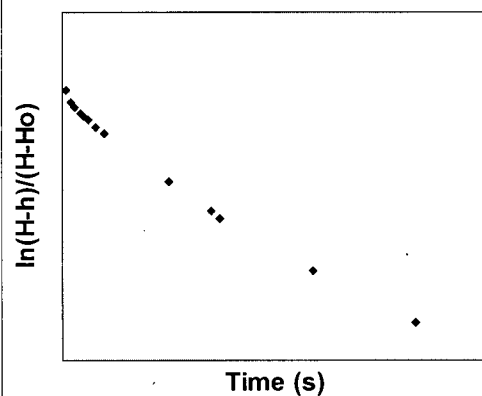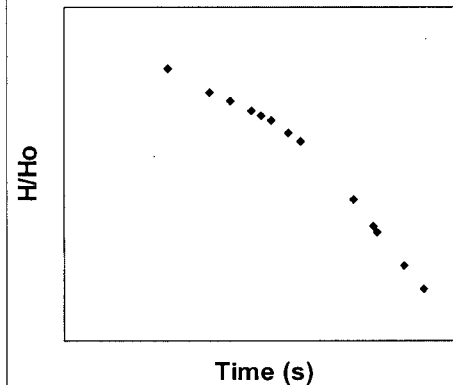
SLUG TEST   PIEZOMETER 302

Date	Actual Time	Elapsed Time	Elapsed Time (s)	Depth to Water (m)	Total Head Water (m)
Aug3/97	18:50:00	0:00	0	1.194	9.256
	18:54:00	0:00:00	0	0.694	9.756
		0:00:30	30	0.700	9.750
		0:00:40	40	0.704	9.746
		0:00:50	50	0.710	9.740
		0:01:05	65	0.715	9.735
		0:01:20	80	0.720	9.730
		0:01:45	105	0.726	9.724
		0:02:00	120	0.732	9.718
		0:02:30	150	0.738	9.712
		0:03:00	180	0.746	9.704
		0:03:15	195	0.749	9.701
		0:03:30	210	0.752	9.698
		0:04:00	240	0.758	9.692
		0:04:30	270	0.764	9.686
		0:05:00	300	0.771	9.679
		0:05:30	330	0.777	9.673
		0:06:00	360	0.784	9.666
		0:06:45	405	0.793	9.657
		0:08:00	480	0.807	9.643
		0:09:15	555	0.821	9.629
		0:11:00	660	0.84	9.610
		0:13:00	780	0.86	9.590
		0:14:30	870	0.875	9.575
		0:17:30	1050	0.905	9.545
	19:14:00	0:20:00	1200	0.922	9.528
		0:24:15	1455	0.948	9.502
	19:28:00	0:34:00	2040	1.009	9.441
	19:50:00	0:56:00	3360	1.09	9.360
	19:56:00	1:02:00	3720	1.105	9.345
	19:58:00	1:04:00	3840	1.11	9.340
	20:05:00	1:11:00	4260	1.12	9.330
	20:23:00	1:29:00	5340	1.145	9.305

Hvorslev Plot

ln(H-h)/(H-Ho)

Time (s)

Cooper-Bredehoeft Plot

H/Ho
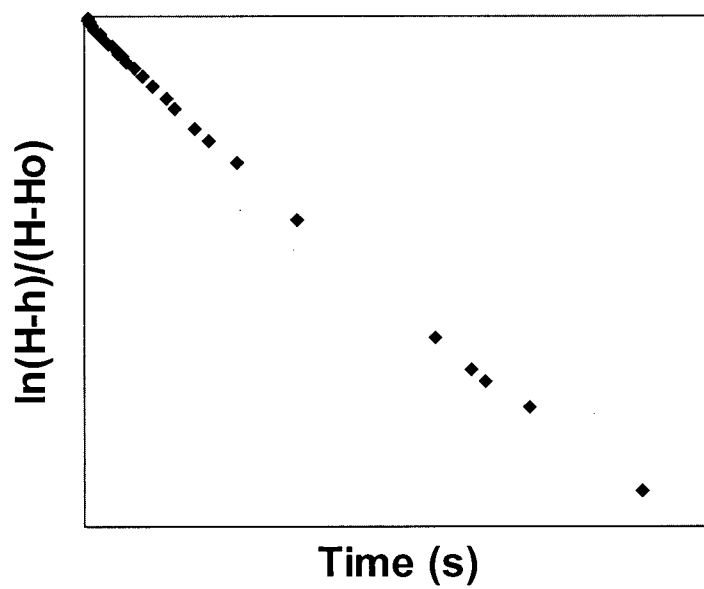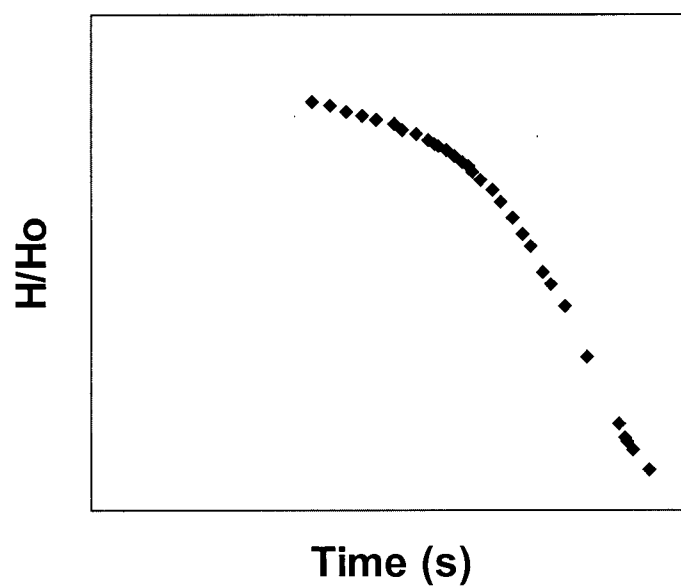
Time (s)

SLUG TEST   PIEZOMETER 402

Date	Actual Time	Elapsed Time	Elapsed Time (s)	Depth to Water (m)	Total Head Water (m)
Aug3/97	18:29:00	0:00	0	0.813	8.817
	18:29:00	0:00	0	0.524	9.106
		0:00:30	30	0.525	9.105
		0:00:40	40	0.531	9.099
		0:00:45	45	0.540	9.090
		0:01:15	75	0.547	9.083
		0:01:45	105	0.557	9.073
		0:02:15	135	0.564	9.066
		0:02:45	165	0.572	9.058
		0:03:15	195	0.578	9.052
		0:04:00	240	0.585	9.045
		0:04:30	270	0.594	9.036
		0:05:00	300	0.599	9.031
		0:05:30	330	0.602	9.028
		0:06:00	360	0.608	9.022
		0:06:30	390	0.613	9.017
		0:07:00	420	0.618	9.012
		0:07:30	450	0.622	9.008
		0:08:15	495	0.627	9.003

Hvorslev Plot

y-axis: ln(H-h)/(H-Ho)
x-axis: Time (s)

Cooper-Bredehoeft Plot

y-axis: H/Ho
x-axis: Time (s)
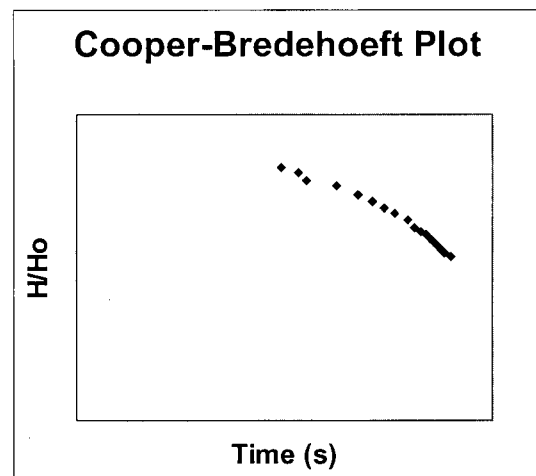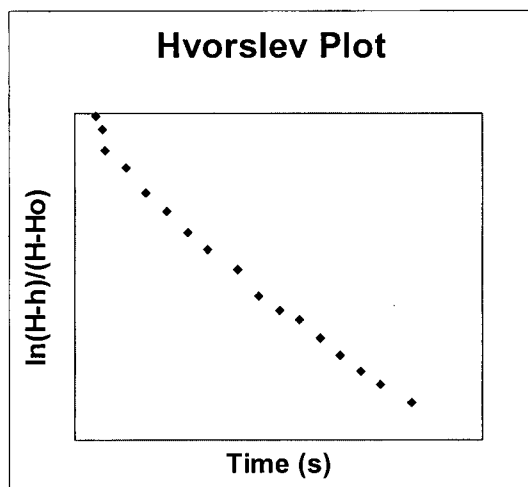
BAIL TESTS   PIEZOMETER 601

Date	Actual Time	Elapsed Time	Elapsed Time (s)	Depth to Water (m)	Total Head Water (m)
Sep27/97	10:43:00	0:00		0.250	9.470
	10:43:00	0:00:00		0.598	9.122
	10:44:00	0:01:00	60	0.420	9.300
	10:44:30	0:01:30	90	0.340	9.380
	10:45:00	0:02:00	120	0.269	9.451
	10:45:30	0:02:30	150	0.260	9.460
	10:46:00	0:03:00	180	0.257	9.463
	10:46:30	0:03:30	210	0.255	9.465
	10:47:00	0:04:00	240	0.255	9.465
	10:49:00	0:06:00	360	0.255	9.465
	10:50:00	0:07:00	420	0.254	9.466
	11:00:00	0:17:00	1020	0.258	9.462
	11:05:00	0:22:00	1320	0.257	9.463
	11:10:00	0:27:00	1620	0.257	9.463
	11:30:00	0:47:00	2820	0.257	9.463
	11:33:00			0.257	9.463
	11:33:00			0.493	9.227
	11:33:10	0:00:10	10	0.354	9.366
	11:33:30	0:00:30	30	0.305	9.415
	11:34:00	0:01:00	60	0.273	9.447
	11:34:30	0:01:30	90	0.266	9.454
	11:35:00	0:02:00	120	0.259	9.461
	11:37:00	0:04:00	240	0.258	9.462
	11:40:00	0:07:00	420	0.258	9.462
	15:27:00	3:54:00	3240	0.285	9.435

Hvorslev Plots

ln(H-h)/(H-Ho)

Time (s)

Cooper-Bredehoeft Plots

H/Ho
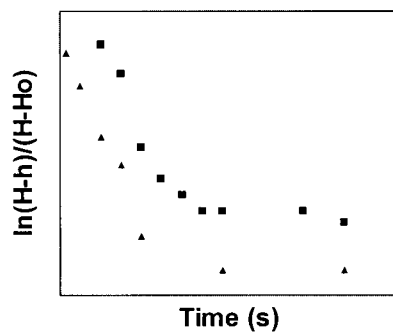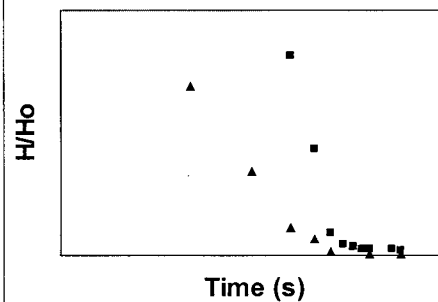
Time (s)

BAIL TESTS   PIEZOMETER 602

Date	Actual Time	Elapsed Time	Elapsed Time (s)	Depth to Water (m)	Total Head Water (m)
Sep26/97	3:52:00			0.198	9.527
	3:52:00	0:00:00		0.839	8.886
	3:53:00	0:01:00	60	0.805	8.920
	3:54:00	0:02:00	120	0.778	8.947
	3:55:00	0:03:00	180	0.751	8.974
	3:56:00	0:04:00	240	0.728	8.997
	3:57:00	0:05:00	300	0.704	9.021
	3:58:00	0:06:00	360	0.683	9.042
	3:59:00	0:07:00	420	0.664	9.061
	4:00:00	0:08:00	480	0.641	9.084
	4:01:00	0:09:00	540	0.625	9.100
	4:03:00	0:11:00	660	0.590	9.135
	4:05:00	0:13:00	780	0.560	9.165
	4:10:00	0:18:00	1080	0.493	9.232
	4:15:00	0:23:00	1380	0.441	9.284
	4:20:00	0:28:00	1680	0.400	9.325
	4:25:00	0:33:00	1980	0.365	9.360
	4:30:00	0:38:00	2280	0.337	9.388
	4:40:00	0:48:00	2880	0.291	9.434
	4:50:00	0:58:00	3480	0.267	9.458
	4:55:00	1:03:00	3780	0.258	9.467
	6:53:00	3:01:00	10860	0.225	9.500
Sep27/97	10:54:00			0.251	9.474
	10:55:00			0.524	9.201
	10:55:30	0:00:30	30	0.512	9.213
	10:56:00	0:01:00	60	0.503	9.222
	10:57:00	0:02:00	120	0.484	9.241
	10:58:00	0:03:00	180	0.469	9.256
	10:59:00	0:04:00	240	0.456	9.269
	11:00:00	0:05:00	300	0.441	9.284
	11:02:00	0:07:00	420	0.417	9.308
	11:04:00	0:09:00	540	0.395	9.330
	11:06:00	0:11:00	660	0.379	9.346
	11:08:00	0:13:00	780	0.361	9.364
	11:10:00	0:15:00	900	0.347	9.378
	11:15:00	0:20:00	1200	0.32	9.405
	11:20:00	0:25:00	1500	0.299	9.426
	11:25:00	0:30:00	1800	0.286	9.439

	11:30:00	0:35:00	2100	0.276	9.449
	11:40:00	0:45:00	2700	0.262	9.463
	11:50:00	0:55:00	3300	0.259	9.466
	12:00:00	1:05:00	3900	0.257	9.468
	12:21:00	1:26:00	5160	0.257	9.468
	15:27:00	4:32:00	16320	0.286	9.439
Sept27/97	15:27:00			0.286	9.439
	15:32:00			0.522	9.203
	15:32:30	0:00:30	30	0.514	9.211
	15:33:00	0:01:00	60	0.505	9.220
	15:34:00	0:02:00	120	0.489	9.236
	15:35:30	0:03:30	210	0.47	9.255
	15:36:00	0:04:00	240	0.465	9.260
	15:37:30	0:05:30	330	0.449	9.276
	15:38:00	0:06:00	360	0.444	9.281
	15:39:00	0:07:00	420	0.436	9.289
	15:40:00	0:08:00	480	0.427	9.298
	15:45:00	0:13:00	780	0.392	9.333
	15:50:00	0:18:00	1080	0.366	9.359
	16:02:00	0:30:00	1800	0.328	9.397

Hvorslev Plots

(H-h)/(H-Ho) vs Time (s)

Cooper-Bredehoeft Plots

H/Ho vs Time (s)

BAIL TEST   PIEZOMETER 802

Date	Actual Time	Elapsed Time	Elapsed Time (s)	Depth to Water (m)	Total Head Water (m)
Sep27/97	14:27:00			0.520	9.060
	14:27:00			0.756	8.824
	14:27:30	0:00:30	30	0.753	8.827
	14:28:00	0:01:00	60	0.745	8.835
	14:28:30	0:01:30	90	0.740	8.840
	14:29:00	0:02:00	120	0.735	8.845
	14:30:00	0:03:00	180	0.726	8.854
	14:31:00	0:04:00	240	0.721	8.859
	14:32:00	0:05:00	300	0.713	8.867
	14:34:00	0:07:00	420	0.696	8.884
	14:36:00	0:09:00	540	0.683	8.897
	14:38:00	0:11:00	660	0.673	8.907
	14:40:00	0:13:00	780	0.662	8.918
	14:45:00	0:18:00	1080	0.640	8.940
	14:50:00	0:23:00	1380	0.622	8.958
	15:00:00	0:33:00	1980	0.595	8.985
	15:15:00	0:48:00	2880	0.565	9.015

Hvorslev Plot

Cooper-Bredehoeft Plot

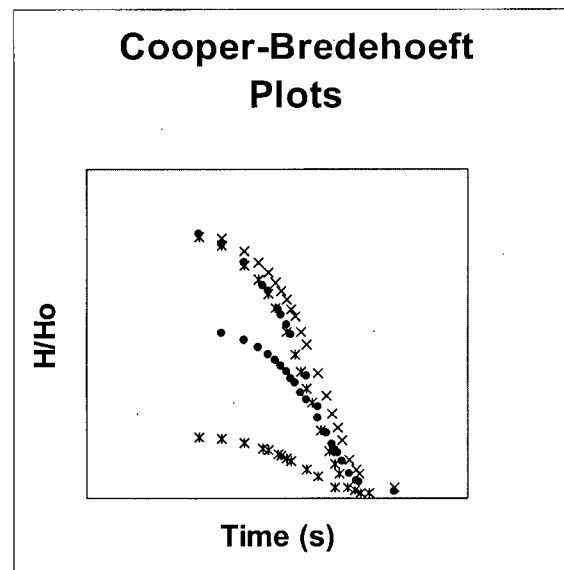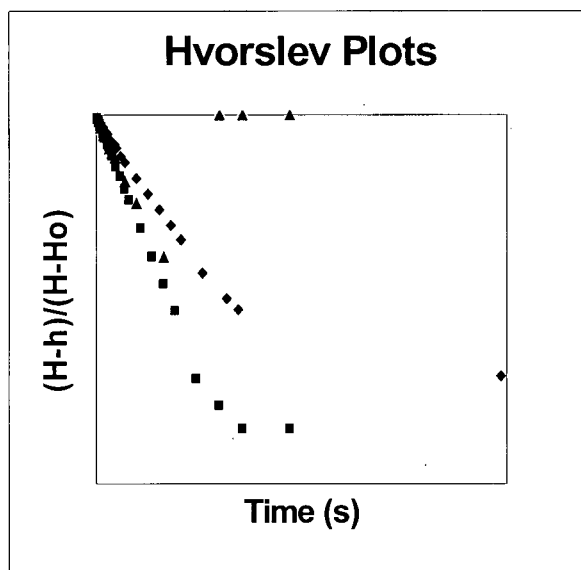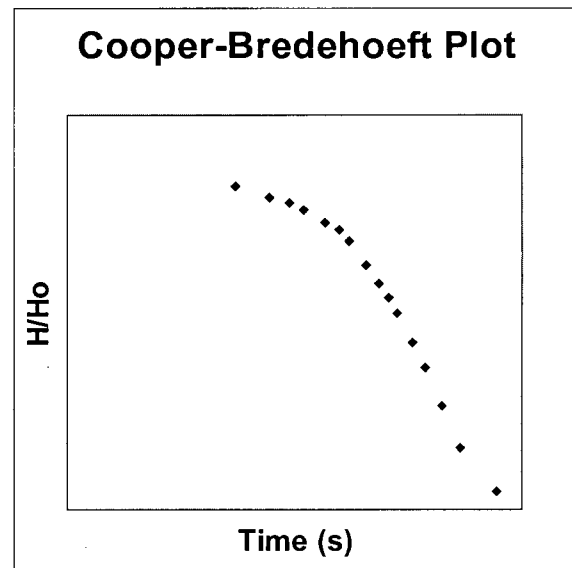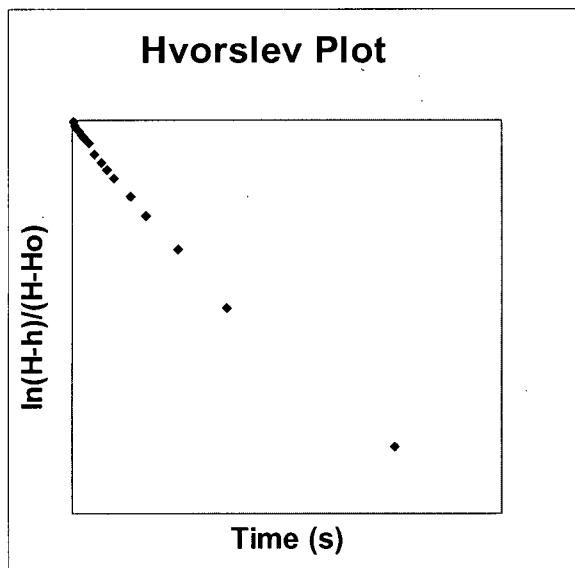# SLUG TEST   PIEZOMETER 902

Date	Actual Time	Elapsed Time	Elapsed Time (s)	Depth to Water (m)	Total Head Water (m)
Aug2/97	0.4416667	0		0.477	8.645
	0.4420139	0	0	0.191	8.931
	0.4423611	0.0003472	30	0.2	8.922
	0.4430556	0.0010417	90	0.212	8.91
	0.44375	0.0017361	150	0.221	8.901
	0.4451389	0.003125	270	0.234	8.888
	0.4465278	0.0045139	390	0.249	8.873
	0.4479167	0.0059028	510	0.259	8.863
	0.4493056	0.0072917	630	0.267	8.855
	0.45625	0.0142361	1230	0.304	8.818
	0.4604167	0.0184028	1590	0.317	8.805
	0.4673611	0.0253472	2190	0.34	8.782
	0.4770833	0.0350694	3030	0.363	8.759
	0.4784722	0.0364583	3150	0.37	8.752
	0.4861111	0.0440972	3810	0.376	8.746
	0.5013889	0.059375	5130	0.398	8.724
	0.5541667	0.1121528	9690	0.438	8.684
	0.7111111	0.2690972	23250	0.469	8.653

Hvorslev Plot

ln(H-h)/(H-Hss)

Time (s)

Cooper-Bredehoeft Plot

H/Ho

Time (s)

154
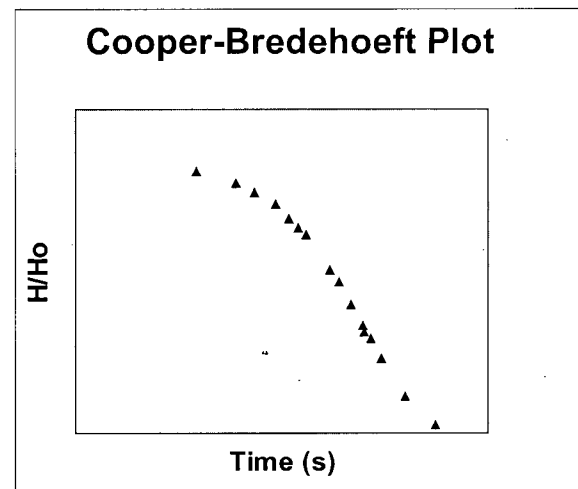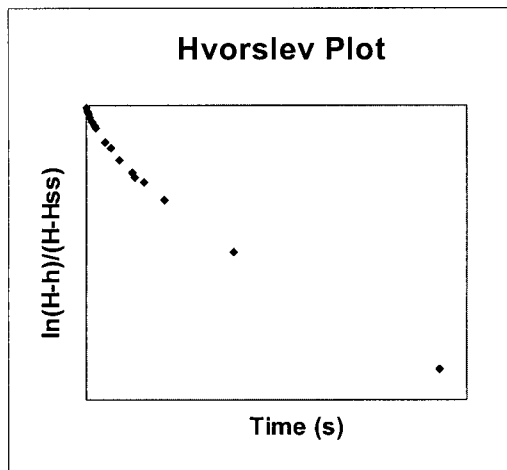
BAIL TEST   PIEZOMETER 902

Date	Actual Time	Elapsed Time	Elapsed Time (s)	Depth to Water (m)	Total Head Water (m)
Sep27/97	9:17:00			0.291	8.831
	9:17:00			0.531	8.591
	9:17:30	0:00:30	30	0.530	8.592
	9:18:00	0:01:00	60	0.529	8.593
	9:19:00	0:02:00	120	0.526	8.596
	9:20:00	0:03:00	180	0.524	8.598
	9:21:00	0:04:00	240	0.522	8.600
	9:23:00	0:06:00	360	0.518	8.604
	9:25:00	0:08:00	480	0.511	8.611
	9:27:00	0:10:00	600	0.506	8.616
	9:35:00	0:18:00	1080	0.490	8.632
	9:40:00	0:23:00	1380	0.481	8.641
	9:45:00	0:28:00	1680	0.473	8.649
	9:55:00	0:38:00	2280	0.455	8.667
	10:05:00	0:48:00	2880	0.439	8.683
	10:15:00	0:58:00	3480	0.425	8.697
	10:30:00	1:13:00	4380	0.409	8.713
	15:04:00	5:47:00	20820	0.321	8.801

Hvorslev Plot

y-axis: ln(H-h)/(H-Ho)
x-axis: Time (s)

Cooper-Bredehoeft Plot

y-axis: H/Ho
x-axis: Time (s)
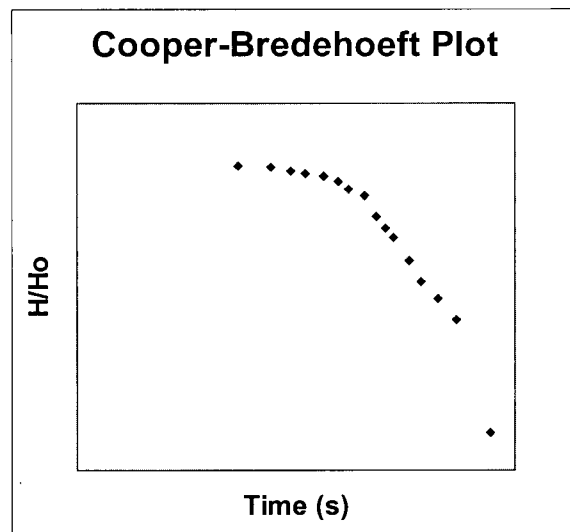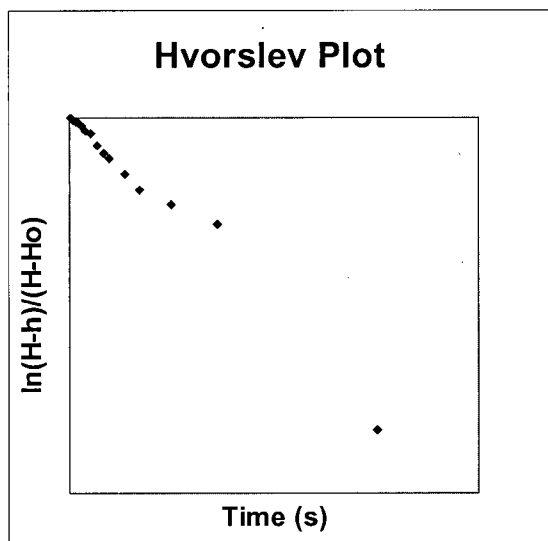
D   WATER SAMPLING FIELD METHODS

This appendix describes how water samples were collected from the piezometers in September '97 and March '98, and which chemical parameters were measured in the field. It is divided into three sections: 1) piezometer preparation 2) sample collection and 3) field analyses.

PIEZOMETER PREPARATION

Immediately after installation, a piezometer is developed to clear away sediment from the base of the standpipe and around the screen. Just before taking a groundwater sample, purging is done to remove stagnant or non-representative water in the piezometer casing, filter pack, and formation. This section explains how development, purging, and sample retrieval were carried out on site.

Piezometer Development

All piezometers were developed using a Waterra™ inertial pump, applying high flow rates to free as much material as possible. The shallow piezometers were pumped to dryness three times. Due to the low hydraulic conductivity of the peat, this process required up to two days. Water clarity improved significantly (from grey to colourless) at all piezometers except 202. It is possible that the filter cloth covering the screen was pushed up or torn when the piezometer was inserted, allowing silt and clay to enter the piezometer.

At least three well volumes (one well volume is the volume of water in the standpipe) were pumped from each of the deep piezometers, stopping when good water clarity was achieved. To avoid cross-contamination by the Waterra™ pump, the foot valve and attached hose were rinsed with a 15% nitric acid solution, then twice with tap water between sampling locations.

Piezometer Purging

Before taking a water sample from the deep piezometers, at least five well volumes were purged using a peristaltic pump at flow rates of around 750 mL/min. The pump was powered by a car battery and connected to a flow-through cell (see **Plate D-1**). The cell consisted of a plastic erlenmyer vacuum flask capped with a rubber stopper having three holes: one for incoming water, another for the pH or Eh probe, and another for the temperature probe. Water left the cell via the vacuum outlet. Separate lengths of tubing were inserted into each piezometer to prevent cross-contamination. Water clarity was good at all three locations and conductivity, pH, and temperature stabilized within minutes. Due to the slow recovery rates of the shallow piezometers, purging just prior to sample collection was not feasible.
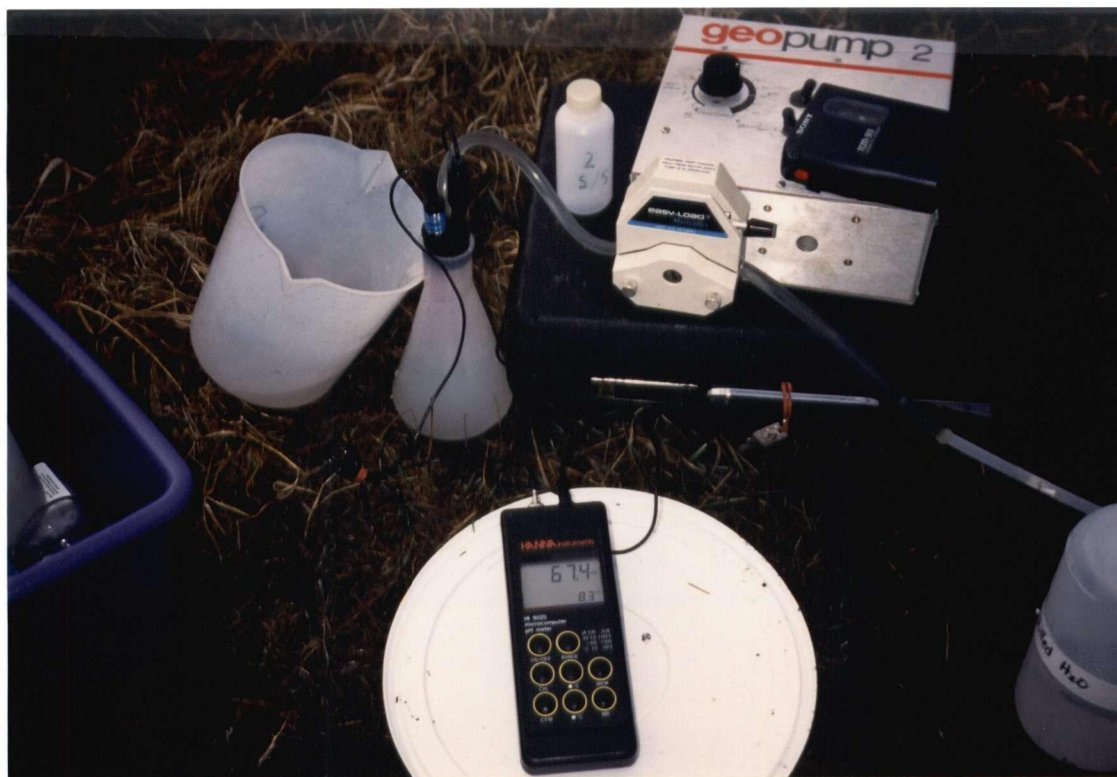
Plate D-1   Set-up of peristaltic pump (geopump) and flow-through cell (centre) with pH meter attached

SAMPLE COLLECTION

Samples were collected from the deep piezometers using the peristaltic pump once pH, conductivity, and temperature readings in the flow-through cell had stabilized (see **Plate D-1**). At the shallow piezometers, samples were collected using either a Waterra™ pump (September '97) or nylon bailer (March '98) within 24 hours of development, or as soon as the water levels had returned to equilibrium. Oxygenation of the water in the standpipe was not a concern since relatively high levels of ferrous iron (over 3 mg/L) were detected. To avoid cross-contamination, both the Waterra™ pump and bailer were rinsed twice with tap water and once with distilled water between sampling locations.

FIELD ANALYSES

The geochemical parameters measured in the field included Eh, ferrous iron, pH, conductivity, temperature, and alkalinity. At all deep piezometers, Eh, pH, and temperature were measured in the flow-through cell, and conductivity and alkalinity were measured on bailed samples. At the shallow piezometers, all parameters were measured on bailed samples. Further description of the methods and equipment used is given below.

Eh

Redox potential was measured using a Cole-Palmer ORP (Redox) Combination Electrode probe with built in reference electrode and platinum band. This was hooked up to the pH meter. Before departure to the field, the Eh probe was tested in the lab with Quinhydrone solutions made up in pH 7 and pH 4 buffers. In the field, the platinum band was cleaned regularly to prevent fouling by organics and other agents in the peat waters, and care was taken to minimize sample exposure to air.

Ferrous Iron

Ferrous iron was measured using a HACH Ferrous Iron test kit. This method uses a 1,10 Phenanthroline indicator which turns the sample orange upon reaction with ferrous iron. Concentrations of up to 10 mg/L, in increments of 0.2 mg/L were read using a colour wheel. All containers were rinsed twice with tap water and once with distilled between stations. Care was also taken to minimize exposure to air.

pH and Temperature

An Orion liquid-filled pH probe connected to a Hanna HI 9025C pH meter was used to measure pH. Temperature was measured with a temperature probe connected to the pH meter. The pH meter was calibrated before each use using buffers 4.01 and 7.01, and rinsed with distilled water between readings. Care was taken to minimize sample exposure to air, since oxidation, degassing, and temperature increase affect pH.

Conductivity

A hand-held conductivity meter (Hanna Dist WP 3) was inserted into the sample to measure conductivity. It had been pre-calibrated in the lab using standardized KCl solutions.

Bicarbonate

As an approximate measure of bicarbonate (HCO_3) concentrations in these waters, the ASTM standard test method for alkalinity of water (D 1067-92) by electrometric titration was followed. This assumes that most of the acid-neutralizing capacity of the water comes from bicarbonate, which is reasonable given the neutral pH of these groundwaters and surface waters. Fifty mililitres of sample were titrated with small additions of 0.02N hydrochloric acid to a pH of 4.0.

Next, pH was plotted against the volume of acid added, and the bicarbonate inflection point (around pH 4.3) was interpolated. All titration data is plotted in **Figure D-1**. Assuming that all of the acid-neutralizing capacity comes from dissolved carbonate, and

knowing that bicarbonate is the dominant species at these neutral pH's, the bicarbonate concentration was calculated using: ·

$$\text{mg/L HCO}_3 \quad = \frac{(\text{mL of titrant})(0.02 \text{ meq/L})(61 \text{ mg/meq})(1000 \text{ mL/L})}{\text{mL sample}}$$

$$= (\text{mL of titrant}) (24.4)$$

Replicate alkalinity titrations were done at every fifth sampling location to test the reproducibility of the bicarbonate values.
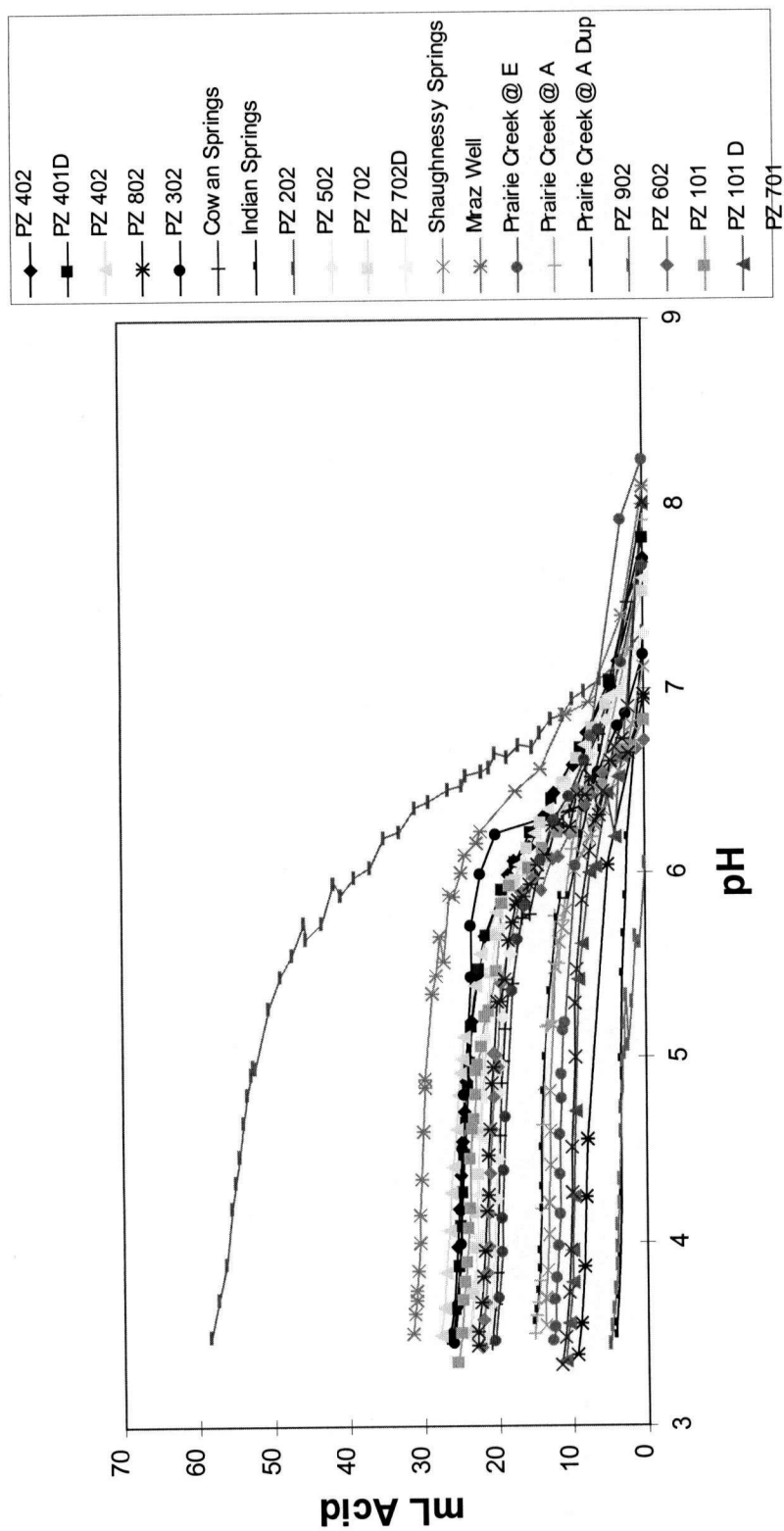
Figure D-1 Alkalinity titration data

The legend of the figure contains the following entries:

PZ 402
PZ 401D
PZ 402
PZ 802
PZ 302
Cowan Springs
Indian Springs
PZ 202
PZ 502
PZ 702
PZ 702D
Shaughnessy Springs
Mraz Well
Prairie Creek @ E
Prairie Creek @ A
Prairie Creek @ A Dup
PZ 902
PZ 602
PZ 101
PZ 101 D
PZ 701

E LAB ANALYSES OF CHEMICAL PARAMETERS

This appendix summarizes the protocols followed in the lab and in the field for water samples requiring lab analysis. It is divided into two sections: 1) sample preservation and storage and 2) lab instrumentation and analysis.

SAMPLE PRESERVATION AND STORAGE

Bottled water samples were collected for laboratory analysis of dissolved uranium, dissolved cations (Ca, Mg, Na, K, Fe_{TOT}), dissolved anions (NO_3, PO_4, Cl, and SO_4), and dissolved carbon (total, organic, and inorganic). Two sets of samples were taken, one for uranium and cations, and the other for cations and dissolved carbon, since each group shares the same preservation and storage requirements.

Uranium and Cations (U, Ca, Mg, Na, K, Fe_{TOT})

Before departure to the field, all sampling and storage material was acid-washed in a 20% nitric acid solution, rinsed with distilled water, air-dried in a fume hood, and sealed in zip-lock plastic freezer bags. In the field, water samples were syringe-filtered using sterilized 0.45 μm Millex-Ha Millipore filters, and stored in 30mL or 60mL nalgene bottles. Before capping, they were acidified to a pH < 2 using 50% v/v nitric acid. Syringes that had to be used more than once were soaked for 3 hours in a 20% nitric acid solution, then in distilled water, then sealed in a clean zip-lock bag. Back at the lab, these samples were placed in the refrigerator at 4°C until analysis.

Anions NO_3, SO_4, Cl, PO_4 and Dissolved Carbon

In September '97, nitrate concentrations were measured using a Hach test kit. Samples were filtered in the field using a hand pump and vacuum flask fitted with Whatman 1 Qualitative filter paper. They were stored in 100mL nalgene bottles in a cooler at 4°C,

and analyzed that same day. All sampling and storage equipment was rinsed with distilled water before and after use, with care taken to avoid contact with nitric acid.

In March '98, nitrate concentrations were measured using an ion chromatograph, along with other anions. Before departure to the field, new 60 mL nalgene bottles were rinsed twice with deionized water, air-dried in a fume-hood, and sealed in clean zip-lock bags. At the time of collection, samples were syringe-filtered through sterilized 0.45 μm Millex-Ha Millipore filters and then bottled. They were frozen within 6 hours of collection, and thawed only in time for analysis.

LAB INSTRUMENTATION AND ANALYSIS

Analyses for uranium, major cations (Ca, Mg, Na, K), anions (NO_3, SO_4, PO_4, Cl) and dissolved carbon (TC, IC, OC) were done in the lab within six weeks of sample collection. Descriptions of the laboratory procedures and instrumentation are given in this section.

Uranium

Aqueous uranium (^{238}U) concentrations were measured by inductively-coupled mass spectrometry (ICP-MS). ICP-MS is ideally suited to analysis of trace heavy metals since it is rapid and sensitive to concentrations in the parts per billion range. Also, interferences by element isotopes of similar mass are not a problem with uranium.

First, external and internal standard solutions, and blank solutions were prepared. External standards are known concentrations of uranium whose measured response signal is plotted to create a calibration curve. Solutions of 1 μg/L, 10 μg/L, and 25 μg/L uranium in a 1% nitric acid matrix were prepared from a 1000 mg/L standard reference solution. One percent is roughly the same concentration of nitric acid in the field samples after acidification to pH < 2. All dilutions and additions were carried out using pre-calibrated Eppendorf micropipetters.

Internal standards are known amounts of some non-analyte that are added to all samples in order to detect and correct for fluctuations in matrix composition, instrumental drift or blockages, and other processes that may cause loss of sample during analysis. Indium was chosen as the internal standard because its natural occurrence in the environment is negligible, it lies in the same mass range as uranium, it is easily ionized in the ICP, and it does not exhibit any interfering chemical effects. A 1 mg/L Indium solution was prepared from a 1000 mg/L Indium reference standard, then added to external standards, samples, and lab blanks to a concentration of 20 µg/L. The laboratory blank consisted of the 1% nitric acid matrix plus internal standard.

During analysis, the ICP-MS was set in pulse-counting mode, the number of counts being proportional to the concentration of analyte in the sample. First the external standards were measured, followed by the samples in order of expected uranium concentration. Pulse counts were later converted to uranium concentration values using the calibration curve.

To ensure quality results, a number of measures were taken:

· sample replicates were done every 5 samples, and the lab blank and 10 µg/L standard were run every 10 samples. Repeating the 10 µg/L standard allowed any shift in the calibration curve through the course of analysis to be detected.

· a 30 second instrument rinse with 1% nitric acid was done between samples, but if remnant U in the sample loop was suspect, the lab blank was run again as a rinse.

· uranium values were corrected for instrumental drift, based on fluctuations in internal standard read-outs. The correction formula used is:

Corrected U = Uncorrected U * Average In counts / In counts

164

Anions (NO_3^-, SO_4^{2-}, Cl^-, PO_4^{3-})

Nitrate samples collected in September '97 were analyzed by Hach's Medium-Range Nitrate (0-4.5 mg/L NO_3-N) and Low-Range Nitrate (0-0.15 mg/L NO_3-N) test methods. These used powder pillows and a DR 2000 Spectrophotometer, and are based on the Cadmium Reduction Method outlined in Standard Methods for Wastewater Analysis. A $NaNO_3$ solution of known concentration was used as a control standard. Water samples from 102 and 402 underwent some orange tinting due to iron-oxide precipitation, which may have biased the results high.

For the March '98 water samples, concentrations of nitrate, sulfate, chloride, and phosphate were obtained by ion chromatography within two weeks of sample collection. This work was carried out by a lab technician in the Oceanography department at UBC, using a Dionex DX-100 Ion Chromatograph. As an accuracy check, two reference solutions of known concentration were analyzed every 10 samples.

Cations (Ca^{2+}, Mg^{2+}, Na^{2+}, K^+, Fe_{TOT})

Samples were analyzed by Flame Atomic Absorption (AA) and Atomic Emission (AE) using a ThermoJarell Ash Video 22 AA/AE spectrophotometer in the Civil Environmental Lab at UBC. Flame AA was used for iron, magnesium, and calcium; and AE was used for sodium and potassium.

External standards were prepared for Ca, Mg, Na, K and Fe by making dilutions of 1000 mg/L standard reference solutions. Their concentrations were chosen to straddle the expected range of cation concentrations in the samples while remaining within the instrument's optimal measurement range. Dilutions were made using glass pipettes and volumetric flasks, and a 1% nitric acid matrix was maintained for all standards and diluted samples.

165

During the analysis, samples were ordered from least to most concentrated. The machine was re-zeroed and re-calibrated every 10 samples, and lab replicates were also done every 5 samples. Calcium, iron, and magnesium concentrations were calculated automatically by the instrument, whereas non-linearity in the calibration curves for sodium and potassium required that each be interpolated manually. This was not a concern since non-linear calibration curves are often encountered when operating in AE mode.

Dissolved Carbon

A Shimadzu TOC-500 Total Carbon / Inorganic Carbon Analyzer was used to find concentrations of total dissolved carbon (TC), dissolved inorganic carbon (IC) and dissolved organic carbon (OC) in the samples. It uses the Combustion Infrared Method, described in Standard Methods for Wastewater Analysis. TC and IC were measured individually, and OC was calculated by difference. This analysis was done by a technician in the Civil Environmental Lab at UBC.

Four standards were used to calibrate the instrument: 10 and 100 mg/L TC, and 10 and 100 mg/L IC. As a precision check, two samples were analyzed twice, and as an accuracy check, two other samples were spiked with known amounts of analyte.

When the carbon analyses were carried out, the samples had previously been thawed and refrozen. On the second thawing, a reddish-brown precipitate was observed in many of the samples, guessed to be a mixed precipitate of iron oxide, organics and silica. If they do contain organics, the dissolved carbon concentrations should not be interpreted quantitatively.

QUALITY CONTROL RESULTS

Various measures were taken to ensure quality results at all stages of sampling and analysis. This included the use of blanks, field duplicates, lab replicates, and control standards.

The results of this work are summarized in **Table E-1.** The left side gives the percent relative error values calculated for the control standards, lab replicates, and field duplicates. Absolute concentrations of analytes measured in the blanks is given on the right. Areas of concern are highlighted and discussed in the upcoming sections.

Control Standards

Where possible, solutions with known amounts of analyte were used to check the accuracy of results, particularly that of the standards. All relative errors were less than 8%, which is acceptable.

Lab Replicates

Lab replicates are the same samples analyzed twice in the lab. Agreement between these was consistently above 95%, which is excellent and therefore eliminates concern about instrument precision. Replicates were not carried out during anion analysis because these were done by another technician.

Field Duplicates

Field duplicates are separate samples taken at the same time from the same location. Duplicates were taken at piezometers 101, 401, 502, and at the exit point of Prairie Creek from the flats. The agreement between duplicates at 401 and 502 is excellent, but at 101 calculated errors are a consistent 25%, and at the stream, 100%. The variation in the Prairie Creek samples is not surprising since they weren't taken at exactly the same time from exactly the same spot along the stream.

The seriousness of the 25% variability seen at 101 is lightened somewhat by the fact that concentrations of most analytes at 101 are among the lowest measured in these groundwaters, some even near detection limits. Thus, the relative error between duplicates at other locations is likely to be lower.

Field and Laboratory Blanks

Five kinds of blanks were prepared for both the acidified and non-acidified samples: the Development blank, Bailer & Bottle blank, Syringe blank, Trip blank, and Cleaning blank. A brief description of each is given below:

· The *Development blank* consisted of tap water rinsed through the Waterra™ tubing right after the development of piezometer 402. Its purpose was to detect any cross-contamination by the Waterra™ during development and sampling.

· The *Bailer and Bottle blank* consisted of distilled water washed through the nylon bailer and sampling bottle after prior rinses with tap water. It would detect any contamination of the sample by these items.

· The *Cleaning blank* was made up of distilled water that had been used in the final soak of bottle cleaning. This made sure that negligible amounts of analyte remained after cleaning.

· The *Syringe blank* was made up of distilled water passed through the syringe and filter after an acid cleaning in the field. It detects any carry-over of analyte after cleaning (especially NO_3).

· The *Trip blank* is distilled water brought out to the field, opened, acidified if required, and stored with the rest of the samples. This measures contamination during the entire process of transport, sampling, storage, and analysis.

168

Of all of these blanks only the Development blank had significant amounts of analyte. Its concentrations represent less than 15% of the measured concentrations in the groundwater at 402, except for phosphate (which is already near the detection limit) and chloride. Chloride has a higher concentration in the blank than in the groundwater, due to either analytical error or to chloride already present in the tapwater used to rinse the Waterra™ tubing. Even if cross-contamination were occurring, pumping piezometers dry during development leaves virtually no water to contaminate fresh inflowing water. In general, the blanks results show that contamination of the water samples during all phases of field work and analysis is negligible.

Error Bars

The largest contribution to error in the water chemistry data is sampling irreproducibility, since lab replicate errors are negligible by comparison. Therefore, error bars are based on the field duplicates, except for temperature, pH, Eh, and Fe^{2+}, which are based on the measuring instrument or method. Ranges of error are summarized in **Table E-2.**

Table E-1 Quality control results

PARAMETER	CONTROL STANDARDS	LAB REPLICATES	DUPLICATES						BLANKS				
			101	401	502	Prairie Crk at A	702		Cleanng	Trip	Devlpmt	Syringe	Bail & Bot
	%	%	%	%	%	%	%		abs	abs	abs	abs	abs
HCO3			4	2		1	2						
Ca	1	2	26	1	1	97	n/a	mg/L	0	0	11	0	0
Mg	8	0	25	0	0	122	n/a	mg/L	0	0	3	0	0
Na	n/a	0	25	0	0	112	n/a	mg/L	0	0	4	0	0
K	n/a	0	25	3	0	128	n/a	mg/L	0	0	1	0	0
Fe	0	0	0	0	0	100	n/a	mg/L	0	0	0	0	0
U	n/a	4	19	12	5	143	n/a	ug/L	0	0	4	0	0
NO3	-2	n/a	195	58.5	0	4	n/a	mg/L	1	0	1	0	2
PO4	-2	n/a	23	5	n/a	20	n/a	mg/L	1	0	1	1	1
SO4	3	n/a	6	7	13	6	n/a	mg/L	0	0	8	0	0
Cl	7	n/a	14	10	14	3	n/a	mg/L	0	1	34	0	0
TC	5	5	12	15	5	n/a	n/a	mg/L	n/a	n/a	15	n/a	0
IC	n/a	4	10	19	7	n/a	n/a	mg/L	n/a	n/a	12	n/a	0
OC	n/a	7	100	10	2	n/a	n/a	mg/L	n/a	n/a	3	n/a	0

%: percent relative error
abs: absolute sample concentration

170

Table E-2 Error bars assigned to each chemical parameter

Parameter	Error
Temperature	$\pm 0.5\ ^\circ C$
Conductivity	$\pm 10\ \mu S/cm$
pH	± 0.1 pH unit
Eh (measured)	$\pm mV$
Fe^{2+}	± 0.2 mg/L
Fe_{TOT}	$\pm 5\%$
NO_3	$\pm 10\ \%$ (20% at PZ 101)
PO_4	$\pm 10\ \%$ (20% at PZ 101)
SO_4	$\pm 10\%$
Cl	$\pm 10\%$
Ca	$\pm 5\%$ (20% at PZ 101)
Mg	$\pm 5\%$ (20% at PZ 101)
Na	$\pm 5\%$ (20% at PZ 101)
K	$\pm 5\%$ (20% at PZ 101)
U	$\pm 10\%$
HCO_3	$\pm 5\%$
Total Carbon (TC)	$\pm 10\%$
Inorganic Carbon (IC)	$\pm 10\%$
Organic Carbon (OC)	$\pm 20\%$

F GEOCHEMICAL MODELING USING PHREEQC AND WATEQ4F DATABASE

This appendix explains the revisions made to the WATEQ4F database used by the PHREEQC program to do the geochemical modeling for this thesis. Aqueous species concentrations and mineral saturation indices calculated for the groundwater samples collected at the Prairie flats are also presented.

Revisions made to WATEQ4F database

Since the original compilation of the WATEQ4F database in the 1980's, several advances have been made in uranium chemistry. The $UO_2(HPO_4)_2^{2-}$ species has been discarded (Sandino and Bruno, 1992), and the E^0 value for the UO_2^{2+}/U^{4+} couple has been re-measured (Giridhar and Langmuir, 1991). This has caused significant changes in the Gibbs free energy values for U^{4+}, UOH^{3+}, UO_2^+, and $U(OH)_4^0$ and some U^{4+} minerals, which have been accounted for in the thermodynamic tables found in Langmuir (1997, p. 551-2). Since the logK and ΔH values for other U^{4+} and U^{6+} species in the WATEQ4F database matched those given by Langmuir (1997), the standard state conditions were also assumed to be consistent. Therefore, the WATEQ4F database was updated according to Langmuir (1997) through the following revisions.

$UO_2^{2+} + 2PO_4^{3-} + 2H^+ = UO_2(HPO_4)_2^{2-}$ eliminated

$UO_2^{2+} + 4H^+ + 2e^- = U^{4+} + 2H_2O$ log K = 8.89

$U^{4+} + H_2O = UOH^{3+} + H^+$ log K = -0.65

$UO_2^{2+} + e^- = UO_2^+$ log K = 1.49

$U^{4+} + 4H_2O = U(OH)_4^0 + 4H^+$ log K = -12.0

$UO_{2(am)} + 4H^+ = U^{4+} + 2H_2O$ log K = 4.16

$UO_{2(c)} + 4H^+ = U^{4+} + 2H_2O$ logK = -4.99
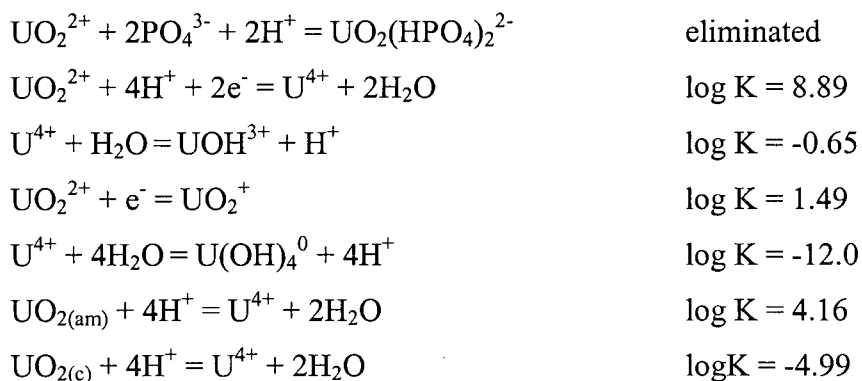
Prairie Flats Geochemical Modeling

Mineral saturation indices and concentrations of aqueous species at equilibrium were calculated for each groundwater sample in the March '98 data set using PHREEQC and the revised WATEQ4F database. Input parameters included pH, calculated Eh (from Fe^{2+} concentrations), temperature, major anion concentrations (NO_3, Cl, PO_4, and SO_4), major cation concentratons (Ca, Mg, Na, K, Fe_{TOT}), and uranium concentrations (see **Table 4-5**). The output is given in **Table F-1**:

Table F-1 PHREEQC output for Prairie Flats groundwaters

Location	Eh (V)	pE	SI UO_2	SI $UO_{2(am)}$	SI U_4O_9	SI U_3O_8	SI Calcite	U-CO_3 M	U-PO_4 M
PZ 101	0.236	4.0	-8.0	-16.4	-26.2	-14.8	0.2	3.9E-08	1.3E-11
PZ 102	0.041	0.7	1.5	-6.7	3.1	-4.0	-0.4	1.5E-07	3.3E-10
PZ 202	-0.024	-0.4	2.6	-5.6	6.0	-3.7	0.6	1.6E-05	4.2E-11
PZ 302	0.018	0.3	1.2	-7.1	1.9	-4.9	0.1	3.5E-07	1.8E-10
PZ 401	0.236	4.0	-7.2	-15.5	-23.3	-13.0	0.7	2.8E-06	3.5E-11
PZ 402	0.035	0.6	2.2	-6.1	5.6	-2.3	-0.2	1.5E-06	7.5E-10
PZ 502	-0.041	-0.7	3.1	-5.2	7.9	-2.5	0.1	4.6E-07	1.2E-12
PZ 601	0.077	1.3	0.3	-8.0	-0.8	-5.6	-0.5	9.4E-08	3.7E-10
PZ 602	0.047	0.8	1.6	-6.6	3.7	-3.2	-0.3	4.3E-07	7.5E-10
PZ 701	0.236	4.0	-7.6	-15.8	-24.8	-14.4	0.2	2.9E-07	1.5E-11
PZ 702	-0.035	-0.6	1.8	-6.5	3.2	-5.3	0.2	2.7E-07	1.2E-11
PZ 802	0.018	0.3	2.3	-5.8	5.8	-2.7	-0.9	4.2E-08	4.7E-10
PZ 902	0.177	3.0	-0.6	-8.8	-2.2	-4.1	-3.1	2.4E-08	3.5E-09

*U-CO_3 and U-PO_4 refer to the total concentrations of all uranyl-carbonate and uranyl-phosphate species, respectively

** SI is the Saturation Index with respect to the given mineral phase

Results of a sensitivity analysis testing the effects of pH, HCO_3 concentration, Eh, and U concentration on uranium mineral saturation indices are tabulated below:

Table F-2 Output of PHREEQC sensitivity analysis on U mineral saturation

pH	Eh (V)	HCO$_3$ mg/L	U ug/L	SI UO$_2$	SI U$_4$O$_9$
7.53	-0.1	555	75.4	3.99	9.76
	0			0.61	-0.38
	0.1			-2.77	-10.52
	0.2			-6.17	-20.72
6	0	555	75.4	4.81	13.39
6.5				3.79	10.31
7				2.25	5.13
7.53				0.61	-0.38
8				-0.82	-5.13
7.53	0	100	75.4	2.64	7.76
		300		1.39	2.74
		500		0.74	0.17
		700		0.3	-1.61
7.53	0	555	10	-0.27	-3.89
			50	0.43	-1.09
			100	0.73	0.12
			500	1.43	2.91
			1000	1.73	4.12